Bulletin of Romanian Chemical Engineering Society

1 2016

ISSN 2360-4697
Edited by SICR and Matrix Rom

The journal is included in the international database
INDEX COPERNICUS INTERNATIONAL

ISSN 2360-4697

Bulletin of Romanian Chemical Engineering Society

Volume 3 2016 Number 1

Contents

THEORY OF SYSTEMS, PROCESS CONTROL, PAST, PRESENT AND FUTURE - THE WAY THEY GO ALONG WITH PROCESS ENGINEERING TOWARDS A SUSTAINABLE SOCIETY

Paul Şerban AGACHI[1,2]

[1]Full Professor, Chemical Engineering, Department of Chemical, Material and Metallurgical Engineering, Botswana University of Science and Technology, Palapye, Botswana
[2]Chemical Engineering Doctoral School, University Babeș-Bolyai, Cluj-Napoca, Romania

Abstract
The paper makes an excursion in the history of Process Engineering (PE) and Process Control (PC) together with the Theory of Systems (TS) seen as interdependent. Starting with the development of the mankind, from its basic needs, going to the nowadays consumerist philosophy, the paper describes the development of civilization from the Neolithic tool manufacturing to the present stage of intelligent manufacturing; it shows the necessity of improvement of approaching the processes from systemic point of view, then controlling them in order to improve the performances, efficiency, the environmental impact for a future sustainable development. Solutions for a sustainable society are provided through close collaboration of the three apparently different fields.

Key words: Process engineering, Process control, Theory of systems, Sustainability.

Manufacturing processes are traced well back in the history of mankind long time before the antiquity. The Industrial Revolution (XVIIIth century) was the moment, the milestone, when the shift from batch to continuous processing occurred and incurred the development of the PC. The Industrial Revolution was the dawn of the consumerism stage in mankind's history and led to an unprecedented escalation in demand, both with regard to quantity and quality, for bulk chemicals such as sulfuric acid and soda ash. This meant two things: one, the size of the activity and the efficiency of operation had to be enlarged, and two, serious alternatives to batch processing, such as continuous operation, had to be examined. This created the need for an engineer who was not only understanding with how machines behaved, but also understood chemical reactions and transport phenomena (W. F. Furter (1982) A Century of Chemical Engineering Plenum Press, New York). Nowadays, Process Engineering (PE), the new development of

Chemical Engineering, is going on under the imperative of sustainable development with its consequences [1].
In parallel, the Automatic Control (AC) is a quite fresh field of development. Of course, interest for small mechanical robots existed from the antiquity to the medieval times, the Chinese water clock being an example. Actually, this is not AC, but PC. But the Industrial Revolution was the inspiring period of the beginning of the process control (see Jacquard weaving looms, XVIIIth century). Passing through Maxwell's analysis of the steam engine governor in 1868, the "primitive period of feedback control" finishes in 1900. It is standard to call the period from then until 1970 the classical period of feedback control and the period from 1970 through present times the modern control period. After 1970's, computers entered in the life of the process industries. The concept of examining the many parts of a complex process or plant together as a single unit, with all the interactions included, and devising ways to control the entire plant is called Systems Engineering (SE) [1].

What was at the beginning?

From the evolutionist point of view (Figure 1), the humankind appeared around 30 Million years ago with early humanoids [2]. It started to produce, prepare, process food only 2-4 Million years ago, to construct a shelter only 200,000 years back, clothes, tools, weapons only 80,000 years back. The goods? Not that time, the population consumed only basic things. Later on, jewels, pottery … Culture is very, very new, first paintings are dated around 40,000 years back and education very, very close to our times: only 10,000 years back. That it is why even today education is considered a luxury! And ethics, morale, even later, these things being under discussion at present.
According to the history written by some archaeologists, it is supposed that the early civilization started in Mesopotamia. But I guess this is because the first archeological discoveries were done in the colonialist era and in the colonial countries, mainly by the British. Of course, there are other newer discoveries contesting that, but is rather difficult to compete with tradition and conservative spirit. So, first pottery - 30,000 years ago, first glassware - 3,500 years ago apparently were done there, looking that the cradle of civilization was in the Middle East and the history of manufacturing continues through the Middle Eve to the present time.
The world population evolved very slowly for a long time, but because of the several Agricultural Revolutions beginning 9,000 years BC, sharply increased in 200 years (1000 AD - 1800 AD), from 500 Million to 1 Billion [3]. This population needed more and better quality food, better shelter, better clothes,

mobility and transportation vehicles. And thus, the Industrial Revolution appeared as a consequence.

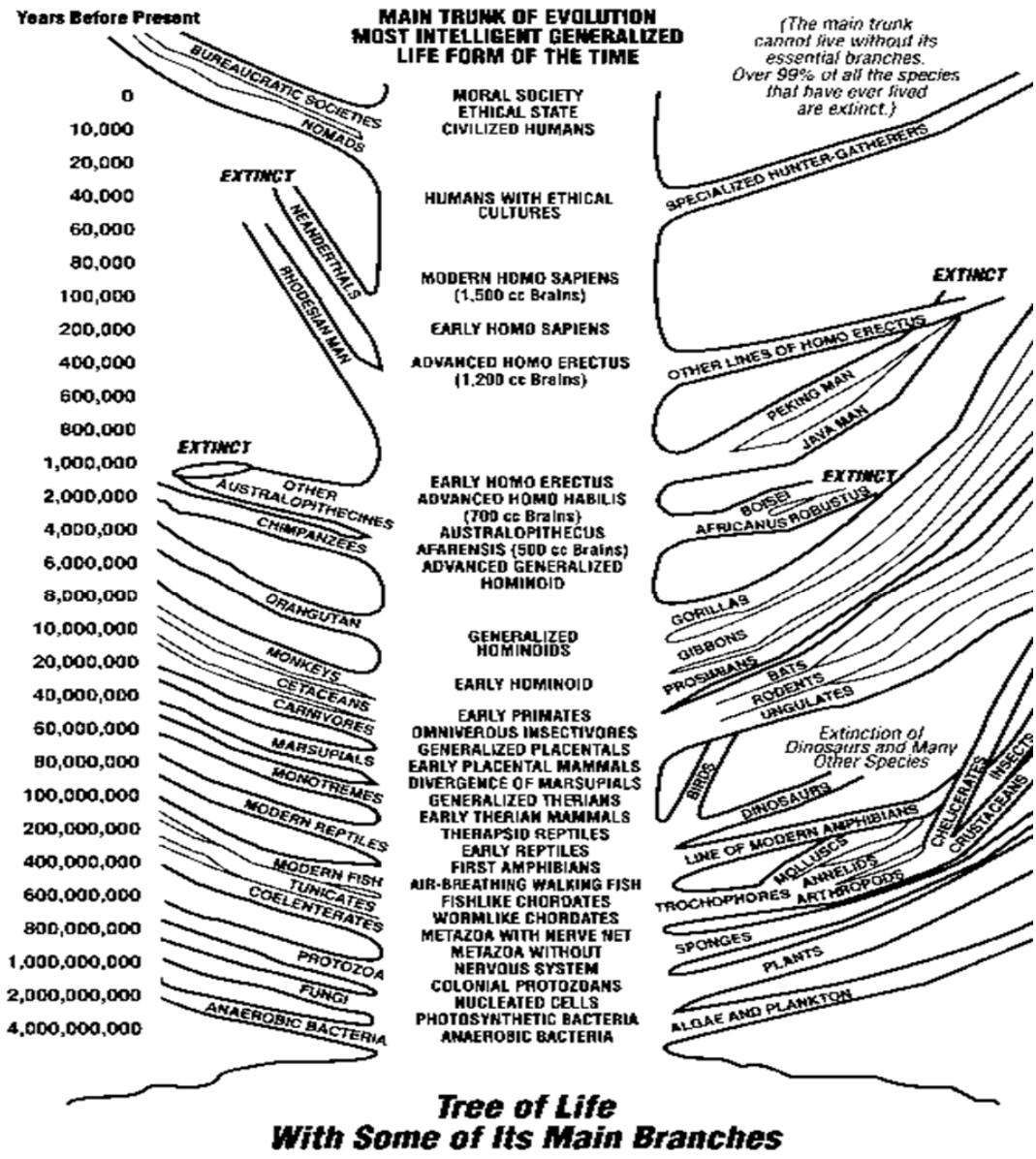

Fig. 1. Evolution of the mankind (source: http://www.see.org/garcia/e-ct-2.htm [2])

A new discipline in the XIXth century- Chemical Engineering

Of course, we may say that the manufacturing of chemicals existed long time before the Industrial Revolution: soap is estimated to have been produced in the

third millennium BC in Mesopotamia; pigments produced 17,000 years ago in ancient Egypt, Assyria, China, Europe; ceramic, 30,000 - 13,000 BC in Japan, Europe, China; glass, 3,500 BC in Mesopotamia. Scented oils, wines, metals, substances for tanning the leather (produced 7,000 BC in South Eastern Asia) were also products of chemical technology, although we do not necessarily consider them as such.

But actually, products of chemical synthesis were obtained only during and after the XVIIIth century: Sulfuric Acid Production (1749), Potassium Carbonate (Potash) (1790), Alkali & Sodium Carbonate - Le Blanc Process (1810).

Fig. 2. Le Blanc Process in Cheshire factory (department.monm.edu, (the IChemE))

We have to mention here that the first oil refinery in the world and first well drill for commercial exploitation were in Ploiești, Romania (1856).

Later, the imminent progress of chemical industries were shown through other extremely important discoveries set in production: Soda Ash & The Solvay Process (1873), the contact method for Sulfuric Acid production (1900), Potassium Nitrate (1903), Synthetic Ammonia (1910), Rayon plant for viscose rayon (1910), Cellulose acetate, acrylics (Lucite & Plexiglas), Polystyrene (1920-1931), Polyethylene (1939) and Epoxy (a very strong adhesive) (1936); Catalytic Reforming to produce higher octane gasoline and create toluene for TNT (1940). Synthetic rubber - Styrene-Butadiene Rubber (1941), First man-made nuclear reactor (1942), Benzene produced from petroleum (1950). And the list may continue until today.

A new era emerges when the danger of over pollution was already visible: US Congress passes the "Clean Air Act" establishing national air quality standards (1970) and later, the "Clean Water Act" to confront water pollution (1972). The

pre-concepts of sustainable environment were set. As a consequence, Catalytic converters are introduced in many automobiles (1975).
In what we have seen up to the mid XIXth century, each industrial manufacturing was under the common approach of Chemistry, Industrial Chemistry or Chemical Technology. But, George Davis (1850-1907), the founder of the new profession, Chemical Engineering, identified broad features in common to all chemical factories. He noticed that all processes inspected (he worked as an inspector for the Alkali Act of 1863, "a very early piece of environmental legislation that required soda manufacturers to reduce the amount of gaseous hydrochloric acid released to the atmosphere from their factories"[4]) have in common most of the same stages: conditioning of the raw materials, processing, separation, packing. At the same time, he fought for the introduction of a new profession, that of the Chemical Engineer. "Many processes can be carried on very successfully by chemists in the laboratory, but few are able to make chemical processes go on the large scale, and simply because they have a lack of physical and mechanical knowledge combined with their chemistry," he wrote in a letter to the editor of the Chemical News in June 1880. He is the author of author of Handbook of Chemical Engineering in 1888. Although he was severely criticized by his colleagues, the chemists, he established a first course of 12 lessons in the University of Manchester, in 1887. The immediate result was the establishment of the Department of Chemical Engineering at Glasgow and West of Scotland Technical College offering day and evening classes in 1888 and a new curriculum at Massachusetts Institute of Technology (MIT): Course X, Chemical Engineering established by Lewis M. Norton in the same year.

Process Control (PC), e new field in the engineering of the XIXth century

Industrial revolution in its content meant invention of advanced grain mills, looms, furnaces, boilers, and the steam engine. Chemicals but also other products as fabric, or food were produced on a large scale only after the mid XIXth century. This enhanced production to address the needs of the already demanding population, accused the need of tighter control of the processes in order to produce a larger quantity of products and of a certain quality. And, now, a new field, PC, comes on the stage. As one may see, the development of the PC is strongly related to the manufacturing processes. These roots are traced in the ancient times of the humanity, starting with the metal, fabric and pottery production. The industrial manufacturing and actually the engineering were the innovations of the XVIIIth century, during the Industrial Revolution. The consumerism led to an escalation in demand, both with regard to quantity and quality, for food, clothing, footwear, housing, transportation, which stimulated the production of construction materials, textiles, chemicals etc. Each global conflict,

after its end (e.g. first and second World Wars, WW I and WW II), induced the same behavior and the same reaction on behalf the society and production companies. The production became mass production with huge quantities of products delivered at deadlines and at a certain quality expectation. The mass production, under these circumstances, could not be anymore controlled manually because of the expectations. In the meantime, in the second half of the XXth century, the environment became important, fact which imposed the environmental constraints on the manufacturers. Top on that, the globalization of the economy amplified the competition among world companies and only those capable to reduce costs and to respect the environment, resisted on the market. Together with these facts, an important impact on the development of the technology and especially computing facilities had the cold war and space race between the major world powers: the US and USSR. All these sequences led to a tremendous development of the control equipment, techniques as a part of process control development. PC was seen as a major tool for development and complying with the new constraints [1].

Milestones in the modern history of PC are C. Drebbel's contribution in inventing the first temperature control device for a furnace, around 1624, D. Papin's invention of the first safety valve for his steam engine – pressure regulator in 1704, E. Lee's first controlled positioning system for a wind mill in 1745 [5,6], T. Polzunov's first level controller for his steam engine (1765), J. Watt's fly ball governor in 1768 [7,8] – speed regulator for his rotary steam engine (Figure 3). The first obviously advanced combination between process engineering and process control was H. Jacquard's loom in 1801 (Figure 4) which stored the model of the silk fabric on punched cards [9,10]. Actually, in that period in France, there were several looms having similar control systems.

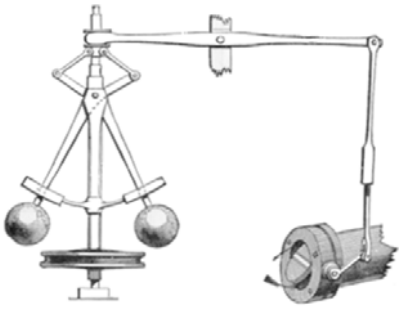

Fig. 3. J. Watt's fly ball governor

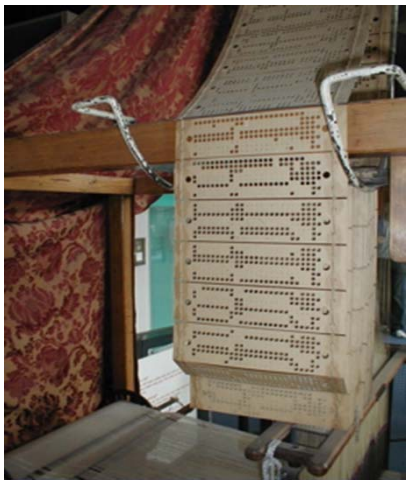

Fig. 4. Jacquard's loom

The more advanced the automated industrial cases were, more needs of solving problems of stability and performance of the controlled systems appeared. The first publication in the field of control systems was elaborated by J.C. Maxwell in 1868 and approached a theoretical analysis of the stability of Watt's fly ball governor (1868) [7]. The next papers on the subject of automatic control appeared only in the first half of the XX th century (1922 - 1934) and have to be noted the first in the field of control in Chemical/Process Engineering [11-15].

A major innovation represented G. Philbrick's "Automatic control analyzer – Polyphemus", actually the first analogue computer (1937-1938) just before the WW II [16]. The WW II brought extremely important innovations in the field of automatic control: automatic rudder steering, automatic gun positioning systems, automatic pilot of V1 and V2 etc. The innovative ideas of Ziegler and Nichols about how to tune the controllers in a loop stem from that time progress! [17]

Immediately after the WW II, the field of PC exploded. It was helped by the construction of the mega computers ENIAC (1946) [18] and UNIVAC (1951) [19], Shockley's patent on transistor (1950) [20] and Feynman's premonition regarding nanospace expressed at the American Physics Society Meeting in Caltech *"There's plenty of room at the bottom"* (1959) [21]. The new frontier of challenging the outer space launched by the US president John Fitzgerald Kennedy produced the portable computer which influenced thoroughly the more recent history of PC. The first industrial control computer system was built 1959 at the Texaco Port Arthur, Texas, refinery with a RW-300 computer from the Ramo-Wooldridge Company [22] and the second one was installed in 1964 by Standard Oil California and IBM at El Segundo refinery in a FCC Unit, under the name 1710 Control System [23][1].

Thus, there were practically three stages in Process Control development:

- ✓ First one, of Measurement and Control Devices (WW I – mid XXth century), dominated by manual control and operation of the industrial processes; there were used sometimes field mechanical controllers;
- ✓ Second one, of Classical Feedback Control (1950s –1970s), when most of the processes were supervised and controlled automatically in the simplest way – feedback control; the control equipment was either electronic or pneumatic, rarely hydraulic;
- ✓ Third stage, of Computer Assisted Control (1970s – present), as main feature, by the control systems including a micro or minicomputer; most processes are controllable and they need classical control systems, but

[1] I had the privilege to work for that refinery exactly in the computer controlled domain and they were very proud of these past achievements

around 20% of them from process industry are less controllable and need Advanced Control techniques and equipment.

It is worth to mention in the development of Chemical Engineering, that the computer control of chemical processes gains credibility (1959).

The use of computers in process control can be detailed in several stages of complexity. In the first stage of complexity a microchip to perform some calculations inside the controller or even computer is embedded, allowing more complicated control algorithms: optimal, adaptive, fuzzy, ratio, inferential, feed-forward control algorithms. A second stage of complexity is the Advanced Process Control (APC) characterized by a combination of hardware and software control tools used to solve complicated multivariable control problems or mixed integer-discrete control problems. It involves the computer techniques (hardware and software) applied to control, the good understanding of the process (process modeling and design), the good understanding of control techniques and optimization (Model Predictive Control (MPC), Distributed Control Systems (DCS) etc.). In the processes with multiple variables (hundreds or thousands) an efficient operation of the process, of the plant or of the industrial platform, can be done only through APC. Central Control Rooms looking like cosmic flight control centers are supervising and operating the whole plant. New skills of the operators are requested, because the implications of their actions are on a large scale. With APC one can save energy, raw materials, time, reduce costs and make the processes more competitive in terms of quality and costs. The third stage of complexity is expressed by the Wise Machinery (WM), a new concept which involves not only complying the standards or set points, but also, the intervention without the human assistance of the machine for its own functional efficiency and safety [24]. For that, the WM involves the complex industrial equipment, the Data Acquisition System (DAS) and the "Optimal Parametrical Control System (OPCS)" They are intended for finding operative and optimal solution of all possible management tasks arising in vital activities of process and machine's equipment in the limits of its life cycle. PCS is based on Bio-cybernetic Control Systems (BCS) which is principally a novel and industry evaluated decisions making system, which functions on the basis of formalization the unconscious activity process of a brain in maintaining the functions of an organism. It is a new civilization in itself.

The newcomer: Theory of Systems (TS)

Actually, it is not a newcomer since, from the very first developments of flyball governor [7], Airy's automatic telescope (1840), in the XIXth century, the scholars needed to invent new mathematical tools of solving their new problems. So, Airy, when he saw that during watching the moon movement, his automatic telescope

was not able to steadily fix the position, but only with oscillations, he tried to explain and calculate and he invented *Partial Differential Equations.* The *Stability Theory*, part of Automatic Control and Theory of Systems practically was established with Maxwell's study of the flyball governor. Immediately after that, Routh [25] and Vyshnegradsky [26] contributed with numerical techniques and studies of the stability of controllers. A.M. Lyapunov studied the stability of nonlinear differential equations using a generalized notion of energy in 1892. O. Heaviside invented the *operational calculus* in the last decade of the XIXth century. He studied the transient behavior of systems (very new at that time and even today this approach is rare among process engineers), introducing a notion equivalent to that of the *transfer function*.

"During the eighteenth and nineteenth centuries, the work of A. Smith in economics [The Wealth of Nations, 1776], the discoveries of C.R. Darwin [On the Origin of Species By Means of Natural Selection 1859], and other developments in politics, sociology, and elsewhere were having a great impact on the human consciousness. The study of Natural Philosophy was an outgrowth of the work of the Greek and Arab philosophers, and contributions were made by Nicholas of Cusa (1463), Leibniz, and others. The developments of the nineteenth century, flavored by the Industrial Revolution and an expanding sense of awareness in global geopolitics and in astronomy had a profound influence on this Natural Philosophy, causing it to change its personality" [27].

In the first quarter of the XXth century, A.N. Whitehead [28], with his philosophy of "organic mechanism", L. von Bertalanffy [29], with his hierarchical principles of organization, C. Odobleja [30] with his "Psychologie consonantiste", N. Wiener [31] and others had begun to speak of a "general system theory".

A definition: Systems Theory - the transdisciplinary study of the abstract organization of phenomena, independent of their substance, type, or spatial or temporal scale of existence. It investigates both the principles common to all complex entities, and the (usually mathematical) models which can be used to describe them [32]. Examples of systems are given in Figures 5 - 7.

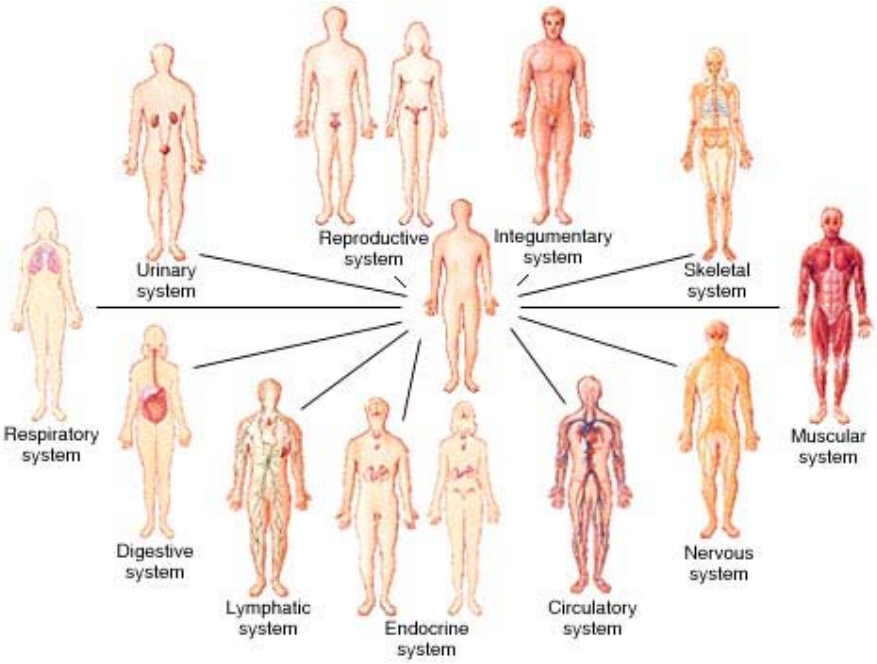

Fig. 5. Human body system (source: http://voud.dvrlists.com/human-organ-systems/)

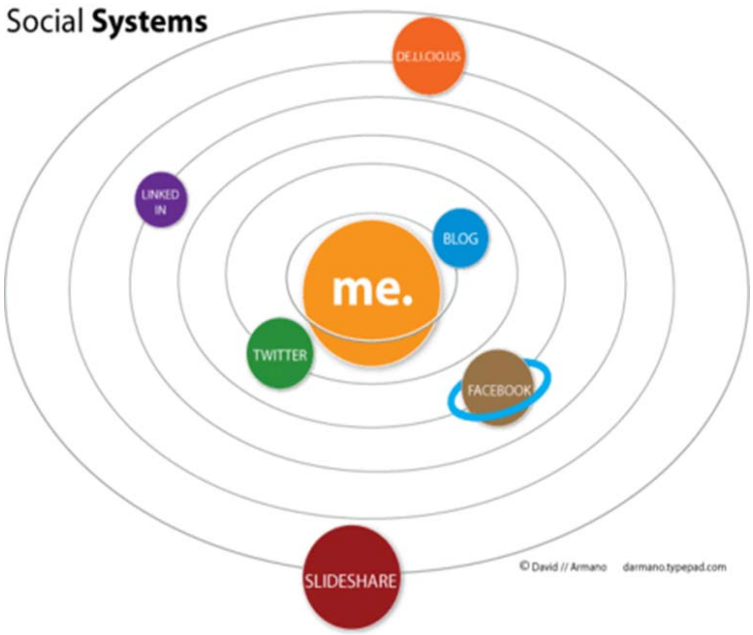

Fig. 6. Social system
(source: http://darmano.typepad.com/logic_emotion/2007/12/social-systems.html)

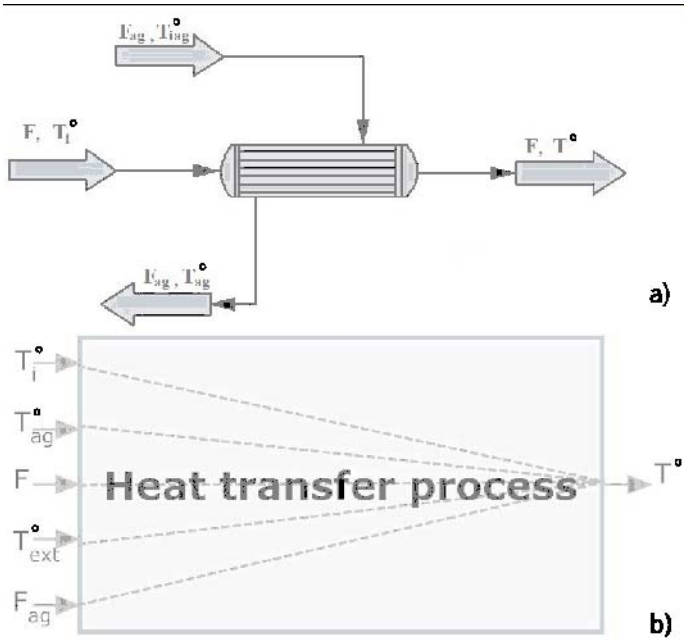

Fig. 7. Physical system (source: Basic Process Engineering Control, De Gruyter, 2014)

The System theory is nowadays the science which encompasses and embraces all other sciences giving a holistic view towards the approach of the systemic problem either it is of social/ administrative or mechanical/chemical nature. The strong belief of the author is that all systems are behaving basically in the same way and their approach should be similar.

And, finally, the Sustainable Society

Sustainable development was set on the agenda by the Brundtland Commission (UN World Commission of Environment and Development). Its definition:

”meeting the needs of the present without compromising the ability of future generations to meet their own needs” is acknowledged world-wide. In practice it is translated to better use of the available resources, better distribution of prosperity world-wide and taking into account already present environmental problems and a future growing world-population [33].

It is obvious we are living in a non-sustainable society with a non-sustainable economy (Figure 8).

Only 25% of the Earth resources are transformed in products and services; the rest, is garbage.

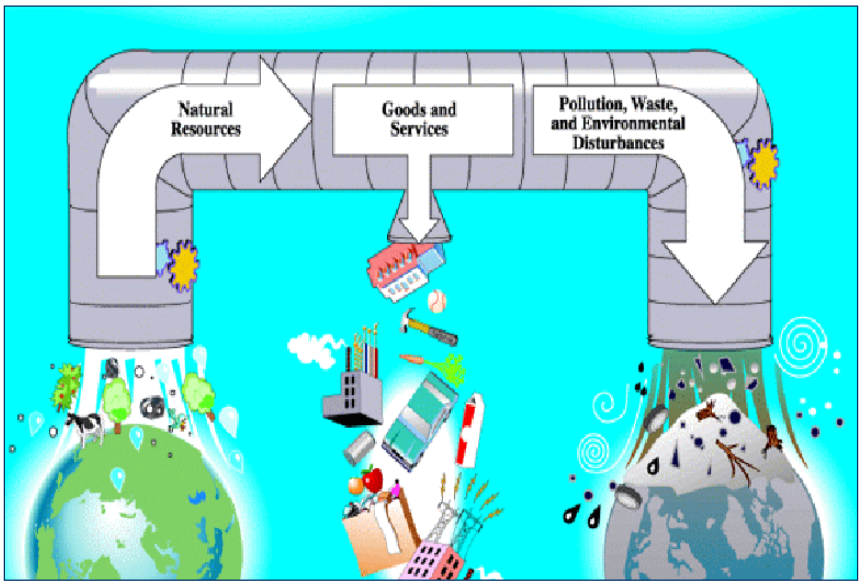

Fig. 8. Non sustainable humankind (source: Jean-Claude Charpentier, Among the trends for a modern Chemical Engineering: CAPE an efficient tool for Process Intensification, Product Design and Engineering, ESCAPE 17, Bucharest, 2007. Plenary lecture).

How do we approach this situation? How do these related sciences treat it?

Along their evolution, these four separate domains of activity, changed according to the new challenges. One huge challenge is the improvement of the eco-efficiency of all our activities.

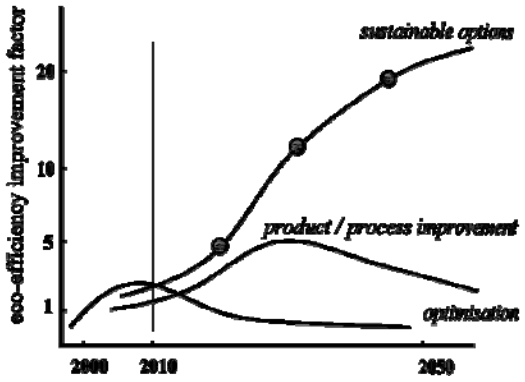

Fig. 9. Eco-efficiency factor function of time

According to different authors, the improvement needed is 4-20 fold: FACTOR 4 (Von Weizsacker, 1998), 10 (Schmidt-Bleek, 1993), 20 (AllChemE, 2001). We

are not now in the situation to increase 20 times the efficiency of production, but we will be obliged. WISE Machinery seems to be a solution.
Thus, Chemical Engineering changed its paradigms from the first one - Unit Operations starting from Davies, but explicitly stated by Walker in 1923, then the second paradigm - Transport Phenomena in the late '50s (Bird), the third paradigm: Chemical Product Engineering (or better Product-Process Engineering), stated most clear by Hill, 2009, to, finally, the fourth paradigm - Sustainable Chemical Engineering, nowadays [34]. Alexandru Woinaroschy is somehow subjective and conservative keeping close to Chemical Engineering although it is obvious the shift from Chemical to Process Engineering. These paradigms changed fundamentally the thinking prior to their apparition: from a sort of applied chemistry complicated with some mechanics/ mechanical engineering (Paradigm I), then from Unit Operations which treated separately individual parts of the process, to a more integrated approach of Transport Phenomena which was transversal (Paradigm II), then from Transport Phenomena to the holistic approach of Product – Process Engineering (Paradigm III) and lastly to the complicated involvement of the environmental and reserve constraints of Sustainable Process Engineering (Paradigm IV). New Mass Indices, Environmental Factors, Environmental Indices are requested and computed.
The principles of PE can be applied to the health of the environment as it is the example of using PE, PC and TS in preventing floods and draught (Figure 10) [35], or counteracting river pollution [36, 37].
Moreover, principles of PE, PC and TS can be applied to other systems than chemical engineering systems, but also to them.

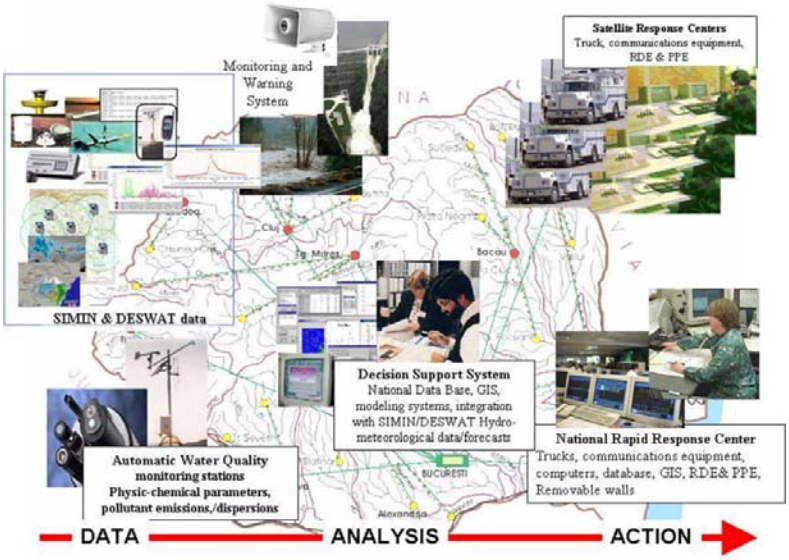

Fig. 10. Decision Support System for preventing flood and draught in Jijia Catchment

Applying the mass conservation principles and the fluid dynamics, we can anticipate the flood wave much before the flood is actually taking place. Based on some predictive models, the system which includes SCADA monitoring, an expert system, and Model Predictive Controllers, can prevent the flood by assuring some supplementary buffering capacity.
Coming back to manufacturing processes, for example, for a simple process of heating, +2°C deviation from the desired prescribed temperature value, for a simple heat exchanger, with a throughput of water of 5t/h, means a waste of 2.7k Euros/year/heat exchanger which the simple feedback control loop saves. With a number of 100 heat exchangers in a plant which is very usual, the amount estimated is of 270 kEuros/year. And here, we do not save only money but resources as well, according to sustainability principles.
But the principle of feedback which is very usual in PC and TS, can be applied to any other process from another far different field of activity. Feedback control principles are very well applied to medical treatment (Figure 11), or to educational systems (Figure 12). Supposing English subject is taken out of the program of the 5th graders. The result will be observed on the labor market only after 13 years. The difficulties created by this stupid measure are felt by the economy very late and, according to the dynamics of the processes they will be corrected with difficulty and with serious consequences. Here, a Model Predictive Control approach should be needed, but I wonder if the responsible persons would ever have had some knowledge about how to govern intelligently.

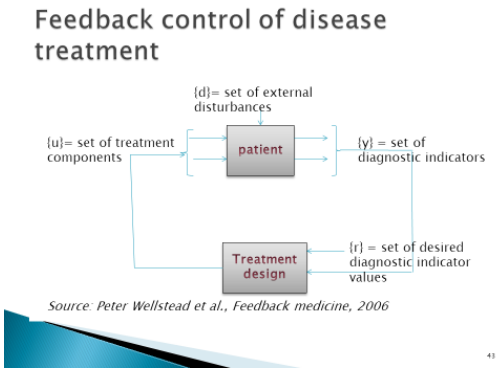

Fig. 11. Medical treatment with feedback

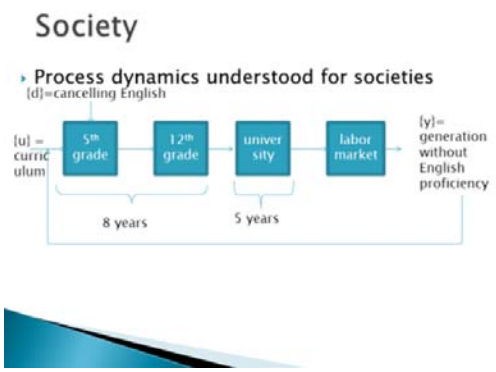

Fig. 12. Feedback in education systems
(Source: APS, Plenary lecture, 8th International PhD Summer School, Miskolc, 6-10 August, 2012)

Further on, advanced control methods could be used anesthesia, but also in the drug treatment of different organs since processes of transport through blood vessels or aerial tracts, mass transfer through membranes, chemical reactions at cell level are present in the human body (Figure 13).

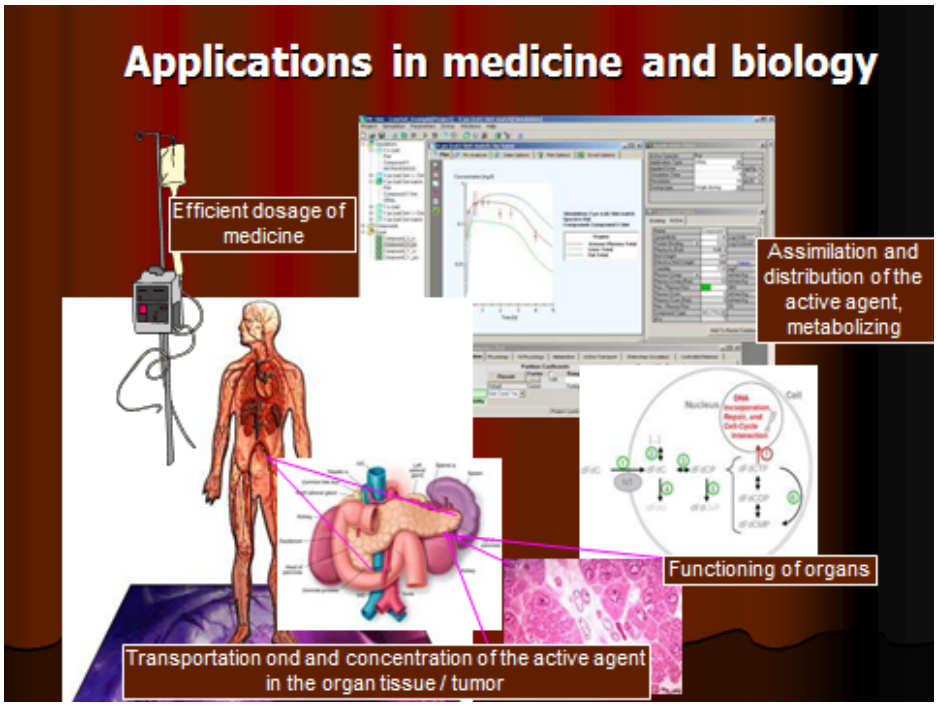

Fig. 13. Applications in medicine (source: APS, Plenary lecture, 36th Congress of Slovak Society of Chemical Engineering Tatranske Matliare, May 25-29, 2009)

But to come back to our original purposes, we might mention the huge impact the new Process Engineering through process intensification and advanced control have on the dimensions and performances of the processes. First example is taken from PVC batch suspension process (Figure 14) where a Model Predictive Control can reduce the batch time with 9% for every batch (average duration – 10 hours) and thus, save 9.5 Million Euros/year at a production of 40,000t/year [38].

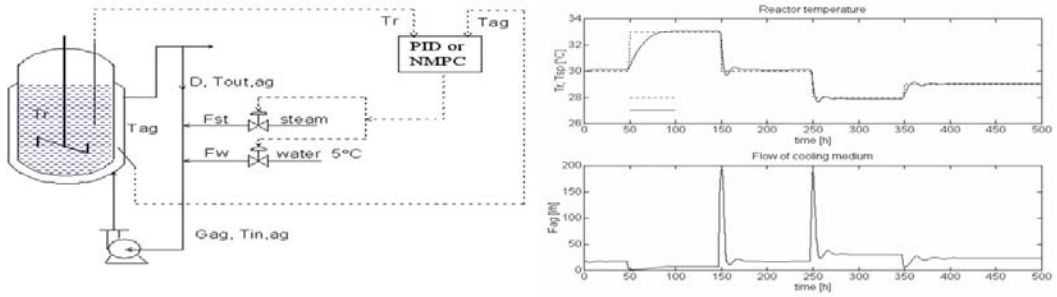

Fig. 14. MPC for a PVC batch suspension reactor

In the end, I want to cite Professor Jean-Claude Charpentier, former President of European Federation of Chemical Engineers [39]: “here I am presenting one

vision of how a future plant employing process intensification may look versus a conventional plant (Figure 15); operating with nonpolluting processes, involving process intensification, saving about 30% of raw materials, energy and operating costs".

Fig. 15. Comparative operation of the conventional and the future PE plant

Together with this advanced approach and repeating what I have mentioned previously about the most advanced type of control, *Optimal Parametrical Control System (OPCS)* which are intended to find operative and optimal solution of all possible management tasks arising in vital activities of process and machine's equipment and which is principally a novel and industry evaluated decisions making system, which functions on the basis of formalization the unconscious activity process of a brain in maintaining the functions of an organism, we may face with a new civilization in itself. This gives hope for the future of mankind but featuring a threat at the same time if we do not know how to cope with the new developments and the newly born Artificial Intelligences parallel to our natural human ones.

REFERENCES

[1] Agachi, P.,S., Cristea V.,M., Basic Process Engineering Control, De Gruyter Gmbh, Berlin, Boston, 2014, Introduction.

[2] Garcia, J., D., Creative transformation, A Practical Guide for Maximizing Creativity. Chapter 2, SEE Publishers, 1991, http://www.see.org/garcia/e-ct-2.htm.

[3] DeLong Bradford, J., Estimating World GDP. One Million BC – Present, http://www.j-Bradford-delong.net/TCEH/1998_Draft/World_GDP/Estimating_World_GDP.html.

[4] George E. Davies, https://en.wikipedia.org/wiki/George_E._Davis.

[5] Mayr, O., The origins of feedback control, *Scientific American*, 223(4), (1970), 110-118.

[6] Mayr, O., Feedback Mechanisms in the historical collections of the national museum of history and technology, Smithsonian Institution Press, 1971.

[7] Maxwell, J.C., On governors, *Proceedings of the Royal Society of London*, 16, (1868), 270 – 283 [This is presumably the first scientific article on feed back control].
[8] Centrifugal governor, http://en.wikipedia.org/wiki/Centrifugal_governor.
[9] Eclectica, Jacquard's loom and the stored program concept, http://addiator.blogspot.ro/2011/10/jacquards-loom-and-stored-programme.html.
[10] Essinger, J., Jacquard's Web: How a Hand-loom Led to the Birth of the Information Age, New Ed., Oxford University Press, 2007.
[11] Minorsky, N., Directional stability of automatically steered bodies, *J. Am. Soc. Nav. Eng.*,34, (1922), 280; [The article came after WWI when serious attempts for stabilization of the rudder of the naval units have been done].
[12] Nyquist, H., Regeneration theory, *Bell Syst. Technol. J.*,11, (1932), 126; [The article is related to papers by Black and Bode, representing another approach of a feedback system. [Nyquist developed an original theory for the feedback systems analysis and design].
[13] Grebe I., Boundy R.H., Cermak R.W., The control of chemical processes, *Trans. Am. Inst. Chem. Eng.*, 29, (1933), 211; [The article is the first to approach the control of chemical processes].
[14] Hazen, H. L., Theory of servomechanisms, *J. Franklin Inst.,* 218, (1934), 279; [Hazen is the first to describe how automatic equipment will replace human labor; he distinguished for the first time the „open cycle" (without feed-back) from „closed cycle" (with feed-back) what it is called nowadays open-loop and closed loop control].
[15] Ivanoff A., Theoretical foundation of the automatic regulation of temperature, *Journal of the Institute of Fuel*, 7, (1934), 117; [One of the first papers analyzing theoretically the temperature control].
[16] Holst, P., George A. Philbrick and Polyphemus: the first electronic training simulator, *IEEE Annals*, 4(2), (1982), 143.
[17] Ziegler J.G., Nichols N.B., Optimum settings for automatic controllers, *Transactions ASME*, 64, (1942), 759; [The first paper approaching the controller closed - loop tuning which was quite new at that time. The methods described are still used on a large scale for individual control loops].
[18] Goldstine H. H. and Goldstine A., The Electronic Numerical Integrator and Computer (ENIAC), 1946, reprinted in The Origins of Digital Computers: Selected Papers, Springer-Verlag, New York, 1982, 359-373; [First digital computer created at the University of Pennsylvania, for the US army; it had a calculation speed 1,000 times higher than the electromechanical machines].
[19] UNIVAC conference oral history, 17-20 May 1990, Charles Babbage Institute, University of Minnesota; [The second numerical computer created by the same team as ENIAC, delivered in 1951 to the US Census Bureau].
[20] US 2502488(1950), Semiconductor Amplifier; [Shockley W. submitted his first granted patent involving junction transistors].
[21] Feynman R., There's plenty of room at the bottom, *Caltech Engineering and Science*, 23(5), (1960), 22-36; [The conference presents the vision of the nano space and nano technology].
[22] Strycker W.P., Use and application of control systems via a digital computer, SPE Production Automation Symposium, 16-17 April 1964, Hobbs, New Mexico, Conference paper. [The

paper describes the concept and practice of installing first computer control system in process industries, initially controlling off line, from distant IBM computer center in San Francisco, via telephone lines with printer or punched cards reader terminals, and afterwards on line with a process computer installed at the refinery]

[23] Astrom, K., Wittenmark, B., Computer Controller Systems: Theory and Design, Prentice-Hall Inc., USA, 1997, 3.

[24] Bravy K., The compatibility of viability maintaining of machinery with viability maintaining of an animal's organisms, New technologies for the development of civil and military organizations in the modern post-industrial world, November 30, 2004, Ashdod, Israel, Conference paper.

[25] Routh, E.J., A Treatise on the Stability of a Given State of Motion, London: Macmillan & Co., 1877.

[26] Vyshnegradsky, I.A., On Controllers of Direct Action, Izv. SPB Tekhnolog. Inst., 1877

[27] F.L. Lewis, Applied Optimal Control and Estimation, Chapter 1: Introduction to modern control theory, Prentice-Hall, 1992.

[28] Whitehead, A.N., Science and the Modern World, Lowell Lectures (1925), New York: Macmillan, 1953

[29] Bertalanffy, L. von, A quantitative theory of organic growth, *Human Biology*, 10, (1938), 181-213.

[30] Odobleja, Ș., Psychologie consonantiste, Tome I-II, Editions Maloine, Paris, 1938.

[31] Wiener, N., Cybernetics: or Control and Communication in the Animal and the Machine, Cambridge: MIT Press, 1948.

[32] Heylighen, F., Joslyn, C. Principia Cybernetica Web, http://pespmc1.vub.ac.be/ CYBSYSTH. html, 1992.

[33] Bruntland Commission Report, Our common future, Oxford University Press, 1987.

[34] Woinaroschy, A., A paradigm-based evolution of chemical engineering, *Chinese Journal of Chemical Engineering*, 24, (2016), 553–557.

[35] Hoa, P., Mogos-Kirner,M., Cristea, M., Csavdari,A., Agachi, P.,S., Simulation of Jijia River Catchment using Efficient Full Dynamic and Diffusive Wave Model,The 8th International Conference on Environmental Engineering and Management - ICEEM/08, Iasi, Romania, 9-12 September 2015.

[36] Ani E., C., Cristea V.,M., Agachi, P.,S., Process engineering tools to reduce river in-stream pollution, Science Direct, *Chemical Engineering Transactions*, (2011), 1075-1080.

[37] Ani E., C., Cristea V., M., Agachi, P.,S., Factors Influencing Pollutant Transport in Rivers. Fickian Approach Applied to the Somes River, *Revista de Chimie*, 66(9), (2015), 1495 – 1503.

[38] Nagy,Z., Agachi,S., Model Predictive Control of a PVC Batch Reactor, *Computers &Chemical Engineering,* 6, (1997), 571-591.

[39] Charpentier, J., C., Among the trends for a modern chemical engineering: CAPE an efficient tool for process intensification and product design and engineering, Plenary lecture, ESCAPE 17, Bucharest, 27-30 May, 2007.

GENERAL STRATEGIES IN PRODUCT ENGINEERING

Alexandru WOINAROSCHY[1,2*]

[1]University Politehnica of Bucharest, Faculty of Applied Chemistry and Material Sciences, Department of Chemical and Biochemical Engineering, 1-7 Polizu street, 011061Bucharest, Romania

[2]Academy of Technical Sciences of Romania

Abstract
The diversity of industrial products has a huge growth, and correspondingly, very strong market fights have evolved between producer companies. Product engineering paradigm was imposed by the fight for technical and economical product performances generated by a strong competitive market environment. Two general strategies for design of chemical homogeneous products are presented: a concise strategy and an extended strategy. The two general strategies present similarities, but there are some meaningful differences.

Key Words: product engineering, design strategy, homogeneous product

1. Introduction

The diversity of industrial products (in many cases with close properties and with the same utilization) has a huge growth, and correspondingly, very strong market fights have evolved between producer companies. This raises questions about which products and what properties should have these products in order to win over the market. Product engineering paradigm was imposed by the fight for technical and economical product performances generated by a strong competitive market environment.

Nowadays, it is far more important what and how much is sold, than what and how much is produced [1]. Until recently, the main purpose of chemical engineering has been to obtain the lowest cost process. In contrast, chemical product design tries to obtain the most added values for a product through enhanced product properties. This is a more complex task than a mathematical treatment to maximize profit, because the profit depends in some unidentified way upon the complex set of product properties. Due to this, product engineering problems can't be solved by traditional chemical engineering approaches, there are necessary the new tools [2, 3].

Up to present two strategies for the design of chemical homogeneous products were developed:

- concise strategy;

*Corresponding author: E-mail address: a_woinaroschy@chim.upb.ro

- extended strategy.

2. Concise strategy for the design of chemical homogeneous products

This strategy consists in three steps presented in Figure 1.

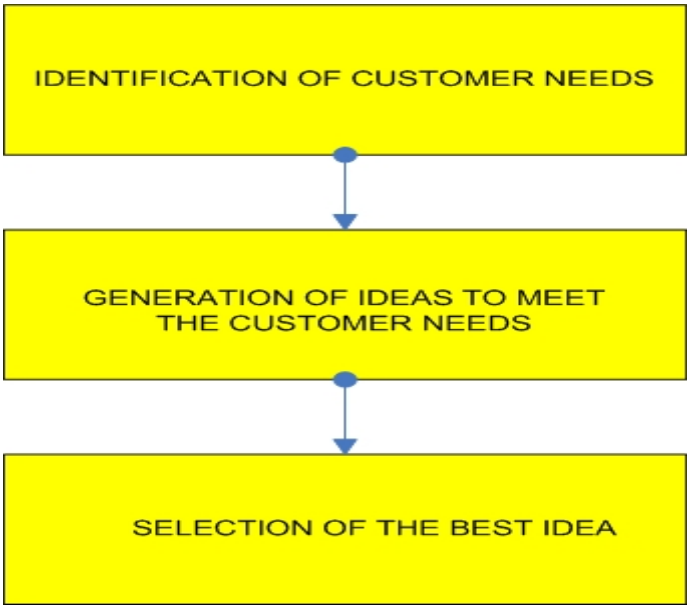

Fig.1. The steps of concise strategy for the design of chemical homogeneous products

The first step, identification of customer needs, consist mainly in:
- customers interviewing;
- identification of expressed requirements;
- translation of requirements into product specifications.

The primary source in identification of customer requirements are the final product users, respectively the beneficiaries of the chemical product properties. It is desired not to be individuals, rather organizations, including government agencies. Particularly important are so-called vanguard users, which express requirements in advance with the market: they often invent small product improvements and, usually, they clearly indicate undesired features of the existing products.

The second step, generation of ideas to meet the customer needs, implies:
- initial ideas generation;
- filtering of ideas;
- ideas screening.

For the initial ideas generation, the primary sources are: product development team, potential customers, literature and patent searches in similar or related areas, product experts, private inventors, consultants, synthesizing tangent

compounds using methods such combinatorial chemistry, computer aided molecular design (CAMD [4]), etc.

It should be investigated around 100 ideas generated as free and as unrestricted. Ideas generation are based on adjustment or innovation. Adjustment consists in problems solving by existing technologies or by close to these whilst innovation consists in problems solving by the use of new information. In Figure 2 is presented the choosing between innovation and adjustment, respectively the emphasize between technology and market for several big companies [1].

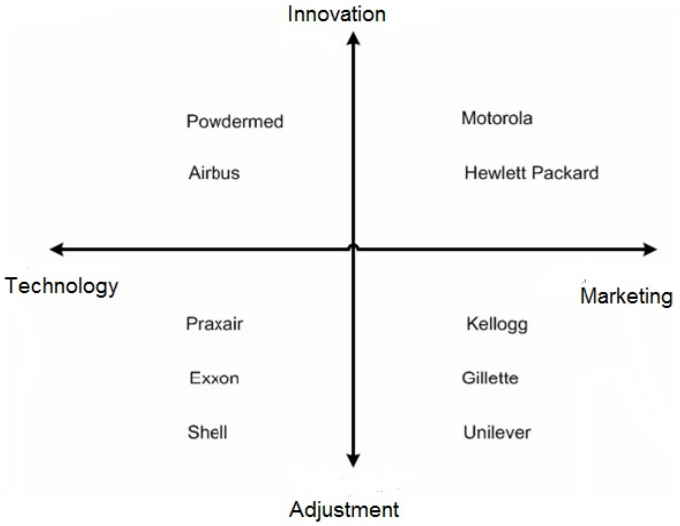

Fig.2. Innovation vs. adjustment and technology vs. marketing for several big companies

The filtering of ideas implies the elimination of redundant ideas, and also of the eccentric ideas (even with the risk that they contain innovator germs). After these eliminations will remain about 20 ideas deserve to be considered further.

In ideas screening for each idea j with the weight ω_j and its attribute i is given the score $s_{i,j}$. The overall score S_j of the idea j is the sum of the products $s_{i,j}$ ω_i :

$$S_j = \sum_i s_{i,j}\,\omega_i \tag{1}$$

Frequently, used attributes are:
(1) Scientific maturity;
(2) Facilities-based engineering;
(3) Minimum risk;
(4) The low cost;
(5) Safety;
(6) Environmental impacts.

At the end of screening will remain about 5 ideas deserve to be considered further.

In the last step of the concise strategy, selection of the best idea, there are used technical or subjective criteria. The subjectivities is decreased by the use of selection matrices based on the next three key issues: the used criteria must be independent; must be avoided the redundancy, and must be formulated a complete list of criteria.

3. Extended strategy for the design of chemical homogeneous products

This strategy consists in three steps presented in Figure 3.

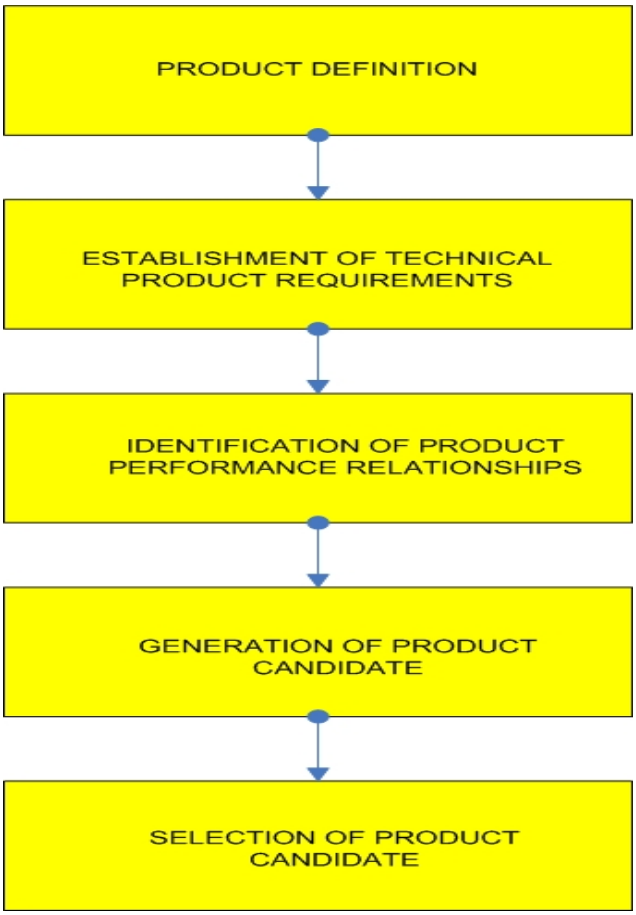

Fig.3. The steps of extended strategy for the design of chemical homogeneous products

In the first step, product definition, the analysis of customer needs will lead to a specification of technical product targets. There are investigated the current products, if any, in the marketplace — price, composition, the specific function of any components, strengths and weaknesses (from both a customer/consumer and a supplier perspective), any hidden costs, and total market size. Even if there is no

product just like an intended product currently in the market, there may be other kinds of products indirectly fulfilling the same end function.

For the second step, establishment of technical product requirements, should be considered the implications each mechanism will this have on the physical properties of the product. Where there are multiple properties that must be met simultaneously, it may be assumed that the complete required property set can be decomposed into subsets of properties which can be achieved separately through their own components. This will allow the complete property set to be achieved by combining all components. It is useful to consider if there are classes of compounds that can provide some of the required properties which they were present as components, as well as any classes of compounds that would be inappropriate in the new product.

In the third step, identification of the product performance relationships, for each property subset, the understanding of the underlying chemical engineering phenomena can be used to derive a set of equations that can predict the relevant behavior as a function of composition. While simplifying assumptions may be made, one must be careful not to oversimplify, verifying qualitatively that the models will be useful for predicting the relevant behavior. All physical parameters that will be needed to apply the model with any candidate compound should be listed. In the absence of direct experimental data, one must decide how the needed physical parameters will be obtained (e.g. tabulated data, appropriate correlations, group contribution methods, etc.).

In the fourth step, based on an understanding of the underlying chemistry, for each property subset a list of potential candidates as large as is possible should be generated. This list may be done by computer generation of alternatives, or by searching through tabulated databases. Using the various product property models, and any other relevant factors, each list may be culled by eliminating candidates that are inappropriate.

At the last step, step 5 - selection of product candidate, for each property subset overall performance may be defined by assigning a weighting factor to each property in the set. Raw material costs for compounds that simultaneously meet all the important criteria within that property subset should be obtained, and using the property models and weighting factors all remaining candidates should be ranked for their raw material costs on an equal overall performance basis. Any compounds that are less expensive than those used in current products on an equal overall performance basis, including hidden costs, may then be identified. Assuming that the complete required property set can be achieved by combining the components for each property subset, an overall composition to recommend for experimental study may now be identified.

4. Subsequent stages of both strategies

There are necessary for both strategies several subsequent stages [2]: risk assessment and financial analysis which imply a process predesign. This stages are not discussed here.

5. The design of chemical structured products

Structured products achieve their properties through a microstructure that is determined by the interaction of its components and the manufacturing process [5]. Product engineering for structured products is particularly difficult, as the product and process must be designed simultaneously. In absence of a current general strategy for the design of chemical structured products, two primary approaches are possible [2]:

(1) generation and systematic reduction of the number of alternative through heuristics;

(2) optimization of the set of all potential alternatives through mathematical programming.

6. Conclusions

Both presented strategies are useful tools in product engineering, but sometimes the complexity of the tasks impose supplementary procedures. The concise strategy is practical and oriented to the customer. The extended strategy is more elaborate and promote innovation, especially due to the identification of product performance relationships. The product designed by these procedures can be the starting point for mathematical optimization. Since the product that offers maximum performance regardless of costs is unlikely to be the product that offers maximum profitability, there is value in simultaneously simulating and optimizing the effects of product performance, consumer response, and microeconomics.

REFERENCES

[1] Cussler, E. L., Moggridge, G. D., 2011, *Chemical product design*, 2nd ed. Cambridge University Press, New York.
[2] Hill, M., Chemical Product Engineering-The third paradigm, *Computers & Chemical Engineering*, 33 (5), (2009) 947-953.
[3] Woinaroschy, A., Raiciu, A.D., 2015, Elemente de inginerie de produs, Ed. AGIR, Bucuresti.
[4] Gani, R., 2010, *Solvent Selection through ICAS-ProCAMD*, Tutorial document, CAPEC, Technical University of Denmark.
[5] Edwards, M. F., *Product Engineering: Some Challenges for Chemical Engineers*, *Transaction IChemE*, 84, part A, (2006), 255 – 260.

PERVAPORATION OF AQUEOUS ETHANOL SOLUTIONS THROUGH PURE AND COMPOSITE CELLULOSE/BIOCELLULOSE MEMBRANES

Ali Al JANABI*, Al Sakini Ahmed HAMEED, Tanase DOBRE

University Politehnica of Bucharest, Faculty of Applied Chemistry and Material Sciences, Department of Chemical and Biochemical Engineering, 1-7 Gh. Polizu street, 0110661, Bucharest, Romania

Abstract.
The pervaporation performance in terms of total permeate flux, separation factor with respect to the separation of ethanol/water was assessed for composite membranes based on composite cellulose, obtained from solutions containing dissolved cellulose in NaOH - thiourea solutions, biocellulose and tetraethyl orthosilicate (TEOS). The phase inversion method was employed for membrane preparation using cellulose/bio cellulose/TEOS solution. The casting solution was spread as a thin film on to a glass plate (for non-supported membranes) or on a paper support (for supported membranes) and then exposed to ambient air for 24 h. NaOH and thiourea were removed from the film by treating with 1M HCl solution and rinsing with distilled water to a neutral pH. The rinsed membrane was kept in distilled water for 24 h and further dried at room temperature. Three content of biocellulose, 0% ,10% and 30%, with different operation temperature has been used in experiment. Pervaporation performances, which were evaluated in terms of total permeate flux and pervaporation separation factor, strongly depended on membrane biocellulose content, on ethanol concentration and operation temperature. The experiment showed that the flux increases with decreasing the ethanol content and with increasing the operation temperature.

Key words: alcohols dehydration, cellulose membrane, biocellulose membrane, permeate flux, pervaporation, separation factor

1. Introduction

The following four process, namely liquid- liquid extraction, extractive distillation, chemical adsorption and azeotrope distillation, are used in separation of mixtures containing organic compounds and water. The disadvantages of these techniques are represented by demand of external entrainer, extensive amount of energy and downstream processing to recover key component [1]. In the last year's pervaporation is considered a promising process for dehydration of solvent [2, 3]. The process was already mentioned in the early of the 20th century; first major research efforts were made by Binning et al. beginning with 1950 year at the American Oil Company [4]. Pervaporation (PV) is an emerging membrane separation technology with the merit of low operating costs. The disadvantages of

* Corresponding author: Email address: alialjanabi35@yahoo.com

the pervaporation are the high capital cost and the low maximal capacity [5]. In PV process, the feed liquid mixture is placed in contact with one side of non-pours membrane and one of these liquids is removed as permeate from other side as vapor at low-pressure [6, 7]. In recent decades, the world's present economy is highly dependent on various sources of fossil energy production such as, coal, natural gas, oil etc. but these sources are non-renewable [8]. Ethanol is one of the most renewable promising future fuels due to its simplicity of production process, high energy value and environmentally friendly comportment.
The ethanol derived from fermentation has received a wide popularity as a fuel [9, 8, 10]. Pervaporation is one of the good processes that are used to reduce the effect of product inhibition and improve the sugar utilization and solvent productivity in fermentation process [11]. Repeat units characterizing the structure of some pure membranes widely employed for pervaporation of organics (hydrophobic membranes) or water (hydrophilic membranes) from organics-water mixture, especially from ethanol-water system, are shown in figure 1 [12].

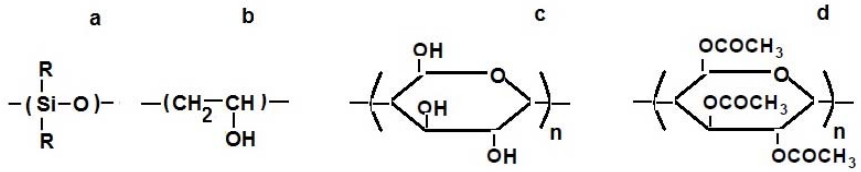

Fig. 1. Repeating units in membranes for processing water-ethanol system (a- polydialkylsiloxane (hydrophobic), b- polyvinyl alcohol (hydrophilic), c- cellulose (hydrophilic), d- cellulose triacetate (hydrophilic))

Cellulose is called biocellulose (BC) when it is obtained by mean of some bacteria through biosynthesis, using glucose as substrate. The most efficient producer of bacterial cellulose is *Acetobacter xylinum* (or *Gluconacetobacter xylinus*), a gram-negative strain of acetic-acid-producing bacteria [13, 14]. The BC can be used with many polymers as composite membrane due to its good mechanical properties, high water absorption capacity, very low porosity, high adsorption capacity for some compounds, stability; properties due to a highly crystalline material structure [15].
Composite organic-inorganic membranes based on TEOS ($Si(OCH_2CH_3)_4$), as an inorganic precursor, have been widely applied to separate aqueous-organic systems [16, 17]. In synthesis of these membranes the silanol groups (–Si–OH), obtained by TEOS hydrolysis, give siloxane bonds (–Si–O–Si–) by dehydration reaction with other silanol groups or dealcoholizes reaction with ethoxy group (–Si–O–CH_2CH_3). For cellulose membranes, siloxane structures are dispersed among cellulose chains resulting in a more open network of hybrid membrane, *i.e.*, exhibiting a larger free-volume [12].

This work has aimed at preparing and characterizing cellulose based hybrid membranes with biocellulose as well as at their testing for pervaporation separation of ethanol-water system. The effect of, ethanol concentration and operation temperature on pervaporation performances, expressed as total permeate flux, separation factor was evaluated.

2. Experimental

Materials

Cotton cellulose powder (50 μm diameter, 0.600 g/cm^3 density), tetraethyl orthosilicate (TEOS) min 98 % as well as crystals of urea ($C_2H_4N_2O$) and thiourea ($C_2H_4N_2S$) were supplied by Sigma-Aldrich Chemie (Germany). NaOH pellets were purchased from Merck (Germany). All reagents were used without further purification. A porous paper support was used to prepare supported pure and composite membranes

Casting solution preparation

For the synthesis of pure cellulose membranes, a casting solution was prepared according to the following procedure: (i) an alkaline solution containing 9 wt. % NaOH and 5 wt. % urea/thiourea was selected as solvent for cellulose; (ii) cellulose powder (CE) was added to the alkaline solution forming a slurry with 8.5 wt. % cellulose, (iii) never dried biocellulose fibres (BC) were added to the solution at 3 values (0 %, 10 %, 30 %) expresses as BC mass percentage relative to total mass of cellulose, which was stirred for 3 hours at a temperature up to 30°C; (iv) the stirred slurry was frozen at about -18 °C for minimum 24 h; (v) the frozen solution was thawed at room temperature and a hydrogel (casting solution) was obtained. For the synthesis of composite cellulose membranes, the casting solution prepared conforming to (i)-(iv) steps was mixed for 10 min with TEOS with 10% mass relative to CE.

Membrane preparation

Supported and non-supported composite/cellulose membranes were synthesized by the phase-inversion method, as follows: (i) the casting solution with/without BC was spread as a thin film onto a glass plate (for non-supported membranes) or a paper support (for supported membranes) and then exposed to ambient air for 24 h; (ii) NaOH and urea/thiourea were removed from the film by treating with 1M HCl solution and rinsing with distilled water to a neutral pH; (iii) the rinsed membrane was kept in distilled water for 24 h and further dried at room temperature.

Optical microscopy (OM) analysis

Casting solutions with/without BC were analysed by means of IOR ML-4M optical microscope (IOR, Romania) in order to observe in these the quality of dissolved cellulose and the distribution of BC fibrils.

Pervaporation tests

Pervaporation experiments were carried out in a batch stirred cell operated under vacuum. The supported membrane was put on a sintered steel disk, 5 μm average pore diameter, welded to the top of the lower compartment. The upper compartment containing the feed ethanol-water mixture was closed in order to stop any loss from feed. Before starting an experiment, the membrane was equilibrated for 30 minutes with a liquid mixture of the same composition as that of the feed. The swollen membrane was then placed in the pervaporation device and the feed liquid was charged to the upper compartment, wherein a magnetic stirring was used to mix the ethanol-water solution. This stirring aimed at minimizing the mass transfer resistance between the feed liquid and membrane. A vacuum of 100 mbar was applied to the lower compartment by means of a vacuum pump (Sartorius, Japan) and the permeate was collected in an ice trap.

The liquid temperature in the feed compartment and the system mass were measured before starting (t_i , m_i) and after finishing (t_f , m_f) an experiment. Total pervaporation flux, j_p, was estimated using Eq. (1), where m is the mass of the permeate collected during the pervaporation time, $\Delta\tau$, and A the effective membrane area.

$$j_p = \frac{m}{A\Delta\tau} = \frac{m_i - m_f}{A\Delta\tau} \tag{1}$$

Ethanol concentrations in the permeate and feed samples were estimated using an Atago Abbe refractometer (Atago, Japan). Separation factor relative to water and ethanol, $\alpha_{w/eth}$, was calculated with Eq. (2), where X and Y represent the mass fractions of species in the feed and permeate, respectively.

$$\alpha_{w/eth} = \frac{\left(Y_w / Y_{eth}\right)}{\left(X_w / X_{eth}\right)} \tag{2}$$

3. Results and discussions

Optical microscopy images of casting solutions with and without biocellulose, shown in figure 2, indicates the appearance of a basic uniformed structure with some local agglomeration of dissolved cellulose (figure 2a) in which the biocellulose fibrils are orderly distributed (figure 2b and 2c). It can be appreciated that the membrane will result from these type solutions will have a homogenous structure.

The pervaporation experimental measurements are performed in term of total permeate flux j_p, and separation factor $\alpha_{w/eth}$. For that in pervaportion experiments

has been used 7 values of water content in feed (c_w in 17.2-80.6 % range), 3 values of biocellulose mass content in swelled membrane (c_{BC} in 0-30% range), and three values of operation temperature (t in 25-45 °C range). The results, presented in figure 3, show an increase in total permeate flux with all process operational parameters (process factors). Increasing water content in the feed increases the permeate flux due to increase the swelling of membrane and this give more flexibility of membrane chains. On the other hand, the permeate flux getting bigger with temperature due to increase the mobility of the chain molecules of membrane. This phenomenon led to increase the diffusion of components inside of gel membrane.

Fig 2. Optical microscope images of casting solutions with and without BC at 100x magnification: a - without BC, b- 10 % BC, c- 30 % BC;

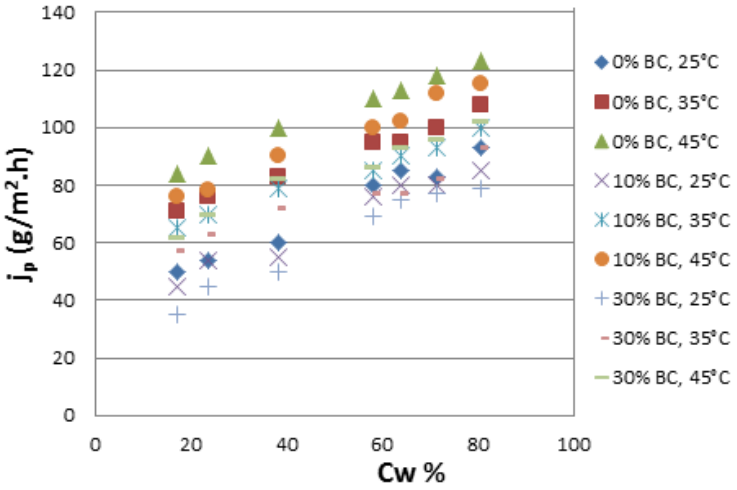

Fig. 3. Effect of water mass percentage in the feed (C_w) on pervaporation flux (j_p) for CE-TEOS-BC membrane

As shown in figure 3, the separation factor, $\alpha_{w/eth}$, is strongly dependent on c_w and c_{BC}. From figure 3 one can observe that $\alpha_{w/eth}$ for pure cellulose membrane drops from (11.9-13.5) to (4.5-5.1), for 10% BC membrane from (12 -13) to (4.3-5), where for 30% BC membrane from (13.8 -14) to (4.8-5.8). Accordingly, to these data $\alpha_{w/eth}$ decreases with increasing of c_w and decreasing the BC percentage.

This behaviour of composite cellulose membrane suggested that membrane is strongly hydrophilic due to the high hydrophilicity of biocellulose. An enhancement of membrane swelling by an increase in c_w, which has negative influence on separation factor and this swelling allows some of ethanol molecules to diffuse through the membrane with water molecules.

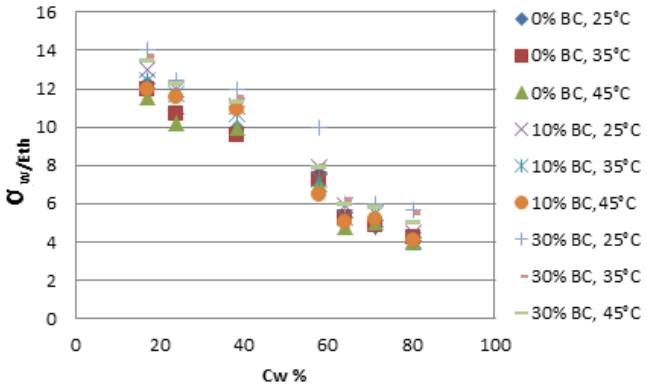

Fig. 4. Effect of water mass percentage in the feed, c_w, on separation factor, $\alpha_{w/eth}$, for CE-TEOS-BC membrane

The data from figures 3 and 4 can be used to obtain the relations describing the dependency of pervaporation flux and separation factor upon process factors (water content of the feed, c_w, biocelluose concentration in the membrane, c_{BC}, and temperature, t) by these using in completing of one factorial experimental plan type 2^3[18]. The dimensionless factor values in Table 1 were computed as it is shown by relationships (3). They serve in rapid determination of characteristic coefficients of regression relationship for 2^3 factorial plan that connects the response process with process factors [18].

Table 1

Matrix of factors influence on pervaporation flux and separation factor for CE-TEOS-BC composite membranes (c_{wc}= 0.5, Δc_{wc}=0.3, c_{BCc}=0.15, Δc_{BC}=0.15, t_c=35, Δt = 10)

No. exp.	c_w kg w/kg m	c_{BC} kg BC/kg CE	t ^{0}C	X_1	X_2	X_3	j_p g/(m^{2}h)	$\alpha_{w/eth}$
1	0.2	0	25	-1	-1	-1	51	12.3
2	0.2	0	45	-1	-1	+1	85	11.5
3	0.2	0.3	25	-1	+1	-1	38	14.1
4	0.2	0.3	45	-1	+1	+1	62	13.8
5	0.8	0	25	+1	-1	-1	93	4.2
6	0.8	0	45	+1	-1	+1	125	3.9
7	0.8	0.3	25	+1	+1	-1	77	5.7
8	0.8	0.3	45	+1	+1	+1	105	5.1
9	0.5	0.15	35	0	0	0	77	4.95
10	0.5	0.15	35	0	0	0	78	4.85
11	0.5	0.15	35	0	0	0	77.5	5.05

$$X_1 = \frac{c_w - c_{wc}}{\Delta c_w}, X_2 = \frac{c_{BC} - c_{BCc}}{\Delta c_{CB}}, X_3 = \frac{t - t_c}{\Delta t} \quad (3)$$

The processing of data from table 1 for obtaining the j_p and $\alpha_{w/eth}$ as functions of c_w, c_{BC} and t goes to relationships (4) and (5). They quantitatively argue all comments above given refering to figures 3 and 4. Except the X_2X_3 interaction, that slowly affects the total pervaporation flux, no other interaction between factors are important in determining j_p and $\alpha_{w/eth}$. It is noteworthy that the linear influences of water concentration in processed mixture (X_1 as dimensionless expression), BC membrane concentration (X_2 as dimensionless expression) and temperature (X_3 as dimensionless expression) are in opposition inside of relations for j_p and $\alpha_{w/eth}$. In other words, if a highly selective membrane is wanted then it will operate with low pervaporation flux.

$$j_p = 79.5 + 20.5X_1 - 9X_2 + 14.75X_3 - 1.75X_2X_3 \quad (4)$$

$$\alpha_{w/et} = 8.825 - 4.1X_1 + 0.85X_2 - 0.25X_3 \quad (5)$$

6. Conclusions

Cellulose membrane was prepared by phase inversion process and tested in pervaporation of water-ethanol mixtures. Composite membranes were obtained on a casting solution by adding biocellulose and TEOS. Total flux j_p and separation factor $\alpha_{w/eth}$, were studied with different operational parameters (mass content of water in feed, c_w= 17.2-80.8%), biocelluose mass loading, c_{BC}= 0-30%, TEOS mass content 10%, operation temperature, t = 25-45 ^{0}C). Experimental results showed an increase in permeate flux j_p of 10 and 30 % bicelluose with all operational parameter, moreover decrease of $\alpha_{w/eth}$ with increasing water content and operational temperature. Analytical expressions for j_p and $\alpha_{w/eth}$ upon pervaporation process factors has been established. The experimental results show that these composite membranes are hydrophilic membrane.

REFERENCES

[1] Khans, M., Usman, M., Guii, N., Butt, M.T.Z., Jamil, T., An overview on pervaporation and advanced separation technique, *Journal of Quality and Technology Management*, Vol. IX, Issue I, (2013), 155 – 161.

[2] Shao, P., Huangr, Y.M., Polymeric membrane pervaporation, *Journal of Membrane Science* 287, (2007), 162–179.

[3] Chengyun, G., Minhua, Zh., Jianwu, D., Fusheng, P., Zhongyi, J., Yifan, Li, Jing, Zh., Pervaporation dehydration of ethanol by hyaluronic acid/sodium alginate two-active-layer composite membranes, *Carbohydrate Polymers*, 90, (2014), 158-165.

[4] Valentínyi Nóra, Mizsey, P., Models with simulation of hybrid separation processes, *Chemical Engineering*, 58, (2014), 17-14.
[5] Szitkai, Z., Lelkes, Z., Rev, E., Fonyo, Z., Optimization of hybrid ethanol dehydration systems, *Chemical Engineering and Processing,* 41, (2002), 631– 646.
[6] Ahmad, S. A., Lone, S. R., Hybrid Process (Pervaporation -Distillation): A Review, *International Journal of Scientific & Engineering Research*, 3(5), (2012), 56-67.
[7] Chang, J.H., Yoo, J.K., Ahn, S.H., Lee, K.H., Ko, Su Mo., Simulation of pervaporation process for ethanol dehydration by using pilot test results, *Korean J. Chem. Eng*., 15(1), (1998), 28-36.
[8] Sadati, S.M., Ghasemzadeh, K., Jafarharasi, N., Vousoughi, P., An overview on the bioethanol production using membrane technologies, *International Journal of Membrane Science and Technology*, 1, (2014), 9-22.
[9] Samnuknit, W., Boontawan, A., Extractive fermentation of ethanol using vacuum fractionation technique, *International Journal of Chemical, Nuclear, Materials and Metallurgical Engineering*, 8(9), (2014), 456-464.
[10] Bai, F.W., Anderson, W. A., Moo-Young, M., Ethanol fermentation technologies from sugar and starch feedstocks, *Biotechnology Advances*, 26, (2008), 89–105.
[11] Liu, G., Wei, W., Wu, H., Dong, X., Jiang, M., Jin, W., Pervaporation performance of PDMS/ceramic composite membrane in acetone butanol ethanol (ABE) fermentation–PV coupled process, *Journal of Membrane Science*, 373, (2011), 121–129.
[12] AlJanabi, Ali A., Parvulescu, Oana Cristina, Dobre, T., Ion, Violeta Alexandra, Pervaporation of aqueous ethanol solutions through pure and composite cellulose membranes, *Rev Chim* (Bucharest), 67(1), (2016), 150-156.
[13] Chen, P., Cho, S. Y., Jin, H. J., Modification and applications of bacterial celluloses in polymer science, *Macromolecular Research,* 18(4), (2010), 309-320.
[14] Evans, Barbara, O'Neill, H. M., Malyvanh, Valerie, Lee, I., Woodward J., Palladium-bacterial cellulose membranes for fuel cells, *Biosensors and Bioelectronics,* 18, (2003), 917- 923.
[15] Yaoa, W., Wu, X., Zhu, J., Sun, B., Zhang, K., Miller, C., Bacterial cellulose membrane – A new support carrier for yeast immobilization for ethanol fermentation, *Process Biochemistry*, 46, (2011), 2054-2058.
[16] Kittur, A. A., Jeevankumar, B. K., Kariduraganovar, M.Y., Dehydration of ethanol/water with cellulose composite membranes*, Int. J. Current Eng. Technol*., 1, (2013), 148-154.
[17] Uragami, T., Wakita, D., Miyata, T., Dehydration of an azeotrope of ethanol/water by sodium carboxymethylcellulose membranes cross-linked with organic or inorganic cross-linker eXPRESS, *Polymer Letters*, 4(11), (2010), 681-691.
[18] Dobre, T., Sanchez, J.M., *Chemical Engineering-Modelling Simulation and Similitude, Chapter 5*, Wiley VCH, 2007

CONDUCTIVITY CELL CONSTANT REVISITED

Ioana-Alina CIOBOTARU*, Florin Mihai BENGA, Oana Claudia BARBU, George Costin LAZAR, Claudiu CAMPUREANU, Traian RUS and Danut-Ionel VAIREANU

University Politehnica of Bucharest, Faculty of Applied Chemistry and Materials Science, Depart. of Inorganic Chemistry, Physical Chemistry and Electrochemistry,

Abstract.
This paper discusses various problems associated with the determination/calibration of the conductivity cell constant, encountered during the practical evaluation of conductivity in liquids, and attempt to present some conventional and non-conventional solutions (some of them based on novel conductivity probe constructive solutions, which allow an easy modification of the probe configuration and hence the variation of the cell constant) to solve these problems. A procedure for manual temperature compensation, as well as one for replatinising the cell electrodes are also presented.

Key words: conductivity, cell constant, manual temperature compensation, calibration

1. Introduction

The electric current is carried out in solutions, conducting polymer or in certain solid material (e.g. SOFC) by ions and hence the process is called ionic conduction. The electrical conductance, *G* and the specific conductivity, also known as electrolytic conductivity or simpler, the conductivity, λ, are a measure of the ability of a solution subjected to an electric field to conduct an electrical current in the above said materials [1-10]. If a substance has a high electrical conductance *G*, the corresponding electrical or ohmic resistance *R* is low and *vice versa* so that the electrical conductance is given, by definition, by the reciprocal of the resistance:

$$G = \frac{1}{R} \qquad (1)$$

The unit of measure for *G* is called Siemens, S or Ω^{-1}.

However, the specific conductivity, λ, (the reciprocal of the electrical resistivity, ρ), the molar conductivity, Λ_m, and the equivalent conductivity, Λ_e are preferred as they carry more information related to the measured species comparing to the conductance. Notations as σ and κ are also used to designate the specific conductivity [4-7], [9-14]. In order to avoid any confusions between the

* Corresponding author: ioanaalinaciobotaru@yahoo.com

conductivity and the cell constant, K_{cell}, for the purpose of this paper, the notation λ shall be used for the specific conductivity, sometimes shortened as conductivity. Although these terms are also present in electronic conductors such as metals, alloys, graphite, semiconductors, the subject of this paper shall be restricted to the electrolytic conductivity (ionic conduction mechanisms).

The determination of specific conductivity is particularly important when one evaluates not only the conduction of liquids, but also the ionic conduction of conductive polymers or ion exchange membranes [11-17].

Conductivity units

There is still some ambiguity when one attaches the units for the conductivity. *Specific conductivity*, by definition, is the conduction capacity of a volume of 1 m^3 of an electrolyte solution when subjected to a potential gradient equal to 1 volt/m and is measured $S \cdot m^{-1}$ or $\Omega^{-1} \cdot m^{-1}$

$$\lambda = \frac{1}{\rho} \tag{2}$$

where ρ is the resistivity. Accepted units are also $S \cdot cm^{-1}$ or $\Omega^{-1} \cdot cm^{-1}$. This duality comes from the fact that in 1971 the unit S, siemens, named after Werner von Siemens, was adopted by the General Conference on Weights and Measures as an SI derived unit and hence the unit for the specific conductivity evolved into $S \cdot m^{-1}$. In USA, it is still accepted the use of $mho \cdot cm^{-1}$, the designatory letters *mho* representing *ohm* spelled backwards and being equal from the mathematical point of view to the reciprocal of that [3], [8].

Molar conductivity is the conductivity of an electrolyte solution normalised with respect to its molar concentration, and hence the unit, $\Omega^{-1} \cdot m^2 \cdot mol^{-1}$ or $S \cdot m^2 \cdot mol^{-1}$, while the *equivalent conductivity* is the conductivity of an electrolyte solution normalised with respect to its equivalent concentration, the unit being $\Omega^{-1} \cdot cm^2 \cdot Eg^{-1}$ or $S \cdot cm^2 \cdot Eg^{-1}$:

$$\Lambda = \frac{\lambda}{c} = \lambda v \tag{3}$$

$$\Lambda_e = \frac{\lambda}{cz} = \frac{\lambda v}{z} \tag{4}$$

2. Experimental

Reagents

All the reagents used were p.a. grade supplied by Sigma-Aldrich, Chempar Ltd and ChimReactiv SRL.

Apparatus and procedure

A series of conductivity meters of diverse range and feature, analogue and digital, with and without automatic temperature compensation such of CyberScan PCD 6500, Phywe Cobra 3 Chem-Unit, Radelkis OK102/1 App-Chem 470, Hanna Instruments 4 were used in conjunction with two, three and four electrode cells. The analogue instruments were also connected to a PicoLog ADC100 computer controlled data acquisition system.

3. Results and discussions

Considerations regarding the conductivity cell constant

Taking into account that the conductivity is the reciprocal of resistivity, one may write a relationship between the resistance and the conductivity:

$$R = \frac{1}{\lambda}\frac{l}{S} = \frac{K_{cell}}{\lambda} \qquad (5)$$

where l is the distance between electrodes and S is the surface area. The ratio

$$K_{cell} = \frac{l}{S},$$

a specific property of the measuring conductivity cell, is called the *cell constant,* and is measured in m^{-1} or cm^{-1}. It should be pointed out that the above relationship, calculated as the ratio of the distance between the electrodes and the electrodes common surface represents the geometrical cell constant and that differs from the real cell constant which is determined experimentally.

Moreover, as there are an increased number of cell designs with a combination of 2, 3 or 4 electrodes, it is almost impossible to determine the real cell constant from its physical dimensions, as the current distribution between these electrode combinations varies greatly. To make things even more difficult, as the practical conductivities vary over six orders of magnitude, from $\mu S \cdot cm^{-1}$ to $S \cdot cm^{-1}$, it is very difficult to use only one cell constant to cover the entire field (e.g. a conductivity cell having K_{cell}=1cm^{-1} may be used for low to relatively high values of conductivity), high conductivity values requiring high cell constants, while low conductivity values require low cell constants, the range of cell constants varying between 0.01 cm^{-1} and 50 cm^{-1} [3].

To overcome this shortcoming, one may use multiple conductivity cells having different cell constants (a high cost option). Another option is to electronically modify the cell constant, obtaining full accuracy over a greater conductivity range using a single conductivity cell [3], but this also increases the investment cost requiring an expensive equipment. Nevertheless, similar results may be achieved using a conductivity cell with a physical adjustable cell constant,

where the cell constant can be changed either by changing the electrodes distance or by changing the electrodes surface [3, 8, 18, 19]. In figures 1 and 2 are represented the main elements of such a cell, where in-between the two platinised platinum electrodes one inserts PTFE templates of different thicknesses and different patterns. By changing the templates, one can easily change the distance between the electrodes and the electrode surface as only the electrode area equivalent with the area of the cut channel will be exposed to the solution.

The feature of this conductivity cell is that one achieves a wide range of cell constants (between 0.5 and 15 cm^{-1}) without the need of electronic compensation, these configurations allowing an extra degree of freedom to modify the hydrodynamic range, should one need to use the cell as a flow-through cell.

The construction of this type of conductivity cell consists of a "sandwich" of two platinised platinum half-cells, inserted into PERSPEX layers, and various interchangeable PTFE templates which have rectangular channels cut, so that a wide range of configurations can be covered (see figure 1 and figure 2). The templates have various thicknesses to provide a controlled variable distance between the electrodes when the templates are inserted between the half-cells.

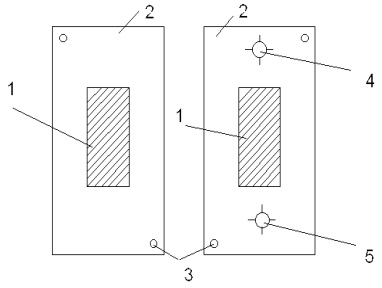

Fig. 1. Platinised platinum half-cells. 1. Platinised platinum electrodes; 2. PERSPEX supports 3. Alignment holes and pins; 4. Fluid inlet; 5. Fluid outlet

The novel variable cell constant conductivity cell presented in this paper consists of two platinised platinum electrodes, 1, (see figure 3), of a geometric surface area S, of 1 cm^2, positioned in a PODEC (parallel opposed dual electrode cell) configuration, at a distance, l, adjustable (between 1.34 mm and 24.59 mm, measured with a Mitutoyo digital micrometer of 0.001 mm resolution). By twisting the micrometer screw, one may now increase or decrease the electrodes distance and hence may adjust the conductivity cell at will. Unlike the configurations presented in figure 1 and 2, which can be used only in conjunction with a flow injection analysis system, this novel cell may also be used in more traditional experiments involving all sorts of shapes and sizes of chemical glassware.

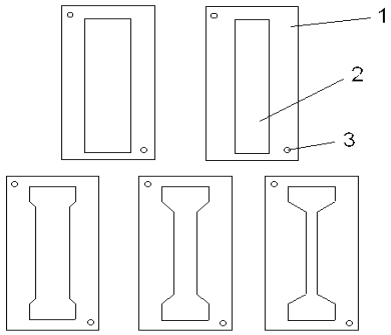

Fig. 2. PTFE templates. 1. PTFE; 2. Channel 3. Alignment holes

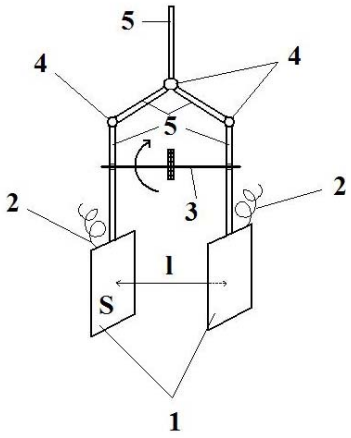

Fig. 3. Variable constant conductivity cell. 1. Platinised platinum electrodes 2. Electrical connecting wires 3. Micrometric screw 4. Articulated joints 5. Insulating rods.

This cell presents also the advantage that, once it is calibrated and the dependence between the cell constant and the electrode distance is established, fig. 4, one may now change the cell constant simply by counting the number of turns of the micrometric screw, fig. 5.

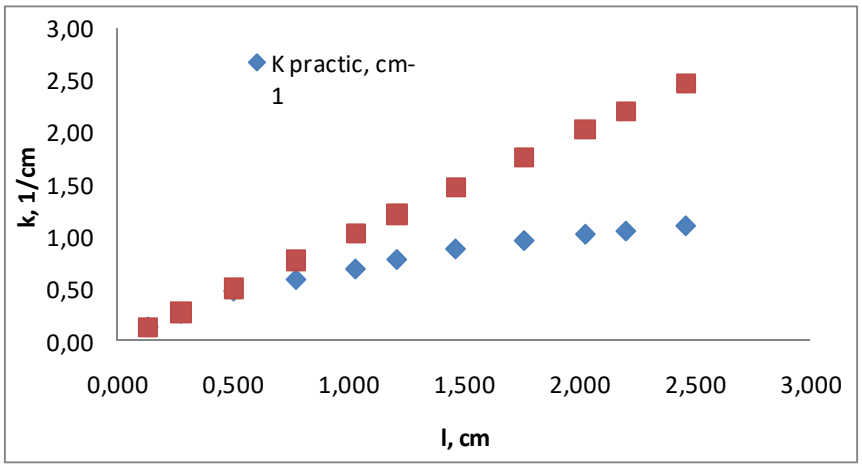

Fig. 4. The dependence of the cell constant, k, versus the electrode distance, l.

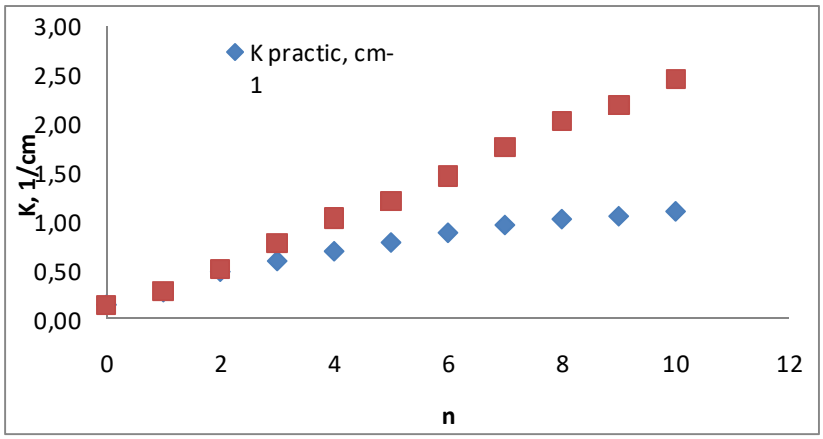

Fig. 5. The dependence of the cell constant, k, versus the number of turns of the micrometric screw, n.

Troubleshootings involving the cell calibration and the determination of conductivity cell constant

As time goes by, the cell is prone to be adversely affected by a number of factors that may lead to the modification of the value of the cell constant (scale, wax, biological growths, oils, gum, etc). A conductivity meter will measure, besides the current that flows between the shortest path between the two electrodes, also the roundabout smaller share of current, so that it is necessary to calibrate the system (determine the conductivity cell constant) [3], [8]. This is

achieved by using calibration standard solutions, which should be near to the high end of the range of operation for the cell conductivity. Normally, a slim beaker should be used and the cell has to be suspended above the bottom rather than left to sit on the bottom of the beaker. As the air bubbles cause errors in conductivity readings by masking certain areas of the electrodes, one has to remove the air by gently tapping the cell or raising and lowering it to get rid of the trapped bubbles. As there is an initial drift, one shall start the calibration procedure only when there is little or no variation in the acquired values (stable readings) [3].

There is an equivalence in the determination of the conductivity cell constant and calibrating the conductivity cell. If one uses an AC compensating bridge (e.g. Kohlrausch bridge), then the cell constant must be determined before the measurements, as the conductivity is calculated as a ratio of the cell constant and the value of the measured resistance (in fact impedance) [3-10]:

$$\lambda = \frac{K_{cell}}{R} \tag{6}$$

In order to determine the cell constant for the above said purpose, one should dry approximately 5 g of KCl in an oven at about 110ºC for 8 hours, and then place it in a dessicator and leave it to cool to the room temperature. A quantity of 0.7455 g should be weigh precisely and transferred into a clean, dry 1000 mL volumetric flask, and filled with distilled water of 25ºC to the mark. If the flask was graded for 20ºC, then the water must have 20ºC. The conductivity cell/probe is soaked in distilled or deionised water for 15 minute, dried and immersed in a slim beaker containing the calibration solution. Using a Kohlrausch bridge or an equivalent system and a thermostated system to maintain the calibration sample at 25ºC, one shall determine now the value of the resistance and knowing the value of the calibration sample conductivity (1413 $\mu S \cdot cm^{-1}$) the cell constant is calculated as $K_{cell} = \lambda R$. Should the calibration take place at a different temperature, then a temperature compensation procedure (as explained below) must be followed to ensure the best accuracy for this determination.

The standard solution may be stored in a HDPE storage bottle for up to one year. For different calibration standards, only the amount of KCl differs, the procedure remains the same. If a proper conductivity meter is used, then the calibration is carried out using a standard calibrating sample solution of known conductivity and adjusting the calibration knob (or pressing the calibration button for digital equipment) until the displayed value is identical to that written on the calibration standard sample.

Calibration troubleshooting

If the cell constant differs with more than 15% from the initial value, as a result of some physical changes or surface deplatination, some conductivity

meters will abort the calibration procedure (see figure 6), suggesting buying a new conductivity cell. The cell may be revived by replatination (as discussed below) or by a fine tuning using a simple external precision variable resistance (a Voltcraft precision resistance decade box R-Box 01 - 1% precision, 0.3 W - was used) connected in series with the conductivity cell, so that the software is tricked to accept the constant cell as being within the manufacturer prescribed range and will calibrate the cell (figure 7), supplying at the same time the value of the conductivity cell constant. As one can see, the difference in the value of the cell constant was only 1% above the accepted limits (1.016 cm^{-1} instead of 1.015 cm^{-1} for a conductivity cell of 1 cm^{-1}).

This procedure was successfully used in the calibration of another novel multiparameter electrochemical cell employed for the characterisation and the determination of the optimum hydrolysis time, reported in details in [21].

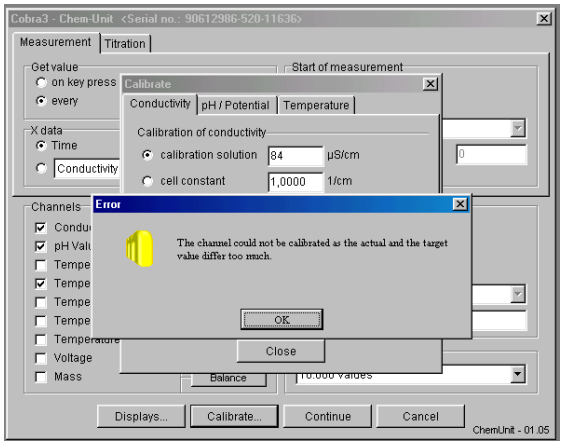

Fig. 6. A screen capture of a calibration failure

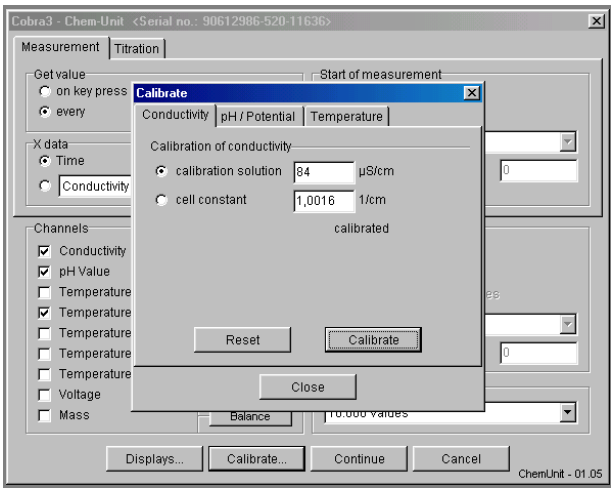

Fig. 7. A screen capture of a successful calibration

Cleaning and storing the cell/probe troubleshooting

As the conductivity measurements are carried out not only in clean solutions but also in solutions loaded with particulate materials, biological materials or organics, the conductivity cells have to be cleaned before storage. Should this case arise, the cell constant changes its value when the platinised platinum is contaminated or partially removed, so that the cell needs cleaning.

For the removal of organics and some biological materials, the cell is cleaned either with a 20% isopropanol solution or with a mild liquid detergent (washing up detergent). After the rinsing, it is immersed in dilute nitric acid (1% wt) and stirred for 3 to 5 minutes. Dilute hydrochloric acid or sulphuric acid may be used when particulate materials such as carbonates are attached to the electrodes. If the cell is heavily loaded, concentrated HCl mixed with a 50% isopropanol solution may be used.

The cell is rinsed several times with distilled or deionised water and recalibrated before use. For a short period of storage, after the cleaning, the cell is immersed in distilled or deionised water (wet storage). If a longer storage period is needed, it may be stored dry, protected with a plastic sleeve [3], [8-10], [18-19]. Obviously, it requires calibration before use and if the calibration does not yield the expected values, it may require replatination.

Cell constant out of range troubleshooting / Electrodes replatination

If the cell does not hold the calibration or the cell constant drifts with more than 50% from its nominal value, the cell/probe should be replaced or replatinised. In order to do this, the black platinum electrodes are cleaned in aqua regia for 30 seconds, a solution of 0.025 N HCl with 3% H_2PtCl_6 and 0.025% $Pb(CH_3COO)_2$ is prepared and the cell is platinised for 10 minutes at a current density of 5-10 $mA \cdot cm^{-2}$, reversing the polarity every 30 seconds, until a consistent black deposit is noticed on the electrodes [18], [19]. The cell is rinsed with distilled water and electrolysed in 0.1 M sulphuric acid for 5 minutes to remove excess chlorine, rinsed again in distilled water and stored either in distilled water (short term) or dry/stored until ready to use. A calibration procedure should be carried out before use. Alternatively, replatination of cell electrodes may be carried out following the procedure described in [1].

Temperature Compensation

Measurements in thermostated solutions cannot be carried out in all cases, either by the impracticability of thermostating the solutions (conductivity of a river or lake water) or by the inherent rapid variation of the solution temperature in a certain given process, so that temperature compensation should be taken into account, as the conductivity varies with temperature roughly in the range of 1-2%/ºC. In the absence of such temperature compensation, the measurements are

prone to unacceptable errors (e.g. a variation of about 25ºC leads to an error of 25x2%/ºC = 50% off). Most manufacturers of conductivity meters have solved this problem by including a temperature sensor and designing the electronic circuits for automatic temperature compensation. However, there are still in use conductivity probes without this feature, so that a manual temperature compensation must be carried out when temperature fluctuates or differs from 25ºC, considered as the reference temperature [3], [8].

A simplified formula for temperature compensation is analogue to that for the variation of resistivity with temperature and is given by:

$$\lambda_T = \lambda_{25^oC}\left[1+\alpha\left(T-25\right)\right] \tag{7}$$

where λ_T is the measured conductivity of the solution at the actual temperature, λ_{25^oC} is the conductivity of that solution at 25ºC (may be taken from tables or measured at that particular temperature), α is the temperature compensation factor (some typical values of α are presented in Table 1) and T is the actual temperature of solution. Where the temperature compensation factor is not known, it can be evaluated by plotting the value of conductivity versus temperature for a given temperature range or by using the default values of 2-2.1%/ºC to compensate the variation of conductivity with temperature [3], [8], [20]. The effect is stronger in low conductivity solutions. Below is given a calculus sample for the manual temperature compensation procedure.

Table 1

Most Common Temperature Compensation Factors [3], [20]

Substance	% change / ºC
HCl 10%	1.56
HNO_3 31%	1.39
H_2SO_4 20%	1.45
KOH 8.4%	1.86
KCl below 5%	2.01
Acids	1-1.6
Bases	1.8-2.2
Salts	2.2-3
Water	2

Manual temperature compensation procedure

A conductivity cell having the cell constant of 1 cm^{-1} is subjected to a calibration procedure, at a temperature of 20ºC, using a standard of 1413 $\mu S \cdot cm^{-1}$ at 25ºC [20]. The equipment does not have an automatic compensation feature, nor a temperature sensor contained, so a manual compensation procedure needs to be carried out. In order to do this, one has to:

a) immerse the conductivity cell into the standard solution and let it 5 minutes for the cell temperature and standard solution temperature to reach an equilibrium;

b) measure precisely the standard solution temperature (let it be 20ºC);

c) determine the standard conductivity value at 20ºC;

$$\lambda_{KCl@20^oC} = 1413\left[1 + 0.0201 \cdot (20 - 25)\right] = 1271\ \mu S \cdot cm^{-1} \quad (8)$$

d) adjust the value on the conductivity meter using the calibration knob to the value of 1271 $\mu S \cdot cm^{-1}$;

e) remove the cell and insert it into a beaker containing a solution of unknown concentration of KCl, at the same temperature and read the displayed value, e.g. 825 $\mu S \cdot cm^{-1}$ (if the substance and/or the temperature are different, one shall replace in the formula (9) the corresponding values for the temperature compensation factor, from tables published in [20] or similar references and the temperature);

f) calculate the conductivity for the corresponding temperature of 25ºC;

$$825 = \lambda_{KCl\ unknown\ sample@25^oC}\left[1 + 0.0201 \cdot (20 - 25)\right] \quad (9)$$

$$\lambda_{KCl\ unknown\ sample@25^oC} = \frac{825}{\left[1 + 0.0201 \cdot (20 - 25)\right]} = 917\ \mu S \cdot cm^{-1} \quad (10)$$

6. Conclusions

Although the cost of conductivity meters came down, it remains still high on the long term, due to the need for more than one conductivity cells/probes to cover the whole range of values or to the need for conductivity cells/probes replacement, once they are decalibrated by deplatinisation or electrode fouling. The paper presents, besides a novel variable cell constant conductivity cell that may be employed in a whole range of experiments requiring different conductivity cell constants, some practical solutions to a number of problems associated with conductivity measurements and the determination of the conductivity cell constant, including that of artificially adjusting and bringing the cell constant within the required equipment range, so that the digital conductivity meter will accept the calibration, even though the cell constant differs more than 15% from its initial value. A procedure for manual temperature compensation, as well as one for replatinising the cell electrodes are also presented.

4. Acknowledgments

Special thanks go to Mr. Corneliu Andrei for providing the logistic support and to Mrs. Mariana Andrei for supplying the necessary reagents.

REFERENCES

[1]. Atanasiu, I.A., Manual de electrochimie generala, Ed. Didactica si Pedagogica, București, (1963), ch 3.
[2]. Murgulescu, I.G., Radovici, O.M., Introducere in chimia fizica, Ed.bAcademiei RSR, București, (1986), 4, ch 4.
[3]. Shreiner, R.H., Pratt, K.W., Standard Reference Materials: Primary Standards and Standard Reference Materials for Electrolytic Conductivity, National Institute of Standards and Technology, Special Publication, Gaithersburg, (2004), 260-142.
[4]. Zosky, C.G., Handbook of Electrochemistry, Elsevier, Amsterdam, (2007), ch 3.
[5]. Badea, T., Nicola, M, Vaireanu, D.I., Maior, I., Cojocaru, A., Electrochimie şi Coroziune, Ed. MatrixRom, București, (2005), ch. 3.
[6]. Vaszilcsin, N., Notiuni de electrochimie, Ed. Politehnica, Timisoara, (2004), ch 3.
[7]. Nemes, M., Vaszilcsin, N., Kellenberger, A., Electrochimie, principii si aplicatii, Ed. Politehnica, Timisoara, (2004), ch 2.
[8]. IC Controls, Conductivity Theory and Measurement, Technical Articles 4-1, available online at http://www.iccontrols.com/files/4-1.pdf.
[9]. Vaireanu, D.I., Electrochemistry, Ed. AGIR, Bucharest, (2006), ch 2.
[10]. Vaireanu, D.I., Handbook of Experimental Electrochemistry, Ed. Printech, Bucharest, (2008), ch 2.
[11]. Vaireanu, D.I., Maior, I., Grigore, A, Săvoiu, D., The evaluation of ionic conductivity in polymer electrolyte membranes, *Rev. Chimie*, 59, 10, (2008), 1140-1142.
[12]. Vaireanu, D.I., Cojocaru, A., Maior, I., Caprarescu, S., Practical considerations regarding the measurement of ionic conductivity by EIS in conductive polymers, *Chem. Bull. "POLITEHNICA" Univ. of Timisoara*, Series Chemistry and Environmental Engineering, 1-2, (2008), 258-261.
[13]. Caprarescu, S, Vaireanu, D.I., Cojocaru, A., Maior, I., Sarbu, A., Removal of Copper Ions from Electroplating Wastewater by Ion-exchange Membranes, *Rev. Chim*., 60, 7, (2009), 673-677.
[14]. Caprarescu, S., Radu, A.L., Purcar, V., Ianchis, R., Sarbu, A., Ghiurea, M., Modrogan, C., Vaireanu, D.I., Périchaud, A., Ebrasu, D.I., Adsorbents/ion exchangers-PVA blend membranes: Preparation, characterization and performance for the removal of Zn^{2+} by electrodialysis, *Applied Surface Science*, 329, 65, (2015), 65-75.
[15]. Baicea, C.M., Luntraru, V.I., Vaireanu, D.I., Vasile, E., Trusca, R., Composite membranes with poly (ether ether ketone) as support and polyaniline like structure, with potential applications in fuel cells, *Central European Journal of Chemistry,* 11, 3, (2013), 438-445.
[16]. Caprarescu, S., Purcar, V., Vaireanu, D.I., Separation of copper ions from synthetically prepared electroplating wastewater at different operating conditions using electrodialysis, *Separation Science and Technology*, 47(16), (2012), 2273-2280.
[17]. Caprarescu, S., Vaireanu, D.I., Cojocaru, A., Maior, I., Purcar, V., A 3-cell electrodialysis system for the removal of copper ions from electroplating wastewater, *Optoelectronics and Advanced Materials – Rapid Communications*, 12, (2011), 1346-1351.
[18]. Vaireanu D.I., Olteanu C., Simion A., Electrochemical modular cell used in flow injection analysis systems, *Rev. Chimie*, 52(3), (2001), 130-133.
[19]. Vaireanu, D.I., Olteanu, C., Mănoiu, A., Mistrianu, M., *Proceedings of the 33rd International Scientific Symposium of the Military Equipment and Technologies Research Agency,* Ed. Ministry of National Defence, vol.4, Military Chemistry, Ecology and Environmental Protection, Bucharest, (2002), 81.
[20]. Deszo, D., Electrokemiai Tablazatok, Ed. Musyaki Konzvkiado, Budapest, (1965), ch 2.

[21]. Ciobotaru, I.A., Maior, I., Cojocaru, A., Caprarescu, S., Vaireanu, D.I., Ciobotaru, I.E., The determination of the optimum hydrolysis time for silane films deposition, *Applied Surface Science*, 371, (2016), 275-280.

STUDY OF THE OLEFIN SELECTIVITY OF A Fe-Ni CATALYST FOR FISCHER TROPSCH PROCESS

Ioan Tudor SIBIANU*, Ioan CALINESCU, Petre CHIPURICI

University Politehnica of Bucharest, Faculty of Applied Chemistry and Materials Science, 1-7 Gh. Polizu street, RO-011061 Romania

Abstract

The aim of this research is to study the synthesis of light olefins via Fischer-Tropsch process while using a Fe-Ni based catalyst. The catalyst consists of several types of alumino-silicate support that has been impregnated with a solution of Fe and Ni nitrate of a molar ratio of 4:6. The impregnated supports have been dried, after which they have been calcinated at a temperature of around 550°C and activated under a continuous flow of Nitrogen and Hydrogen at a molar ratio of 1:1 and a molar flow rate of 30 mL/min for each catalyst. The supports used consisted of γAl_2O_3, ZSM 5, MCM 41, SBA 15.

Each catalyst was tested under various temperatures (250°C, 300°C, 350°C, 400°C) at a Gas Hourly Space Velocity (GHSV) of 950 h^{-1} at 1 atm. For each temperature samples were taken on 30 minute intervals roughly to determine the composition of reaction gases.

Key words: Fischer-Tropsch; Olefins; Catalyst; Support; Iron; Nickel.

1. Introduction

The Fischer-Tropsch process is used for the synthesis of fuel grade hydrocarbons starting from syngas with the help of a catalyst, catalyst which may consist in either the precipitated metal or a support based catalyst where the metal is deposited unto the supports surface by impregnation [1]. Recently there is an ever increasing interest in the synthesis of lower olefins via the Fischer-Tropsch process and using them as intermediates in other branches of the chemical industry. Based on previous studies, iron is a good active site for the synthesis of light unsaturated hydrocarbons that are encountered in the C_2-C_4 range [2-3]. Also among other metals that can exhibit a good selectivity for lower hydrocarbon formation is nickel. The main drawback for nickel is a high selectivity for methane which can be countered with the addition of Fe active sites to the catalyst. Also the addition of a support for the metal active sites can greatly reduce the deactivation of the catalyst

* Corresponding author: Email address: sibianut@yahoo.com

encountered in the Fischer Tropsch process [4-5]. This study focuses on the testing of several support based bimetallic Fischer-Tropsch catalyst.

2. Experimental

2.1. Materials and methods

2.1.1. Reaction Set-up:

The Fischer-Tropsch reactor consisted in a vial which contained 1 gram of catalyst. The vial was approx. 45 mm long 13 mm thick and had both ends elongated and narrowed so they can fit in a small oven that heats the vial. The vial was connected to a catch pot in the event any liquid samples would be formed and collected in order to prevent contamination and blocking of the GC column. The CO and H_2 flow rate were controlled with a series of flow controllers which were calibrated and set to a GSHV of 950 h^{-1} using a 1:1 CO:H_2 mixture. The temperatures used in the reaction process were of 250ºC, 300ºC, 350ºC and 400ºC. The Analysis part of the GC consists of a valve which could go to a loop which could be switched to the GC analysis.

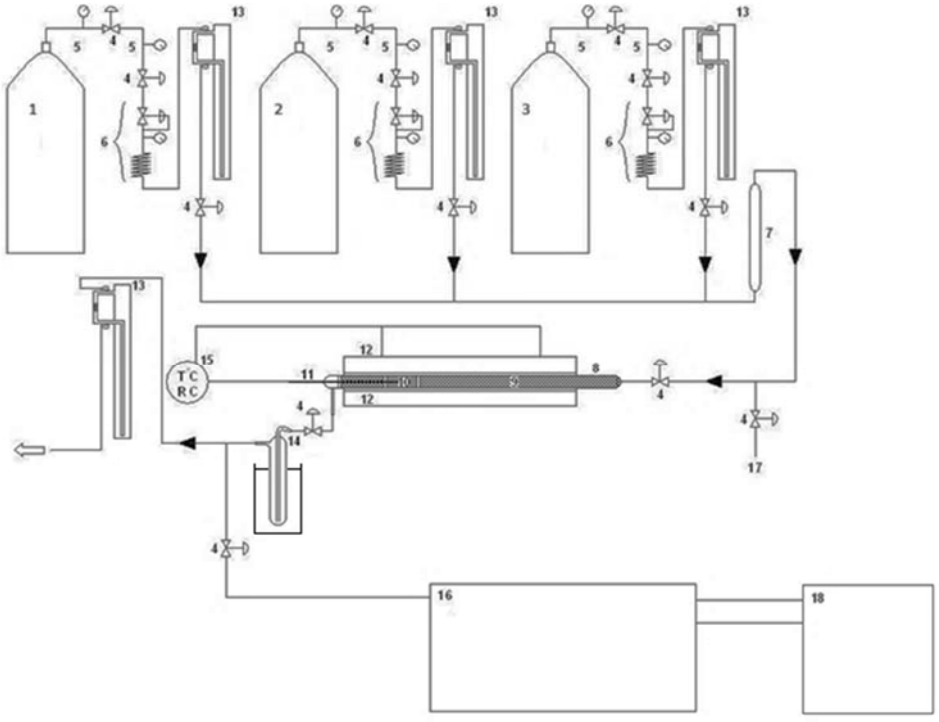

Fig 1. Simplified experimental Fischer Tropsch set-up

Nitrogen at a GSHV of 1140 h^{-1} (1) and hydrogen at a GSHV of 1140 h^{-1} (2) were used to activate and regenerate the catalyst. The syngas necessary for the reaction was supplied from the gas cylinders (2) and (3). Their flow rate was controlled by a series of valves (4), pressure indicators (5) and flow rate reduction

devices (6;13) which led to the quartz tube reactor (8) that has a filling of glass beads (9) and the catalyst bed (10) as well. The heating was supplied by a miniature oven with a temperature sensor and a control switch equipped (11; 12; 15). Liquid samples were collected in the catch pot (14) while gaseous samples were analyzed directly into a Buck type GC (16) and analyzed by a data processing unit using PeakSimple 3.29 version software (18).

2.1.2. Catalyst preparation

A series of 4 supports consisting in γAl_2O_3, ZSM 5, MCM 41 and SBA 15 were prepared and tested using a 4:6 molar ratio Fe:Ni [6-10]. Two types of catalysts were used, one that had been impregnated after the support had been extruded and the over that had been impregnated before extrusion. The support was extruded and left to dry at 150^{o}C for 16 hours and then calcinated at 550^{o}C for 6 hours. Two types of catalysts were prepared in respect with the method of impregnation used. One catalyst type was impregnated after the support was extruded. For this catalyst type the metals were deposited mostly on the outskirts of the catalysts surface and formed a shell of metals on the catalysts surface. The other type of support formed was before the catalyst was extruded. After impregnation the support was dried at 150^{o}C for 16 hours and calcinated at 550^{o}C for 6 hours. For both catalysts a binder had to be used in order to extrude them. The binder consisted in hydroxilated γAl_2O_3 and it was used at a 1:1 mass ratio with the support.

2.1.3. Catalyst composition

The elemental composition of catalyst based on the raw materials used in their synthesis is shown in Table 1.

Table 1.

Composition of catalysts by their raw material elements.

	γAl_2O_3	ZSM 5	MCM 41.	SBA 15
O%	41.35	44.97	42.97	43.1
Al%	46.52	25.17	22.53	24.82
Si%	0	19.39	18.62	17.86
Fe%	4.82	4.16	6.31	5.65
Ni%	7.31	6.31	9.57	8.57

2.1.4. BET analysis:

The internal structures of the catalysts (i.e. specific surface, average pore size and pore volume) were determined by using the BET method on a Quantachrome ASIQWin porosimeter using liquid nitrogen as gas phase.

Samples were initially degassed and afterwards the samples were filled with nitrogen and their internal structural parameters were determined based on the pressure difference recorded by the porosimeter. Results are presented in Table 2.

Table 2.

Structural properties of the fresh and used catalysts

Catalyst	Average Pore size (Å)	Pore Volume (mL/g)	Specific Surface (m^2/g)
γAl_2O_3 fresh	96.57	0.39	282
γAl_2O_3 used	77.55	0.34	253.14
ZSM 5 fresh	90.94	0.25	204.75
ZSM 5 used	90.64	0.29	215.57
MCM 41 fresh	96.60	0.51	602.98
MCM 41 used	98.54	0.42	531.21
SBA 15 fresh	93.57	0.44	440.03
SBA 15 used	92.78	0.45	438.44

2.1.5. Anderson Flory Schultz distribution

Regarding the selectivity of hydrocarbons, one must take into account the probability of chain growth which is given by the Anderson Flory Schulz distribution [11]. The ASF distribution depends on a growth parameter called α. This parameter shows the weight fraction for each hydrocarbon present at a certain value for α. Equation (1) shows how the mass faction can be calculated:

$$W_n = n\,(1-\alpha)^2 . \alpha^{n-1} \qquad (1)$$

where W_n is the mass fraction for a hydrocarbon of n number of carbon atoms, n is the total number of carbon atoms and α is the chain growth parameter.

In Fig. 2, the mass fraction for each hydrocarbon was calculated by using the ASF formula (eq. 1) and in order to get the highest concentration of light olefins, namely ethylene and propylene, α must be located between 0.3 and 0.5.

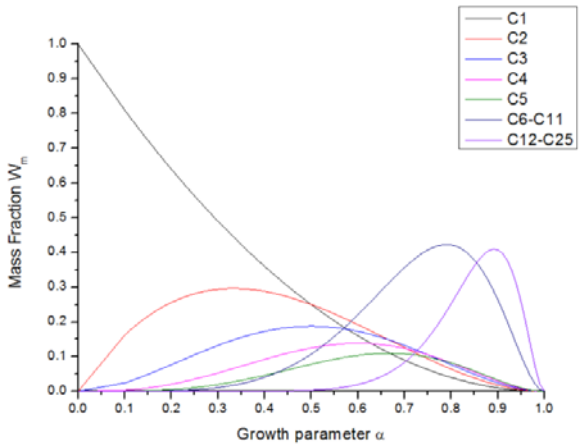

Fig 2. Graphic representation for the ASF distribution for hydrocarbons.

Tables 3.A and 3.B show the chain growth probability parameter (α) which was determined for the catalytic activity of each catalyst. Two values for α were obtained from experimental data. The first one refers to the formation of methane while the second one refers to the formation of C_3 – C_4 hydrocarbons. The fact that the 2 values differ, show that the distribution of the obtained products does not completely follow the ASF mechanism.

From values presented in Tables 3A and 3B, the value for the α parameter is lower than the optimum value for C_2-C_3 formation (0.3-0.5).

In order to increase the value α, the reaction temperature must decrease, the H_2: CO ratio must increase and the pressure must increase as well [12].

However, some of these requirements do not favor the formation of olefins and due to this reason the H_2: CO ratio has to be kept below the value of 2:1, the working pressure shall be kept at 1 atm and the temperature shall be slightly lower than 350ºC. Also since the formation of olefins is favored by a lower residence time, the GSHV has to increase.

Table 3.A.

Chain growth probability parameter α for the used catalysts at 250ºC and 300ºC

Chain growth probability parameter α				
Temperature (ºC)	250		300	
Catalyst type	α for CH_4	α for C3, C4	α for CH_4	α for C3, C4
γAl_2O_3 after extrusion	0.07	0.17	0.06	0.15
γAl_2O_3 before extrusion	0.02	0.03	0.05	0.12
ZSM 5 after extrusion	0.11	0.2	0.09	0.17
ZSM 5 before extrusion	0.15	0.21	0.13	0.21
MCM 41 after extrusion	0.08	0.05	0.06	0.14
MCM 41 before extrusion	0.1	0.19	0.09	0.17
SBA 15 after extrusion	0.12	0.22	0.07	0.15
SBA 15 before extrusion	0.1	0.2	0.1	0.18

Table 3.B.

Chain growth probability parameter α for the used catalysts at 350ºC and 400ºC

Chain growth probability parameter α				
Temperature (ºC)	350		400	
Catalyst type	α for CH_4	α for C_3, C_4	α for CH_4	α for C_3, C_4
γAl_2O_3 after extrusion	0.14	0.23	0.06	0.12
γAl_2O_3 before extrusion	0.09	0.18	0.04	0.08
ZSM 5 after extrusion	0.14	0.24	0.05	0.11
ZSM 5 before extrusion	0.15	0.23	0.03	0.06
MCM 41 after extrusion	0.1	0.19	0.02	0.16
MCM 41 before extrusion	0.13	0.24	0.03	0.07
SBA 15 after extrusion	0.1	0.21	0.02	0.05
SBA 15 before extrusion	0.12	0.22	0.02	0.06

From values presented in Tables 3A and 3B, the value for the α parameter is lower than the optimum value for C_2-C_3 formation (0.3-0.5).

In order to increase the value α, the reaction temperature must decrease, the H_2: CO ratio must increase and the pressure must increase as well [12].

However, some of these requirements do not favor the formation of olefins and due to this reason the H_2: CO ratio has to be kept below the value of 2:1, the working pressure shall be kept at 1 atm and the temperature shall be slightly lower than 350ºC. Also since the formation of olefins is favored by a lower residence time, the GSHV has to increase.

3. Results and discussions

The Fischer-Tropsch samples were analyzed using a Buck 910 GC equipped with a FID and a TCD detector. The mobile phase consisted in helium. The working pressure for the carrier gas (Helium) was 2 bar, for hydrogen was of 1.37 bar and the air pressure was of 0.5 bar. The GC is equipped with a 2 column separation system. The first column is a 6.5-inch silica gel column whose sole purpose is the separation of CO, CH_4, NO_X and CO_2. The other column consists of 13 X zeolite type which separates the organic compounds in the C_2-C_{10} range. By this process, the compounds can be individually separated and processed by the FID. The GC is connected to a Peak simple data acquisition system which provides the necessary chromatograms and from where the selectivity and conversion of the samples are obtained.

In fig 3B the most active catalyst is ZSM 5 with a conversion of 90%, but if we take into account graphs 3F and 3H the temperature at which that conversion was achieved, it was mainly due to the high amount of methane and carbon dioxide

formed. The selectivity's for each olefin are presented in more detail in fig. 3 (A, B, C, D, E and F). Experimental results which can be observed in fig 3.D have shown that the highest selectivity's for olefins were obtained at 350^{o}C and for MCM 41 and SBA 15. This could be due to the internal structures of the catalysts. When the catalyst was extruded the binder has partially covered up the pores of the support which significantly decreased the specific surface and pore volume to the point at which the active sites would have a small space for the reaction to take place and eventually it would lead to the formation of carbon on the catalysts surface which is explained by the high selectivity for CO_2.
In fig. 4 the best results were shown for the catalysts that had been impregnated prior to the extrusion of the catalyst into shape. Out of those 4 catalysts, MCM 41 and SBA 15 had the best results for ethylene and propylene. This is due to the fact that the specific surface is large enough to allow the formation of hydrocarbons without clogging the catalyst. In the case of ZSM 5 and γAl_2O_3 there is an increased selectivity for methane and CO_2 which is due to their smaller surface and pore volume.

4. Conclusions

In this work the aim was to test the effect of using various supports on a certain type of catalyst contain Ni and Fe on conversion of syngas and selectivity of transformation into lower olefins in Fischer Tropsch process.

The use of different structure types of supports has a pronounced effect on the type of compounds obtained. The use of nickel however seems to have a high impact on favoring the formation of methane. As a future goal, the study of using a lower amount of nickel or even avoiding the complete use of nickel as a component for the catalyst might be a solution.

In order to maximize the olefin content in the F-T reaction, the working temperature should be between 300^{o}C and 350^{o}C, the pressure used should be atmospheric, the CO to H_2 ratio used is between 1: 1 and 1: 1.5 and the GSHV has to be high enough to avoid the formation of long chained hydrocarbons.

Also based on lab data the ZSM 5 support would be a good candidate due to its high conversion but due to the high methanation and high CO_2 selectivity, the composition of the metallic active site has to be remade.

The most prominent results have been shown in the case for MCM 41 and SBA15. These two catalysts have had the highest selectivity for olefins.

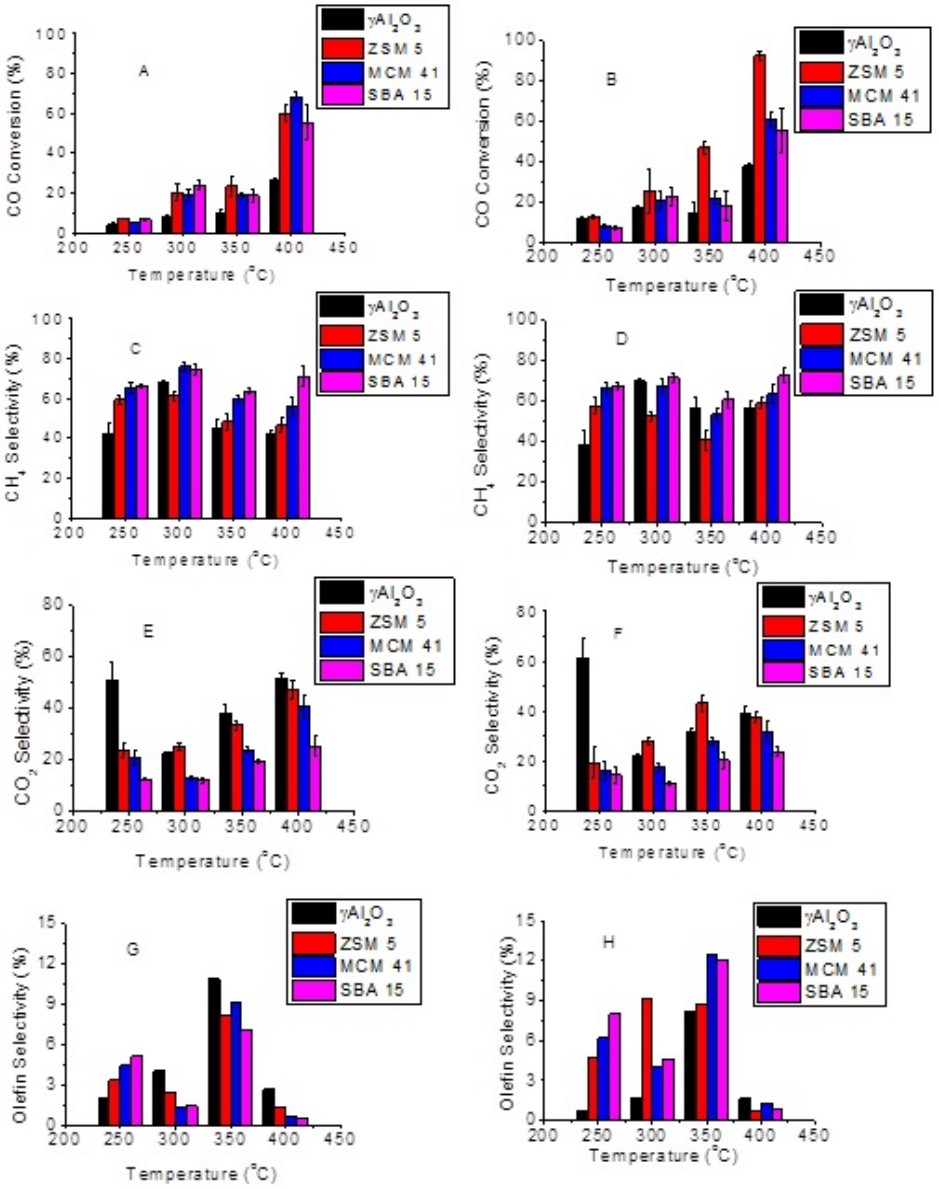

Fig 3. Catalyst behavior during F-T reaction consisting in CO conversion (A; B), CH_4 Selectivity (C; D), CO_2 selectivity (E; F), Olefin selectivity (G; H), for the catalysts prepared before their extrusion (A; C; E; G) and after their extrusion (B; D; F; H).

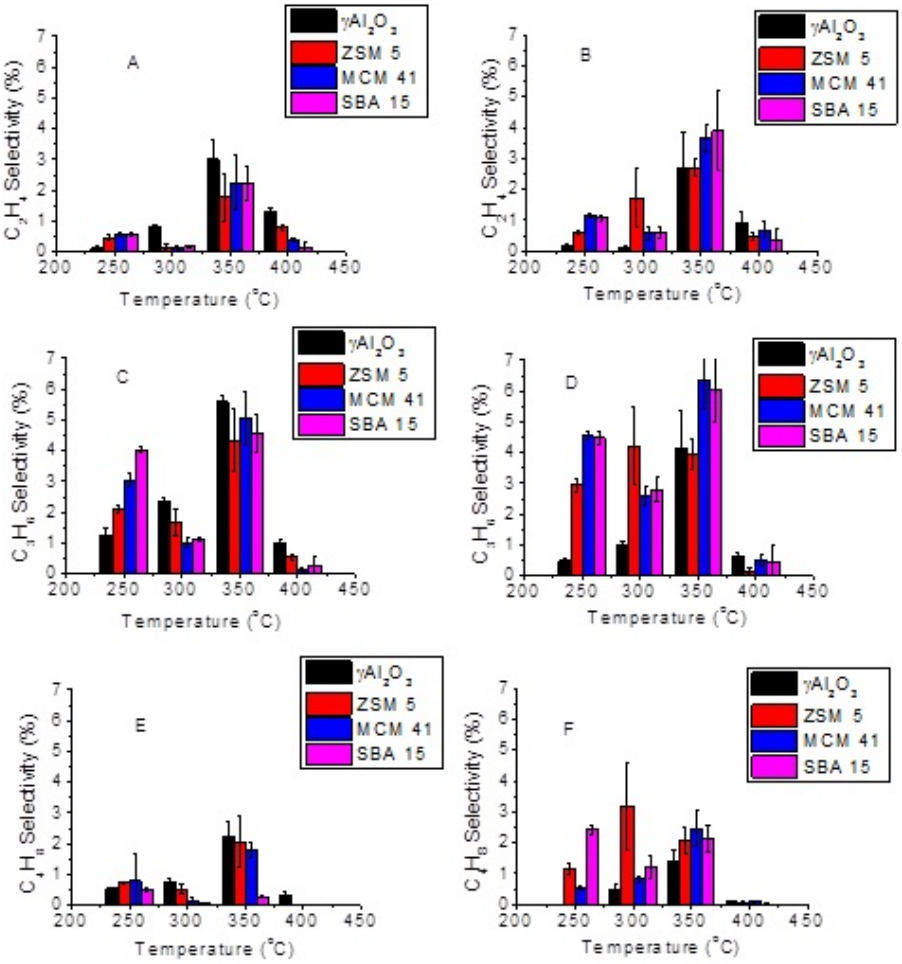

Fig 4. Selectivity for ethylene (A; B), propylene (C; D) and buthylenes (E; F) for catalysts that were impregnated before extrusion (B; D; F) and after extrusion (A; C; E).

REFERENCES

[1] Dry, M.E., High quality diesel via the Fischer-Tropsch process- a review, *Journal of Chemical Technology and Biotechnology,* 77, (2001), 43-50.

[2] Smith, G.V., Notheisz, F., Heterogeneous Catalysis in Organic Chemistry, Elsevier (2000), ISBN 9780126516456.

[3] Hans, S., Principles of Fischer–Tropsch synthesis—Constraints on essential reactions ruling FT-selectivity, *Catalysis Today,* 228, (2014), 113-122.

[4] Feyzi, M., Mirzaei, A.A., Bozorgzadeh H.R., Effects of preparation and operation conditions on precipitated iron nickel catalysts for Fischer Tropsch synthesis*, Journal of natural gas Chemistry,* 19, (2010), 341-353.

[5] Prunier, M.L.; Catalysis of Organic Reactions, CRC Press (2009), ISBN 9781420070767
[6] Li, T., Wang, H., Yang, Y., Xiang, H., Li, Y., Study of an Iron Nickel bimetallic Fischer Tropsch synthesis catalyst, *Fuel Processing Technology*, 118, (2014), 117-124.
[7] Xing, C., Sun, J., Yang, G., Shen, W., Tan, L., Zhu, P., Wei, Q., Li, J., Kyodo, M., Yang, R., Yoneyama, Y., Tsubaki, N., Tunable isoparaffin and olefin synthesis in Fischer–Tropsch synthesis achieved by composite catalyst, *Fuel Processing Technology*, 136, (2015), 68-72.
[8] Kang, S.K., Koo, H.M., Kim, R., Lee, D.H., Ryu, J.H., Yoo, Y.D., Bae, J.W., Correlation of the amount of carbonaceous species with catalytic performance on iron-based Fischer–Tropsch catalysts, F*uel Processing Technology,* 109, (2013), 141-149.
[9] Fischer, N., Steen, E., Claeys, M., Structure sensitivity of the Fischer–Tropsch activity and selectivity on alumina supported catalysts, *Journal of Catalysis*, 299, (2013), 67-80.
[10] Kang, S.K., Bae, J.W., Woo, K.J., Prasad, P.S., Jun, K.W., ZSM-5 supported iron catalysts for Fischer–Tropsch production of light olefin, *Fuel Processing Technology*, 91, (2010), 399-403.
[11] Masuku, C.M., Hildebrandt, D., Glasser, D., Olefin pseudo equilibrium in the Fischer Tropsch reaction, *Chemical Engineering Journal,* 182, (2012), 667-676.
[12] Pour, A.N., Housaindokht, M.R., The olefin to paraffin ratio as a function of catalyst particle size in Fischer Tropsch synthesis by iron catalyst, *Journal of Natural Gas Science and Engineering*, 14, (2013), 204-210.

BIODIESEL PRODUCTION USING A SULPHONATED ACTIVATED CARBON-BASED CATALYST

Cristian Eugen RĂDUCANU, Tănase DOBRE*, Cristina GOGOAŞĂ

Department of Chemical and Biochemical Engineering, Faculty of Applied Chemistry and Materials Science, University Politehnica of Bucharest

Abstract

In this study a heterogeneous catalyst was prepared by direct sulphonation of an activated carbon followed by impregnation with a base component to achieve both acidic and base properties to catalyze used food oil conversion to biodiesel. The prepared catalyst was thermally and chemically stable and showed good catalytic activity when tested in transesterification reactions to yield biodiesel under moderate homogeneous catalyst-like reaction conditions. The highest conversion reached was 94.72 % while the highest biodiesel yield reached was 92.37 % at 65 ºC reaction temperature, 12:1 methanol/oil molar ratio and 0.75 h reaction time.

Keywords: carbon-based catalyst; sulphonated active carbon, biodiesel; oil conversion, green process.

1. Introduction

Having the legislation support behind when started in the beginning of the last decade, biodiesel industry has become a mature one today. We are now able to understand the necessity to dilute the fossil energy with green energy while we are making it. Making biodiesel it became accessible, but the real challenge is to make green biodiesel, keeping the equilibrium between the positive aspects of a commercial-like biodiesel - reaction time and temperature as moderate reaction conditions - and the green specific aspects of a heterogeneous catalyzed process like non-toxic product separation and purification [1].

Heterogeneous catalyzed process can move the feedstock from the conflictual present one, as in vegetable oils, toward the second generation type, as in used cooking oils, yellow grease, brown grease etc.

We now have five major players on romanian's biodiesel market, gathering all together 85 % from near to 500.000 t/year biodiesel, all having the same homogeneous alkaline catalyzed transesterification based technology to

* Corresponding author: E-mail address: tghdobre@gmail.com (TanaseDobre)

convert fresh edible oils to biodiesel, associated with economically and environmental unfriendly, expensive separation product operations [2-4].

In the present work we proposed a heterogeneous carbon based catalyst, extensively studied in the last years, for both esterification and transesterification reaction to convert used food oil and other free fatty acid enriched materials, usable as feedstock, to produce biodiesel [5-11]. Acid and base catalyst properties were obtained both by direct sulphonation and potassium hydroxide impregnation of activated carbon.

2. Experimental

2.1 Materials

The following materials have been used in experimental research: purchased activated carbon (d_p = 1 mm, specific surface area= 200 m^2/g) for catalytic support, methanol (99%), palm used cooking oil from local fast food (used for french fries only), sulphuric acid 98 % (Merck), KOH (Merck pellets). Other properties of reactants and reaction products are shown in table 1

Table 1

Components properties used in this work

Properties		Oil	Methanol	Glycerol	Biodiesel
Molecular mass	g/mol	890	32.04	92.09	840
Density	g/cm^3	0.93	0.792	1.26	0.9
B.p.	°C	> 300	64.7	290	> 300

2.2 Catalyst preparation

Sulphonation: By heating, for 3 h in an oven at 130 ºC, the activated carbon (AC), firstly, supports a thermal pretreatment. Then 50 g of dehydrated activated carbon were immersed in 200 mL sulphuric acid 98 % and kept at reflux under continuous stirring for 6 h at 170 ºC. The final suspension was kept at room temperature for 24 h, and then washed, several times, with distilled water while kept on cold water bath, dried for 3 h at 130 ºC and stored in proper conditions. The weight difference between the resulted AC-S (sulphonated active carbon) and AC was 4.2 g, resulting in 0.084 $g_{H\text{-}SO3}/g_{AC}$.

Impregnation: First 3 g of AC-S were heated at 130 ºC in an oven for 3 h. The starting potassium hydroxide solution for AC-S base impregnation was 1M, prepared by dissolving 0.56 g potassium hydroxide in 10 mL distilled water. Then the dried 3 g of AC-S were immersed in alkaline 1M prepared solution and kept under continuous stirring for 0.5 h at room temperature, an extra 0.75 h at 40-50 ºC to evaporate the water and then dried for 3 h at 130 ºC. The weight difference

between AC-S and AC-S/KOH 1M was 0.8 g. The next solutions for alkaline AC-S impregnation were 1.5M and 2M, following the same steps as with 1M solution (see Table 2). The same procedure was used to perform a second alkaline component impregnation, but for 1 h at room temperature plus an extra 0.75 h for water evaporation. The aim is to study time influence over alkaline properties of the catalyst (Table 3). Impregnation with 3M base solution was performed in the same manner, after several experimental biodiesel, to study catalyst loading along with the reaction time and the oil conversion.

Table 2

AC-S impregnation with alkaline compound for 0.5 h impregnation time

Base.conc. (M)	AC-S (g)	Distilled water (mL)	Added KOH (g)	Impreg. Yield (g)	Impreg.time (h)
KOH 1M	3	10	0.56	0.7	0.5
KOH 1.25 M	3	10	1.12	1.1	0.5
KOH 1.5 M	3	10	0.84	1	0.5
KOH 1 M	3	10	0.7	0.8	0.5

Table 3

AC-S impregnation with alkaline compound for 1 h impregnation time

Base.conc. (M)	AC-S (g)	Distil.water (mL)	Added KOH (g)	Impreg. yield (g)	Impreg.time (h)
KOH 3M	4	10	1.69	1.4	1
KOH 3M	4	10	1.69	1.5	1
KOH 2M	4	10	1.12	1.3	1
KOH 1.5 M	4	10	0.84	1.2	1
KOH 1 M	2	10	0.56	0.6	1

*Catalyst activity test***:** The synthetized catalyst sorts were tested in a transesterification reaction (eq.1) when used food oil is converted to biodiesel. First catalyst activation was performed in a 250 mL three neck bottle by mixing 10.79 g methanol (13.63 mL) with 1.25 g AC-S/KOH xM for 0.5 h at 50 °C at reflux under continuous stirring. Then the 50 ºC preheated oil was fed instantly in reactor. The reaction was kept at reflux and the conditions set was: 12:1 methanol/oil molar ratio, 65 °C reaction temperature, 5 % or 7 % catalyst and maximum 4 h reaction time.

$$TG + 3MeOH \Leftrightarrow Glycerol + 3FAME \quad (1)$$

After completion the solid catalyst was removed from reaction mixture and treated for another run; the reaction products were left to settle 24 h. The reaction mixture was separated both by settling and centrifugation and then the products were purified and prepared for characterization. The biodiesel yield and

the oil conversion were calculated before and after (see Table 4) products purification. Two homogeneous base catalyst transesterification reactions were also performed for comparative data's, using both fresh oil (B0 C) and used oil (B0 W) as feedstock.

Table 4

Catalitic activities on the esterification/transesterification reactions

Exp. no.	Oil (g)	Catalyst			Meth/oil molar ratio	React. time (h)	Oil conv. (%)	BioD pure (%)	Glycerol pure (%)
		(%)	(g)	KOH impregn.					
B0 C	50	1	0.5		6:1	2	99.18	95.36	89.15
B0 W	25	2	0.5		10.6:1	0.25	98.44	93.22	96.64
B7	25	7	1.75	2M-1h	12:1	2	89.69	88.64	85.27
B2	25	5	1.25	2M-1h	12:1	4	94.72	84.92	69.77
B3	25	7	1.75	2M-0.5 h	12:1	4	83.83	88.98	85.27
B9	25	7	1.75	1.5M-1 h	12:1	4	74.88	67.80	77.52
B6	25	5	1.25	2M-1 h	12:1	2	67.06	55.08	42.64
B8-Run2	25	7	1.75	2M-1h	12:1	4	50.29	46.61	15.50
B11	25	7	1.75	2M-1h	12:1	0.75	76.28	81.36	73.64
B12	25	5	1.25	3M-1h	12:1	0.75	83.26	84.32	69.77
B13	25	7	1.75	2M1-h	12:1	0,75	94.16	92.37	85.27
B14	25	3	0.75	3M-1h	12:1	1	94.44	89.83	73.64
B15	25	4	1	3M-1h	12:1	1	79.35	74.58	62.02
B16	25	4	1	3M-1h	12:1	1	80.19	76.69	54.26
B17	25	4	1	3M-1h	12:1	1	84.66	81.78	69.77
B18	25	4	1	3M-1h	12:1	1	86.06	79.66	85.27
B19-Run2	25	10	2.5	3M-1h	12:1	3	68.45	78.81	21.71
B20-Run2	25	5	1.25	3M-1h	12:1	2	61.19	62.71	17.44
B21-Run2	25	5	1.25	3M-1h	12:1	2	62.03	59.32	19.77

3. Results and discussions

As it is shown the AC-S impregnation were performed using potassium hydroxide solution with different molar concentrations. The first tested catalyst AC-S/KOH uses 1M potassium hydroxide solution impregnation with immediately testing in a biodiesel transesterification reaction. The result was not successful. Second prepared catalyst was directly 2M KOH impregnated, tested and reported positive results. After that we reduced to 1.5M and 1.25M the base solution concentration to impregnate the following AC-S catalysts. In order to study catalyst loading, reaction time on oil conversion, the impregnation with 3M base solution was performed. Reaction time was reduced significantly in the

reactions using this type of catalyst, from 4 h and 3 h up to 1 h and even 0.75 h reaction time, along with high oil conversion yielded in these experimental investigations. The effect of time reaction was not taken into consideration, the main reason being the fact that the 1 h and 0.75 h reactions were catalyzed using different catalyst loadings and different base catalyst concentrations, further studies remaining to establish this kind of effect on oil conversion and biodiesel yield.

Catalyst efficiency: The catalyst activity is in direct correlation with the conversion thus the catalyst performance is related to the oil amount transformed into desired (or undesired) product. In this work the highest obtained conversions, over 80 %, were in B2, B14, B13, B7, B18, B3 and B12 experiments. Here the oerrating conditions are: 65 ºC reaction temperature, 12:1 methanol/oil molar ratio, 5% and 7 % catalyst loading and 0.75 h (B13), 1 h (B14, B18 and B17), 2 h (B7) and 4 h (B3) reaction time. The experimental conversions and biodiesel yields, shown in Fig.1, prove the catalyst efficiency by comparing its results with the experimental results of homogeneous base catalyzed reactions B0C and B0W, which presented high conversions and yields as expected. Separation of main products should be considered also an advantage using this catalyst because of the reduced time and number operations.

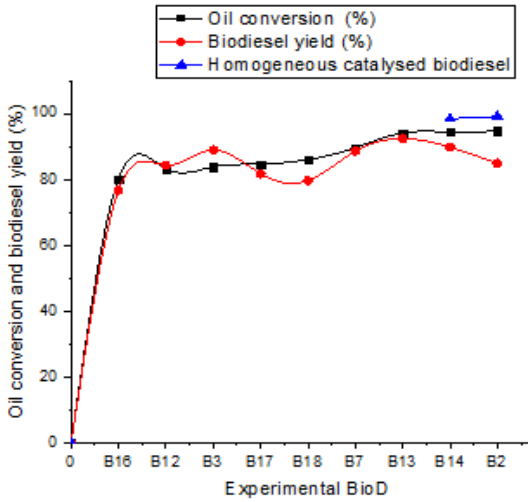

Fig. 1. Oil conversion and biodiesel yield: comparison between heterogeneous and homogeneous catalysed reaction in this experimental

Effect of alkaline impregnation time on biodiesel yield: Visible differences were observed between the reactions involving studied AC-S/KOH 2M-0.5 h and AC-S/KOH 2M-1 h and 3 M-1 h catalysts: catalyst with 1 h impregnation time showed a higher conversion rate, with about 60 % oil conversion after only 0.5h and while the catalyst with 0.5 h impregnation time showed a similar percent after

2.5 h only; the final oil conversion and biodiesel yield were also higher in the 2M-1 h and 3M-1 h catalyzed reactions, implying a correlation between the needed time for base component to stabilize on the catalytic support and outgoing (and the end of) reactions (Fig.2).

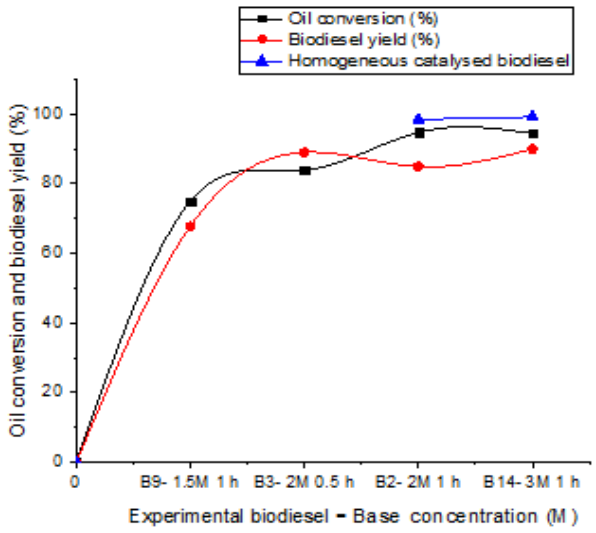

Fig. 2. Effect of alkaline impregnation time on oil conversion and biodiesel yield

Refractive index: The refractive index was determined using an Abbe Refractometer for both experimental biodiesel and glycerol to evaluate their characteristics before the purification operations.

Table 5

Refractive indices for experimental biodiesel

Exp. name	B0C	B0W	B12	B2	B18	B9	B14	B4	B20	B13
Refr. indice n_D^{30}	1.454	1.446	1.451	1.452	1.4528	1.453	1.4485	1.451	1.4585	1.446

The refractive indices variation at the determination time was influenced in the same manner as the methyl esters concentrations. Catalyst loadings along with catalyst base molar concentration had an effect on biodiesel yield and were thus reflected in this variation.

Table 6

Refractive indices for experimental glycerol

Exp. name	B11	B2	B15	B12	B21	B3	B4
Refractive indices n_D^{30}	1.460	1.458	1.458	1.456	1.455	1.449	1.445

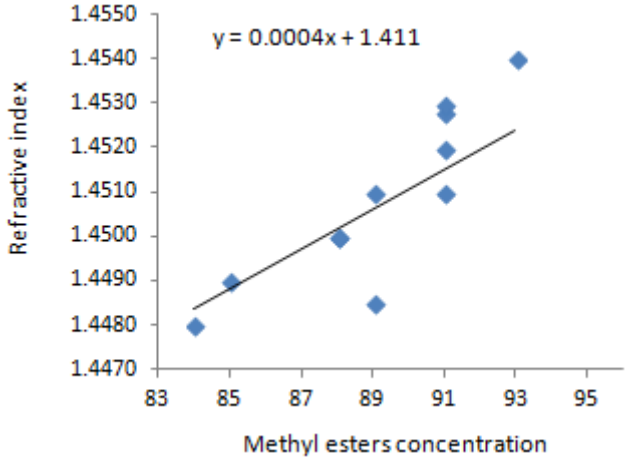

Fig. 3. Biodiesel refractive indices variation with biodiesel concentration

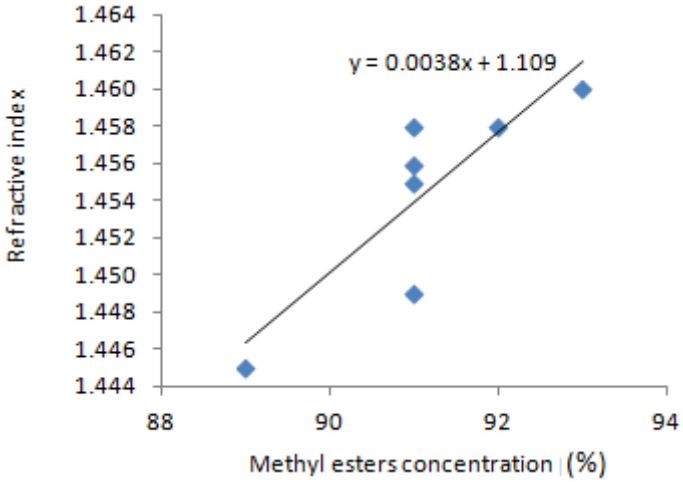

Fig. 4 . Glycerol refractive indices variation with biodiesel concentration

The values for biodiesel and glycerol refractive indices shown in Table 5 and Table 6 will be used as comparative data to evaluate purification method accuracy of both transesterification products in a future laboratory scale study.

Effect of catalyst loading: Heterogeneous catalyzed transesterification reaction has a lower reaction rate and it is a catalyst dependent reaction while the amount of catalyst loading is related to feedstock‘s chemical composition.

For the same reaction conditions except the catalyst amount it can be seen in Fig. 5 that the highest oil conversion and biodiesel yield obtained were over 90 %, when using 5 % and 7 % catalyst loading, with different base concentration.

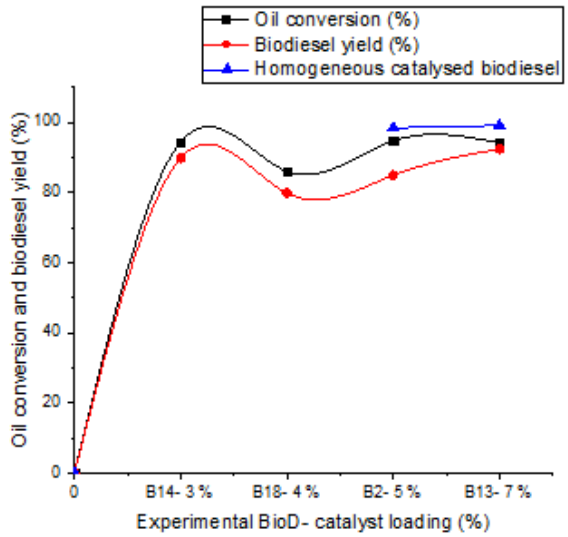

Fig. 5. Effect catalyst loading on biodiesel yield

Catalyst reusability: Reusability is an important feature for a heterogeneous catalyst and also the main difference between a solid and a homogeneous catalyst regarding the commercial viability of the catalyzed processes.

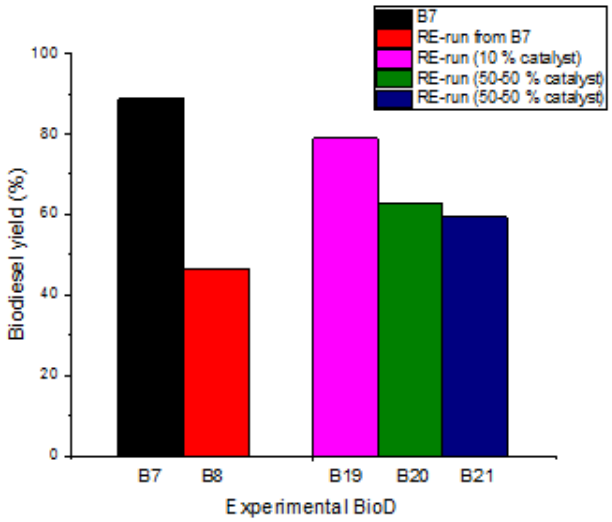

Fig. 6. Catalyst reusability

Catalyst with the highest biodiesel yielded that was selected to re-run in a second reaction, first suffered a methanol washing operation, dried at 130 °C for 3

h and then was fed again in the reactor to catalyze a new transesterification reaction in the same conditions. Catalyst loading for a different catalyst re-run was 10 %, representing 63 % used catalyst and 37 % fresh catalyst (3M). Third and fourth re-runs used 50-50 % different used and fresh catalyst (3M). Fig. 6 shows the biodiesel yield for these re-runs.

4. Conclusions

Reaction conditions were limited on purpose to match the mild homogeneous catalyzed reaction conditions associated to commercial-like biodiesel process: reaction temperature near 60 °C, reaction time 2-4 h (1-2 h commercial process), atmospheric pressure, 12:1 methanol/oil ratio (6:1, 10:1 commercial process) etc.

The AC proved to be an efficient, thermally and chemically stable catalytic support in both strong acid and base medium, at high temperature. AC sulphonated was 50 g in 200 mL H_2SO_4 98% comparing with 1g AC in 50 mL H_2SO_4 98% or 5 g AC in 100 mL H_2SO_4 98% from literature.

AC was successfully sulphonated and impregnated with both base and acid component and showed good catalytic activity in esterification and transesterification reaction to yield high conversion of used food oils to products of interest, to ease the separation of alchil esters and glycerol and to run a second batch as a reusable catalyst.

After studying the effect of impregnation time along with the effect on catalyst concentration we concluded that the minimum base impregnation time should be 1 h and that the higher base component concentration in AC-S KOH catalyst the higher conversion and biodiesel yield were obtained, thus for the future research we should make adjustments regarding the impregnation scheme.

The high conversion from B2, B14, B13, B7, B18, B3 and B12, experimental along with the over 85 % yield in biodiesel, showed and the reusability in B8, B19, B20, B21 (even the yield was only 46.61% to 78.81 %) prove that the heterogeneous catalyst for used food oils conversion to biodiesel can be an alternative for the commercial but conflictual feedstock based, environmental unfriendly homogeneous catalyzed actual processes on romanian biodiesel market.

REFERENCES

[1]. Rathore, V., Newalkar, B.L., Badoni, R.P., Processing of vegetable oil for biofuel production ,through conventional and non-conventional routes, *Energy for Sustainable Development* 31 (2016), 24–49.

[2]. Keera S.T., Sabagh, S.M.E., Taman, A.R, Transesterification of vegetable oil to biodiesel fuel using alkaline catalyst, *Fuel* 90 (2011), 42–7.

[3]. Sharma, Y.C., Singh B., Advancements in solid acid catalysts for ecofriendly and economically viable synthesis of biodiesel, *Biofuels, Bioprod. Bioref*. 5 (2011), 69–92.
[4]. Lubes, Z.I.Z., Zakaria, M., Analysis of parameters for fatty acid methyl esters production from refined palm oil for use as biodiesel in the single-and two stage processes, *Malay J Biochem Mol Biol* 17 (2009), 5–9.
[5]. Lee, A.F., Wilson, K., Recent developments in heterogeneous catalysis for the sustainable production of biodiesel, *Catalysis Today*, 242 (2015), 3–18.
[6]. Agarwal, M., Chauhan, G., Chaurasia, S.P., Singh, K., Study of catalytic behavior of KOH as homogeneous and heterogeneous catalyst for biodiesel production, *Journal of the Taiwan Institute of Chemical Engineers* 43 (2012), 89–94.
[7]. Konwar, L. Wärnå, J., J., Arvela, P.M., Kumar, N., Mikkola, J.P., Reaction kinetics with catalyst deactivation in simultaneous esterification and transesterification of acid oils to biodiesel(FAME) over a mesoporous sulphonated carbon catalyst, *Fuel* 166, (2016), 1–11.
[8]. Melero, J.A., Iglesias, J., Morales, G., Heterogeneous catalysts for biodiesel production: current status and future challenges, *Green Chem.*, 11, (2009), 1285–1308.
[9]. Shu, Q., Gao, J., Nawaz, Z., Liao, Y., Wang, D., Wang, J., Synthesis of biodiesel from waste vegetable oil with large amounts of free fatty acids using a carbon-based solid acid catalyst, *Applied Energy* 87, (2010), 2589–2596.
[10]. Devi, B.P., Gangadhar, K., Prashad, P.S., Prashad, R.N., Ind. Patent, WO 2009/016646 A1, 2009.
[11]. Zhang, H., Luo, X., Li, X., Chen, G.Z., He, F., Wu, T., Preparation and Characterization of a Sulfonated Carbon-based Solid Acid Microspheric Material (SCSAM) and its use for the Esterification of Oleic Acid with Methanol, *Austin Chem. Eng*., 1, (2016), 1024.

CORRELATIONS BETWEEN BIODIESEL PERCENTAGE AND DIESEL FUEL PROPERTIES

Ştefan ŞANDRU*, Diana CURSARU, Ion ONUŢU, Dorin STĂNICĂ EZEANU

Petroleum-Gas University of Ploieşti, Petroleum Processing Engineering and Environmental Protection, 39 Bucureşti Avenue, Ploieşti, Romania

Abstract
Biodiesel ratio in commercial diesel, has known a continuous growth over the years, estimating it will reach 10% until 2020. Having slightly different values of properties, the proportion in which biodiesel is used, will influence the final product. The purpose of this study is to determine correlation equations, for the chosen properties: density and viscosity. Using linear regression, the equations were determined and then tested on a new set of blends.

Keywords: linear regression, biodiesel-diesel blends, correlation equations.

1. Introduction

Biodiesel is a non-toxic and biodegradable fuel used in transport sector. [1] In present it can be found in commercial diesel, with a ratio of 5% and even 7% in some countries. Since it has slightly different values of properties, the proportion in which it is used, will affect the final product. This study approaches two properties, kinematic viscosity and density, in order to determine correlation equations. Using the properties values, determined in laboratory, and linear regression, it was possible to establish these correlation equations [2].

2. Experimental

Biodiesel, chemically, is a blend of methyl or ethyl esters, obtained by transesterification of vegetable oils. The transesterification reaction was performed at 50°C, using corn oil and methanol (molar ratio oil: methanol= 1:3) while being stirred vigorously for 2 hours and in the presence of KOH as catalyst. The separated biodiesel was used for formation of blends with diesel [3]. Hydrotreated diesel fuel, taken from a Romanian oil refinery is the second

* Corresponding author: E-mail address: sandru0318@gmail.com (Stefan Sandru)

component of the blend [4]. The methyl esters were mixed with the diesel fuels 0%, 1%, 3%, 6%, 9%, 12%, 50% and 100%, in order to determine the correlation equations. To test the determined equations, another 4 blends were made with 20 %, 30%, 70% and 80% biodiesel. For this 12 blends, densities and viscosities were determined, with the results shown in Table 1. The selected temperature for measuring the density and respectively the viscosity was done in accordance with the standards used to characterize diesel [5]. The viscosity was determined using the Ubbelohde capillary viscometer bath and density [6] and the density was determined using pycnometer [7].

Table 1.

Density and viscosity values for Biodiesel-Diesel blends

Properties / Biodiesel content (%)	Density at 17 °C (g/cm^3)	Viscosity at 40 °C (mm^2/s)
0 (pure diesel)	0.8410	2.7959
1	0.8430	2.8056
3	0.8436	2.8639
6	0.8447	2.9058
9	0.8458	2.8639
12	0.8466	3.006
20	0.8478	3.006
30	0.8509	3.2219
50	0.8618	3.3412
70	0.8685	3.8076
80	0.8722	3.9378
100 (pure biodiesel)	0.8834	4.3086

3. Results and discussions

A slight increase is noticeable in both properties values, as it can be seen in table 1. Biodiesel has both properties values slightly increased in comparison to diesel, as a consequence the biodiesel ratio increase will also increase the values of the final blend [8, 9]. The eight blends are represented in the graphs below, to ease up the determination of the correlation equations.

From the graphs presented in Figure 1 and 2 we can determine the equations by using the average slope and the intercept point [10]. This was possible due to the steady increase in values.

The correlation equations are presented below.

$$\rho_b = 0.8419 + 0.0004X \quad (1)$$

$$\nu_b = 2.7842 + 0.0145X \quad (2)$$

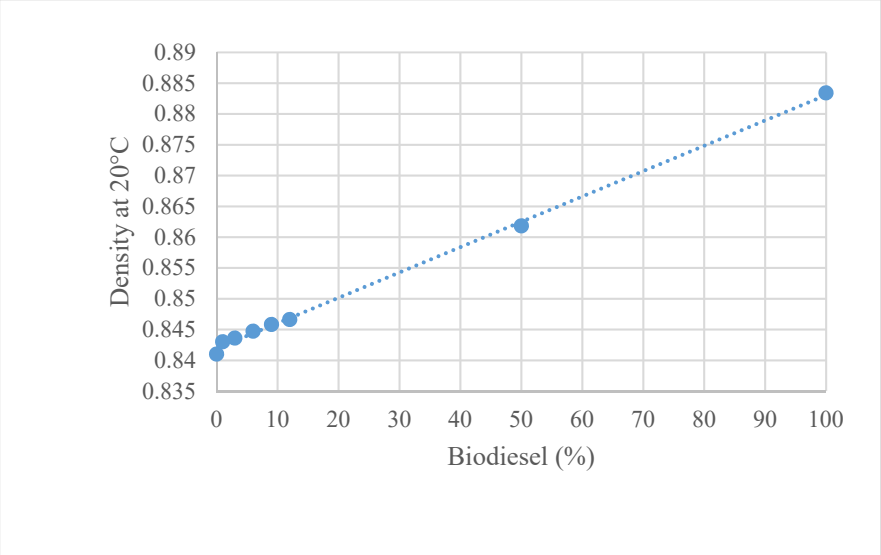

Fig. 1. Densities of methyl ester–diesel fuel blends at 20 ºC

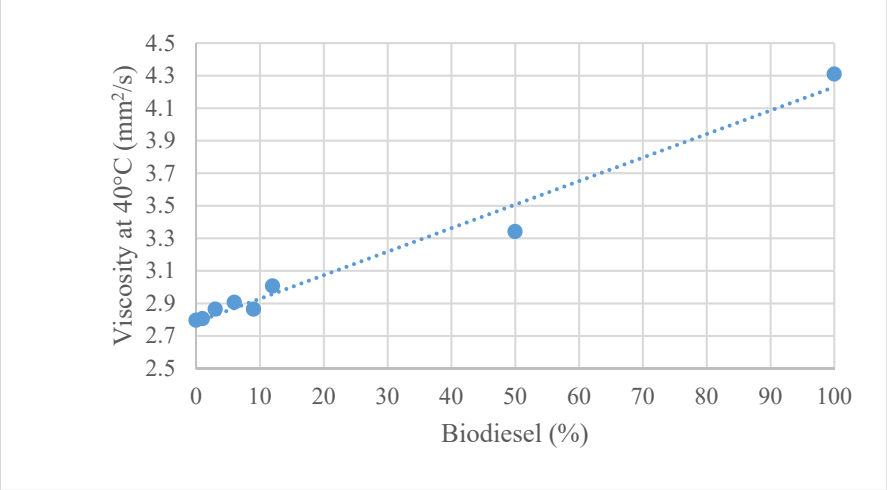

Fig. 2. Viscosities of methyl ester–diesel fuel blends at 40ºC

The first equation (1) corresponds to density and the second (2) is for viscosity. In both cases *X* represents the biodiesel ratio, in the final blend, measured in mL.

Using the newly determined formula, the values for density and viscosity for the initial eight blends was calculated, in order to determine the relative error. The results are presented in table 2 and 3. Since both equations were determined using linear regression, their precision is given by the number of the values used, more values resulting in a higher precision.

Table 2.

Relative error for density measurements

Biodiesel content (%)	Experimental density (g/cm^3)	Calculated density (g/cm^3)	| Calculated density - Experimental density|	Relative error
0	0.841	0.8419	0.0009	± 0.0125
1	0.843	0.8423	0.0007	
3	0.8436	0.8431	0.0005	
6	0.8447	0.8443	0.0004	
9	0.8458	0.8455	0.0003	
12	0.8466	0.8467	0.0001	
50	0.8618	0.8619	0.0001	
100	0.8834	0.8819	0.0015	

Table 3.

Relative error for viscosity measurements

Biodiesel content (%)	Experimental viscosity (mm^2/s)	Calculated viscosity (mm^2/s)	| Calculated viscosity - Experimental viscosity |	Relative error
0	2.7959	2.7842	0.0117	± 0.1146
1	2.8056	2.7987	0.0069	
3	2.8639	2.8277	0.0362	
6	2.9058	2.8712	0.0346	
9	2.8639	2.9147	0.0508	
12	3.006	2.9582	0.0478	
50	3.3412	3.5092	0.168	
100	4.3086	4.2342	0.0744	

If the absolute value of difference between the calculated value and measured value, does not exceed the limits given by the relative error, then it is safe to use the given result. If the value exceeds the limit, then an experimental determination will be needed.

To test the equations, four more blends were made, with 20%, 30%, 70% and 80% biodiesel. As it can be seen in tables 4 and 5, the equations gave results that did not exceed the limit imposed by the relative error.

Table 4.

Trial for density correlation equation

Biodiesel content (%)	Experimental density (g/cm^3)	Calculated density (g/cm^3)	| Calculated density - Experimental density|	Relative error
20	0.8499	0.8478	0.0021	± 0.0125
30	0.8539	0.8509	0.0030	
70	0.8699	0.8685	0.0014	
80	0.8739	0.8722	0.0017	

Table 5.

Trial for viscosity correlation equation

Biodiesel content (%)	Experimental viscosity (mm^2/s)	Calculated viscosity (mm^2/s)	| Calculated viscosity - Experimental viscosity |	Relative error
20	3.0742	3.006	0.0682	± 0.1146
30	3.2192	3.2219	0.0027	
70	3.7992	3.8076	0.0084	
80	3.9442	3.9378	0.0064	

4. Conclusions

This study was conducted on biodiesel made from corn oil. There were made a total of 12 blends with a ratio of: 0%, 1%, 3%, 6%, 9%, 12%, 20%, 30% , 50%, 70%, 80% , 100% biodiesel. For this 12 blends density and viscosity values were determined. The equations were determined, using linear regression, from 8 of the 12 blends. The other 4 were used to determine if the equations are genuine.

In the end it was proved that the determined equations are accurate, and give good and reliable results. To improve the accuracy of the equations, more experimental values are needed. Due to the different types of biodiesel and diesel, these correlation equations are only valid for this type of biodiesel and diesel. For further study artificial neural networks will be taken into consideration to predict the values, especially if the values appear to be random, or have a hidden pattern.

REFERENCES

[1] Tesfa B., Mishra R., Gu F., Powles N., Prediction Models for Density and Viscosity of Biodiesel and their Effects on Fuel Supply System in CI, *Renewable Energy*, 35(12), (2010), 1-3.

[2] Dominik R., Rainer J., Overview and Recommendations on Biofuel Standards for Transport in the EU; Eur. Dir., May 2006.
[3] Ashley D'Ann Koh, Two-step biodiesel production using supercritical methanol and ethanol, PhD Thesis, University of Iowa, Iowa Research Online, 2011.
[4] Shakinaz A. El Sherbiny, Ahmed A. Refaat, Shakinaz T. El Sheltawy; Production of biodiesel using the microwave technique, *Journal of Advanced Research*, 1, (2010), 309–314.
[5] EN 590; EN 14214; Diesel-ASTM D975; Biodiesel- ASTM D6751.
[6] http://www.multilab.ro/viscozitate/baie_vascozimetrica_ubbelohde.html, 2016.
[7] http://www.fisica.uson.mx/manuales/fluidos/fluidos-lab02.pdf, 2016.
[8] G. Knothe, K. R. Steidley: Kinematic viscosity of biodiesel fuel components and related compounds. Influence of compound structure and comparison to petrodiesel fuel components, *Fuel*: 84(9), (2005), 1059–1065.
[9] Sheehan J., Camobreco V., Duffield J., Graboski M., Shapouri H., An Overview of Biodiesel and Petroleum Diesel Life Cycles; www.nrel.gov/docs/legosti/fy98/24772, 1998.
[10] Tesfa B., Mishra R., Gu F., Powles N., Prediction Models for Density and Viscosity of Biodiesel and their Effects on Fuel Supply System in CI, *Renewable Energy*, 35(12), (2010), 11-13.

SURFACE PROPERTIES OF NOVEL AMINO ACID-BASED AND CARBOHYDRATE-BASED SURFACTANTS

Irina Elena CHICAN*, Dana Simona VĂRĂŞTEANU, Loti Cornelia OPROIU, Mircea RUSE

National Research and Development Institute for Chemistry and Petrochemistry-ICECHIM Bucharest Department of Chemical & Petrochemical Technologies, 202 Spl. Independentei, 060021, Bucharest, Romania

Abstract

Surface active properties of four novel amino acid-based and carbohydrate-based surfactants were studied. Critical micelle concentration in aqueous solutions was determined for 1,12-digluconamidododecane (bolaform surfactant), lauroyl hydroxyproline, palmitoyl hydroxyproline and 1,12-dodecanedioyl diglycylglycine (bolaform surfactant). The efficiency, surface excess concentration and minimum area per molecule were calculated. A high efficiency in decreasing the surface tension of distilled water was observed for lauroyl hydroxyproline and palmitoyl hydroxyproline. The critical micelle concentrations of amino acid-based surfactants are placed in the domain of anionic surfactants. The study demonstrates that the synthesized surfactants are viable alternative for the petrochemical compounds.

Key words: surfactant, amino acid, carbohydrate, critical micelle concentration, surface tension.

1. Introduction

Surfactants are used in large quantities in household and industrial activities. After use, surfactants are discharged into water treatment systems or into surface waters, often leading to negative environmental effects. Most surfactants are to some extent toxic to aquatic organisms, interacting with the biological membranes of the organisms. Because of this, there is a trend among the manufacturers of surfactants to replace the surfactants produced from petrochemical feedstocks with surfactants based on renewable raw materials. Surfactants with hydrophilic groups consisting of amino acids or carbohydrates and hydrophobic tails from vegetable oils are gaining increased attention due to the high degree of biodegradability, good surface-active properties and low toxicity [1-4]. In addition to these characteristics, amino acid-based and

* Corresponding author: Email address organica@icechim.ro (Irina Chican)

carbohydrate-based surfactants may present self-assembling capacity into supramolecular structures, such as fibers, ribbons and tubules [5-7]. The amino acid-based surfactants can be tailored in multiple structures. N-acyl derivatives (acyl amino acids) represent the most important class of protein-based surfactants, since they present no toxicity [8, 9] and are highly biodegradable [10]. Acyl-amino acids with anionic, cationic, amphoteric or non-ionic character can be obtained, depending on the ionic nature of the amino acid. The amino acids and alkyl chains can be combined to each other to generate single-chained, double-chained, gemini or bolaform surfactants. Carbohydrate-based surfactants are nonionic surfactants with superior detergency, foaming and wetting properties, gentle action on the epidermis and are highly biodegradable. They are used in institutional or household detergent formulations and in cosmetic industry. In this paper studies regarding the surface active properties of surfactants containing one or two amino acid/carbohydrate-derived head groups are presented. Surfactants were obtained by processes that comply with the principles of green chemistry (use of the aqueous reaction medium, or if it is not possible use of solvents with low toxicity, reaction temperatures up to 50°C). The surface tension and critical micelle concentration (CMC) in aqueous solutions were determined for 1,12-digluconamidododecane (bolaform surfactant), lauroyl hydroxyproline, palmitoyl hydroxyproline and 1,12-dodecanedioyl diglycylglycine (bolaform surfactant).

2. Experimental

Materials and methods

The amino acid-based surfactants used in this study were synthesized according to Schotten-Baumann method [11-14]. Lauroyl hydroxyproline and palmitoyl hydroxyproline was prepared from 4-hydroxyproline (Merck) and lauroyl chloride, respectively palmitoyl chloride (Merck), in alkaline medium. The bolaform surfactant 1,12-dodecanedioyl diglycylglycine was prepared from glycylglycine (Merck) and dodecanedioyl dichloride (Sigma-Aldrich), in alkaline medium. 1,12-Digluconamidododecane was synthesized from 1,12-diaminododecane (Sigma-Aldrich) and gluconolactone (Sigma-Aldrich). The structure of the surfactants was confirmed by FT-IR spectroscopy.

The structures of synthesized surfactants are presented in figure 1:

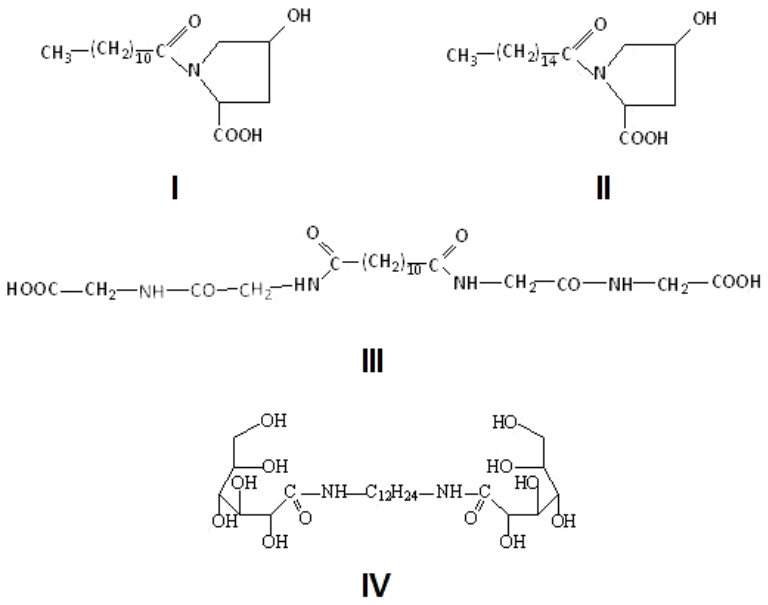

Fig. 1. Structures of amino acid-based and carbohydrate-based surfactants. (I) Lauroyl hydroxyproline; (II) Palmitoyl hydroxyproline; (III) 1,12-dodecanedioyl diglycylglycine; (IV) 1,12-digluconamidododecane

The surface tension and critical micelle concentration (CMC) were measured with a KSV Sigma 700 automated tensiometer. The measurements for CMC were performed using the DuNouy Ring technique. Successive quantities of a surfactant stock solution, prepared in distilled water, were added to a vessel containing 40 mL distilled water. Additions were made such that data were evenly spaced along the log scale of concentration. After each addition the surfactant, solution was stirred for 20 seconds with a waiting time after stir of 10 seconds.

3. Results and discussions

The critical micelle concentration is the point at which sudden variations occur of the various physico-chemical properties (such as surface tension) of the dilute solutions of surfactants and coincides with the formation of micelles on a large scale. Critical micelle concentration is an important parameter in surfactant characterization, since the optimum application domain ranks to the upper limit of the critical micelle concentration. The stock solutions of amino acid-based surfactants (lauroyl hydroxyproline, palmitoyl hydroxyproline and 1,12-dodecanedioyl diglycylglycine) were adjusted at pH 8 with a 25% NaOH solution,

in order to solubilize the surfactant in aqueous solution, ensuring the formation of the active part of the molecule, namely the anion $R\text{-}COO^-$.

The variation of surface tension vs. concentration of aqueous solutions of surfactants was plotted (fig. 1-3). CMC values were acquired from the intersection of the baseline and slope.

Beside the critical micelle concentration other surface properties were determined, namely:

Efficiency, π, of a surfactant, which is given by the difference between the surface tension γ_0 of pure solvent and surface tension γ at CMC.

$$\pi = \gamma_0 - \gamma \tag{1}$$

The surfactants which produce the largest decrease surface tension at CMC possess the highest efficiency. The surface tension of distilled water used in experiments is 71 mN/m.

Surface excess concentration, Γ_{max}, is defined as the difference between the concentration of the surfactant at the interface and in the volume of the solution and was calculated from the Gibbs equation:

$$\Gamma_{max} = -\frac{1}{2RT}\left(\frac{d\gamma}{d\ln c}\right) \tag{2}$$

where: R – gas constant;
T – absolute temperature;
γ – surface tension;
c – concentration of surfactant in aqueous solution.

Gibbs equation was modified by placing the factor 2 in the denominator, used in the case of anionic surfactants, in which the cation, although it is not surface-active, accumulates at the interface, making ion pair with the carboxyl group.

The **surface activity** is defined as $d\gamma/d\ln c$ and is an indicator showing the ability of the substance to decrease the surface free energy. The surface activity is in fact the slope of the concentration-dependent region of the surface tension.

A substance that lowers the surface energy is therefore in excess near the surface.

Minimum area per molecule, A_{min}, is the average area occupied by the surfactant molecule at the air/surfactant solution interface and was calculated according to the equation:

$$A_{min} = 1/N * \Gamma_{max} \tag{3}$$

where: N is Avogadro number;

Γ_{max} – surface excess concentration of adsorbed species;

The critical micelle concentrations of surfactant solutions, determined by surface tension, are shown in figures 2-4. In figure 5 is represented the surface tension of 1% solution of 1,12-digluconamidododecane, comparative with surface tension of distilled water.

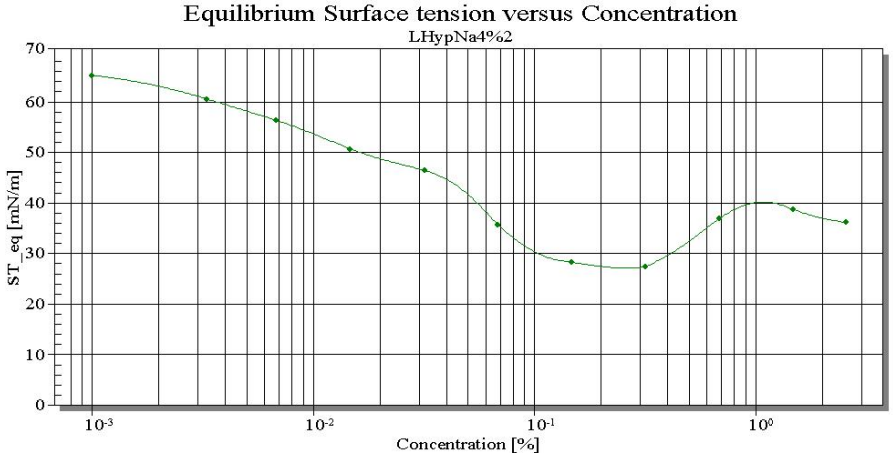

Fig. 2. Surface tension vs. logarithm of concentration curve for lauroyl hydroxyproline sodium salt

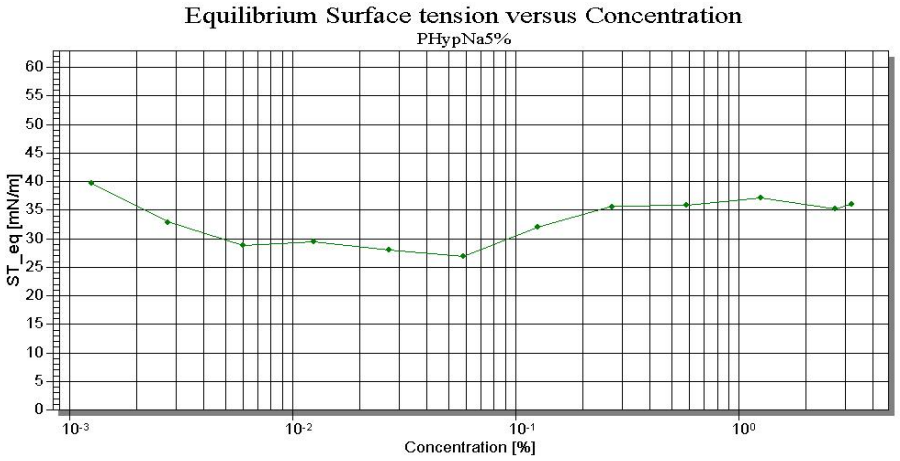

Fig. 3. Surface tension vs. logarithm of concentration curve for palmitoyl hydroxyproline sodium salt

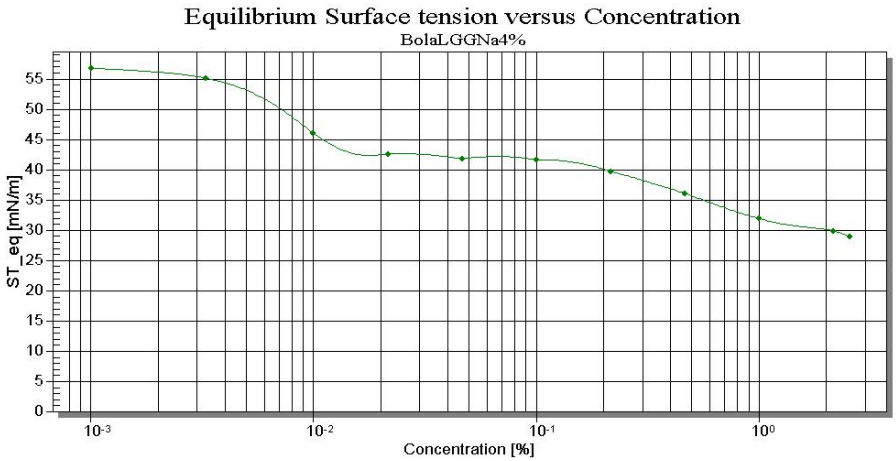

Fig. 4. Surface tension vs. logarithm of concentration curve for 1,12-dodecanedioyl diglycylglycine disodium salt

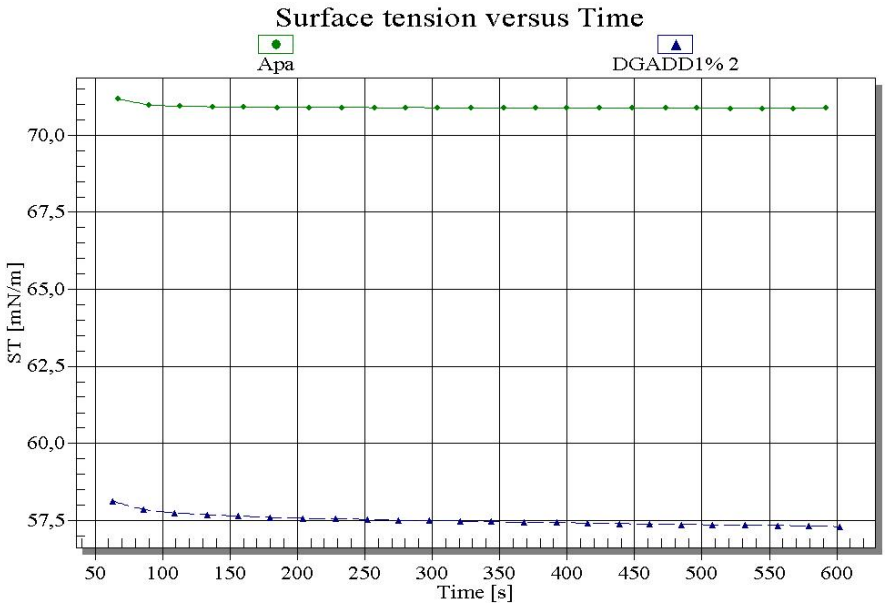

Fig. 5. Surface tension of 1% solution of 1,12-digluconamidododecane, comparative with surface tension of distilled water

In Table 1 are presented the surface properties for amino acid-based surfactants.

Table 1

Surface properties for amino acid-based surfactants

Surfactant	CMC, g/L	Surface tension, mN/m	Efficiency	dγ/dlnc, mN/m	10^{10} x Γ_{max}, mol/cm^2	10^2 x A_{min}, nm^2
Lauroyl hydroxyproline sodium salt	1.45	27.85	43.15	-27.22	5.47	29
Palmitoyl hydroxyproline sodium salt	0.35	27.44	43.56	-3.92	0.79	210
1,12-dodecanedioyl diglycylglycine disodium salt	0.22	41.76	29.24	-15.25	3.08	53
Lauroyl glygylglyginate sodium salt [14,15]	3.60	28.26	42.71	-20.10	4.06	41

If we refer to the sodium dodecyl sulfate, a reference anionic surfactant for studies of surface properties of surfactants, with a critical micelle concentration of 2.3 g/L and a surface tension at CMC of 34 mN/m, it was found that lauroyl hydroxyproline sodium salt and palmitoyl hydroxyproline sodium salt have lower CMC value than sodium dodecyl sulfate and have greater efficacy in lowering the surface tension at CMC.

The CMC of hydroxyproline-based surfactants decreases with increasing of hydrocarbonate chain, the CMC of palmitoyl hydroxyproline sodium salt solution was 0.35 g/L, while the CMC of lauroyl hydroxyproline sodium salt was 1.45 g/L. The explanation lies in the fact that increasing the length of hydrophobic chain causes a more pronounced adsorption of surfactant molecules at the air-water interface due to a higher asymmetry between the hydrophilic and hydrophobic groups.

Minimum area per molecule (A_{min}) is an important parameter to judge the arrangement of molecules in the surface adsorption layer. Regarding the hydroxyproline-based surfactants I and II, there is an increase of A_{min} with the increase of the hydrocarbonate chain, due to the higher hydrophobicity of the molecule II, which lead to reducing the density of molecules at the air-solution interface. By comparing the minimum area per molecule of bolaamphiphilic surfactant III with lauroyl glygylglyginate sodium salt, it can be noted a higher value of A_{min} for bolaform surfactant III, fact that can be attributed to a looser packing of molecules. Bolaform surfactants often present a U-shape conformation at the air/water interface.

Comparing the surface properties for 1,12-dodecanedioyl diglycylglycine disodium salt (bolaform surfactant with one hydrophobic chain and two headgroups) from table 1 with surface properties of lauroyl glygylglycinate

sodium salt (surfactant with one hydrophobic chain and one headgroup), previously synthesized and characterized by our team [14, 15] it can be noted that the CMC of 1,12-dodecanedioyl diglycylglycine disodium salt (0.22 g/L) is smaller than the CMC of lauroyl glygylglycinate sodium salt (3.6 g/L) by one order, indicating a greater micellization ability of bolaform surfactant.

For the carbohydrate-based surfactant 1,12-digluconamidododecane it was acquired only the surface tension of 1% solution, comparative with surface tension of distilled water, since the surfactant presents limited solubility in water. The surfactant 1,12-digluconamidododecane will be tested in terms of self-assembly capacity.

The results indicate that the novel surfactants possess high surface active properties, compared to conventional surfactants, being viable alternative for the petrochemical compounds.

6. Conclusions

The surface properties in aqueous solutions were determined for 1,12-digluconamidododecane (bolaform surfactant), lauroyl hydroxyproline, palmitoyl hydroxyproline and 1,12-dodecanedioyl diglycylglycine (bolaform surfactant). The influence of the hydrophobic chain length upon CMC was studied for hydroxyproline-based surfactants. The CMC value of palmitoyl hydroxyproline sodium salt was lower than the CMC of lauroyl hydroxyproline sodium salt, due to the more pronounced adsorption of surfactant molecules at the air-water interface. The enhanced hydrophobicity of palmitoyl hydroxyproline sodium salt lead also to an increased minimum area per molecule.

A greater micellization ability of bolaform surfactant 1,12-dodecanedioyl diglycylglycine disodium salt was observed from the lower CMC value, compared with lauroyl glygylglycinate sodium salt.

Efficiency of about 40 mN/m of aqueous solutions of sodium lauroyl hydroxyproline and sodium palmitoyl hydroxyproline, indicated that are effective in decreasing the surface tension of water at critical micelle concentration.

The results indicate that the novel surfactants possess high surface active properties, compared to conventional surfactants, being viable alternative for the petrochemical compounds.

Acknowledgements

This work was financially supported by National Authority for Scientific Research and Innovation, in the frame of Nucleu Programme-Project **PN 16.31.02.03**.

REFERENCES

[1]. K. Holmberg, Natural surfactants, *Curr. Opin. Colloid Interf. Sci.*, 6(2), (2001), 148-159.

[2]. P. Clapés, M.R. Infante, Amino Acid-based Surfactants: Enzymatic Synthesis,Properties and Potential Applications, *Biocatal. Biotransf.*, 20(4), (2002), 215–233.

[3]. R.O. Brito, S.G. Silva, R.M.F. Fernandes, E.F. Marques, J. Enrique-Borges, M.L.C. do Vale, Enhanced interfacial properties of novel amino acid-derived surfactants: effects of headgroup chemistry and of alkyl chain length and unsaturation, *Colloids Surf. B: Biointerfaces*, 86, (2011), 65–70.

[4]. S. Gatard, M. N. Nasir, M.Deleu, N. Klai, V. Legrand, S. Bouquillon, Bolaamphiphiles Derived from Alkenyl L-Rhamnosides and Alkenyl D-Xylosides: Importance of the Hydrophilic Head, *Molecules*, vol.18, (2013), 6101-6112.

[5]. S. Roy, J. Dey, Effect of hydrogen-bonding interactions on the self-assembly formation of sodium N-(11-acrylamidoundecanoyl)-l-serinate, l-asparaginate, and l-glutaminate in aqueous solution, *J. Colloid Interface Sci.* 307, (2007), 229–234.

[6]. T. Shimizu, M. Masuda, H. Minamikawa, Supramolecular nanotube architectures based on amphiphilic molecules, *Chem. Rev.* 105, (2005), 1401–1444.

[7]. D. Vărăşteanu, M. C. Corobea, M. Ghiurea, S. Pop, I. Chican, D. Florea, A. Piscureanu, I. Călinescu, Variable morphologies of self-assembled metal-complexed lauroyl-glycylglycine in the presence of montmorillonite-silica nanowires, *Optoelectron. Adv. Mat.*, 7(11-12), (2013), 991-996.

[8]. P. Clapés, M.R. Infante, Amino Acid-based Surfactants: Enzymatic Synthesis,Properties and Potential Applications, *Biocatal. Biotransf.*, 20(4), (2002), 215–233.

[9]. N. Ménarda, N. Tsapis, C. Poirier, T.Arnauld, L. Moine, F. Lefoulon, J.M. Péan, E. Fattal, Drug solubilization and in vitro toxicity evaluation of lipoamino acid surfactants, *Int. J. Pharm.*, 423, (2012), 312-320.

[10]. Infante, M., Pinazo, A., Seguer, Non-conventional surfactants from amino acids and glycolipids: structure, preparation and properties, *J. Colloids Surf. A: Physicochem. Eng. Aspects*, 123–124, (1997), 49–70,

[11]. A. Paquet, Preparation of some long-chain N-acyl derivatives of essential amino acids for nutritional studies, *Biochem. Cell Biol.*, 58(7), (1980), 573–576.

[12]. S.Y. Mhaskar, R.B.N. Prasad, G. Lakshminarayana, Synthesis of N-Acyl Amino Acids and Correlation of Structure with Surfactant Properties of Their Sodium Salts, *J.Am. Oil Chem. Soc.*, 67(12), (1990), 1015-1019.

[13]. E. Jungermann, J.F. Gerecht, I.J. Krems, The preparation of long chain N-acylamino acids, *J.Am. Oil Chem. Soc.*, 78, (1956), p. 172.

[14]. D. Vărăşteanu, A. Piscureanu, I. E. Chican, M. C. Corobea, Aspects regarding the synthesis and surface properties of some glycine based surfactants, *U.P.B. Sci. Bull., B Series*, 73(3), (2011), 147-154.

[15]. D. Vărăşteanu, I. Chican, L. Oproiu, M. Simion, Relationship between structure and surface properties of protein-based surfactants - *International Symposium "Priorities of chemistry for a sustainable development - PRIOCHEM, XIth edition*, 29 – 30 Oct. 2015, Bucharest.

MATHEMATICAL MODELS FOR ENCAPSULATION OF ALUMINUM PIGMENTS IN SiO_2 MATRICES

Alina SMOCHINĂ[1], Draga DRAGNEA, Costin Sorin BÎLDEA

University Politehnica of Bucharest, Department of Chemical and Biochemical Engineering

Abstract

Sol-gel encapsulation is known as a solution for avoiding the degradation of aluminum pigments in water systems and keeping their decorative proprieties. In this paper, we present theoretical models of aluminum encapsulation using TEOS as precursor. After a basic understanding of the TEOS - Water system, more details are gradually added. The models predict the temporal evolution of various species when hydrolysis, water-forming condensation and alcohol-forming condensation are considered. A statistical reaction model is also presented in order to reduce the number of rate constants. To check the model correctness, moieties and atom conservation equations are formulated.

Key words: aluminum pigments, encapsulation, modeling, tetraethyl orthosilicate, SiO_2 matrices

1. Introduction

Aluminum pigments are well-known in paint and coatings industry due to their excellent metallic appearance [6-7]. Traditionally, aluminum pigments are incorporated into solvent-borne paints, but due to environmental concerns, water-borne systems are developed in order to reduce the organic emissions [5]. However, aluminum can easily react with water, leading to aluminum hydroxide and hydrogen [2]. There are different methods of stabilizing aluminum pigments in aqueous media, the most used ones being the adsorption or precipitation of corrosion inhibitors and coating the pigments with a protective layer. In order to avoid the emission of metallic compounds, encapsulation of aluminum pigments is the preferred method. Encapsulation can be achieved by using inorganic polymers (sol-gel process), organic polymers or composite polymers. Organic coatings (such as styrene-maleic anhydride copolymers, saccharides) show good compatibility with resins, but poor stability in alkaline media [7]; encapsulation with inorganic-organic composite polymers are quite promising, but many combinations of inorganic precursor – organic monomer are possible and few systems have been

[1] Corresponding author; *E-mail:* alina.smochina@gmail.com

tested; while, inorganic coatings (as SiO_2 polymer) show excellent stability and are well-known in the literature [4].

The most used inorganic precursor for aluminum encapsulations is tetraethyl orthosilicate (*TEOS*), which has four hydrolysable groups. Other reactions that might occur in the TEOS – Water system involve water-forming condensation and alcohol-forming condensation. The same types of condensation are considered between TEOS – Water species and hydrolyzed aluminum surface. In this work, different mathematical models are built based on these types of reactions, making appropriate assumptions.

2. Aluminum encapsulation modeling: TEOS – Water system

The sol-gel reactions can be described at different levels of detail. In the following, we will present the main reactions in the TEOS – Water system ("*Basic Approach*"); afterwards, the analysis will include all the species that might be formed during TEOS – Water interactions ("*Detailed Approach*").

2.1. TEOS – Water Basic Approach

The modeling starts with description of the main reactions of the TEOS – Water system: hydrolysis, water-forming condensation and alcohol-forming condensation. These involve the following functional groups: "–OR", "–OH", and "-OSi" without considering how are they distributed within the silicon atoms. Thus, there are reactions, each characterized by one reaction rate constant:

Reaction 1: - Hydrolysis

$$SiOR + H_2O \xrightarrow{k_H} SiOH + ROH$$

Reaction 2: - Water-forming condensation

$$2SiOH \xrightarrow{k_{CW}} Si - OSi + H_2O$$

Reaction 3: - Alcohol-forming condensation

$$SiOH + SiOR \xrightarrow{k_{CA}} Si - OSi + ROH$$

where:

k_H – is the rate constant of hydrolysis, expressed in $\frac{L}{mol \cdot min}$;

k_{CW} – is the rate constant of water-forming condensation, expressed in $\frac{L}{mol \cdot min}$;

k_{CA} – is the rate constant of alcohol-forming condensation, expressed in $\frac{L}{mol \cdot min}$;

Based on these reactions, the following equations describe the species concentrations:

$$\frac{d[SiOR]}{dt} = -r_1 - r_3 \quad (1)$$

$$\frac{d[SiOH]}{dt} = r_1 - 2 \cdot r_2 - r_3 \quad (2)$$

$$\frac{d[Si-OSi]}{dt} = r_2 + r_3 \quad (3)$$

$$\frac{d[H_2O]}{dt} = -r_1 + r_2 \quad (4)$$

$$\frac{d[ROH]}{dt} = r_1 + r_3 \quad (5)$$

where:

$$r_1 = k_H \cdot [SiOR] \cdot [H_2O] \quad (6)$$

$$r_2 = k_{CW} \cdot [SiOH]^2 \quad (7)$$

$$r_3 = k_{CA} \cdot [SiOH] \cdot [SiOR] \quad (8)$$

[A] – concentration of species A

2.2. TEOS – Water Detailed Approach

A more realistic scenario is to consider all the species that can be formed during hydrolysis, water-forming condensation and alcohol-forming condensation.

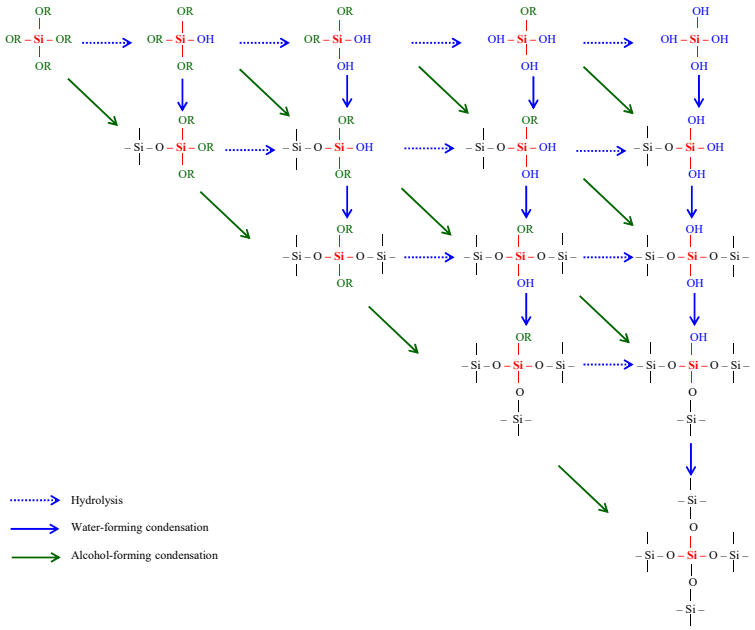

Fig. 1. The species matrix within TEOS – Water system Detailed Approach

Fig. 1 shows 15 different species, displayed in a matrix, which can be formed from *TEOS* by successive hydrolysis and condensation reactions. This model considers only forward reactions, thus assumes that the equilibrium strongly favors the product species. Each Si atom retains a coordination number of 4. The only functional groups that can be attached to Si atom in this system are: "–OR", "–OH", or "–OSi". Hydrolysis reactions occur left-to-right (dotted blue arrows), starting with *Si(OR)4* and ending with *Si(OH)4*; water-forming condensation occurs top-to-bottom (blue arrows) and alcohol-forming condensation (green arrows) proceeds diagonally from *TEOS* to *SiO2*.

Naming and numbering

Because of the large number of species, it is necessary to develop a naming convention describing the functional groups attached to the central silicon atom. This way, a triplet (X, Y, Z) denotes the number of "–OR" groups (X), "–OH" groups (Y), respectively "–OSi" groups (Z). The sum X + Y + Z = 4 for every Si atom and corresponds to the silicon coordination number. The species matrix represented in **Fig. 1** becomes:

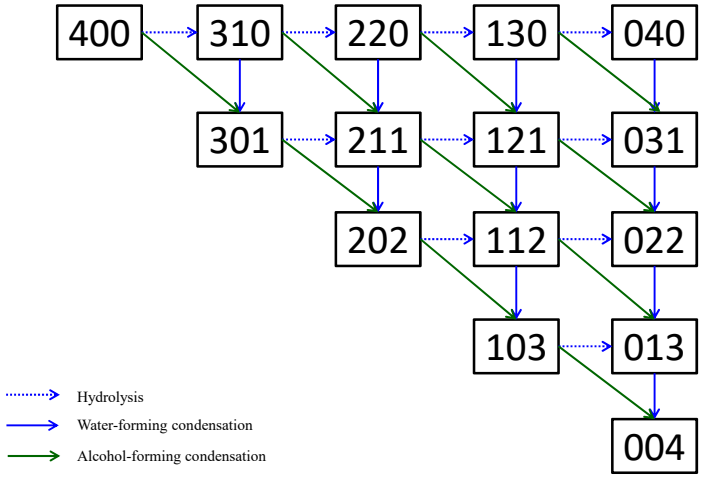

Fig. 2. The species matrix within TEOS – Water system Detailed Approach, represented as (X,Y,Z) triplet

To completely describe the system, 165 rate constants must be estimated from experimental data [1-3]: 10 for hydrolysis, 55 for water-forming condensation, and 100 for alcohol-forming condensation. As this is clearly a daunting task, the number of rate coefficients must be reduced.

One way of reducing the number of rate coefficients is through the use of a probabilistic model, which uses the following assumptions:

- the hydrolysis and condensation rate constants do not depend on the local silicon chemical environment; they depend only on the functional group reactivity.
- the rate coefficient of a given species is the product of a combinatorial probability factor and the appropriate functional group rate coefficient.

$$k_{H_i} = X_i \cdot k_H \quad (9)$$
$$k_{CW_{i,j}} = Y_i \cdot Y_j \cdot k_{CW} \quad (10)$$
$$k^H_{CA_{i,j}} = Y_i \cdot X_j \cdot k_{CA} \quad (11)$$
$$k^R_{CA_{i,j}} = X_i \cdot Y_j \cdot k_{CA} \quad (12)$$

For example, the rate constant $k_{CW_{i,j}}$ of water-forming condensation between species i and j is proportional to the number of hydroxyl groups attached to the reacting Si atoms, Y_i and Y_j.

Implementing the probabilistic model into TEOS – Water system Detailed Approach, the general species concentration equation will be the following:

$$\frac{d[X,Y,Z]}{dt} = r_1 + r_2 + r_3 - r_4 - r_5 - r_6 + r_7 - r_8 \quad (13)$$

where:

$$r_1 = k_H \cdot (X+1) \cdot [X+1, Y-1, Z] \cdot [H_2O] \quad (14)$$
$$r_2 = k_{CA} \cdot (X+1) \cdot [X+1, Y, Z-1] \cdot [SiOH] \quad (15)$$
$$r_3 = k_{CW} \cdot (Y+1) \cdot [X, Y+1, Z-1] \cdot [SiOH] \quad (16)$$
$$r_4 = -k_H \cdot X \cdot [X, Y, Z] \cdot [H_2O] \quad (17)$$
$$r_5 = -k_{CA} \cdot X \cdot [X, Y, Z] \cdot [SiOH] \quad (18)$$
$$r_6 = -k_{CW} \cdot Y \cdot [X, Y, Z] \cdot [SiOH] \quad (19)$$
$$r_7 = k_{CA} \cdot (Y+1) \cdot [X, Y+1, Z-1] \cdot [SiOR] \quad (20)$$
$$r_8 = -k_{CA} \cdot Y \cdot [X, Y, Z] \cdot [SiOR] \quad (21)$$

Hydrolysis (r_1 and r_4). A compound can be formed through hydrolysis of another compound that has one "–OR" group more and one "–OH" group less. The probability of hydrolysis is proportional to the number of "–OR" groups.

Water-forming condensation (r_3 and r_6). In this case, one "–OH" group of a compound reacts with *SiOH*, forming one molecule of water. *SiOH* stands for any "–OH" group attached to a silicon atom. So, the more such groups exist in the mixture, the higher will be the probability of reaction. The formed chemical compound will have a new "–OSi" bond and one "–OH" group less than the original.

Alcohol-forming condensation (r_2, r_5, r_7 and r_8). In this case there are two possibilities. The first way is a condensation of a specie that has one "–OR" group more and one "–OSi" bond less than the product. This condensation requires *SiOH*. But, also, it is possible to have the same alcohol-forming condensation from a specie that has one "–OH" group more and one "–OSi" bond less than the product, reaction which needs *SiOR* (meaning any "–OR" group attached to a silicon atom).

Rearranging the terms, the final master equation for any compound *i*, which has *X* "–OR" groups, *Y* "–OH" groups and *Z* "–OSi" bonds within TEOS – Water System will be the following:

$$\frac{d[X_i,Y_i,Z_i]}{dt} = k_H \cdot \{(X_i+1)\cdot[(X_i+1),(Y_i-1),Z_i] - X_i[X_i,\,Y_i,\,Z_i]\}\cdot[H_2O] + k_{CW}\cdot \{(Y_i+1)\cdot[X_i,(Y_i+1),(Z_i-1)] - Y_i[X_i,\,Y_i,\,Z_i]\}\cdot\sum_j Y_j\cdot[X_j,\,Y_j,\,Z_j] + k_{CA}\cdot[\{(X_i+1)\cdot[(X_i+1),Y_i,(Z_i-1)] - X_i\cdot[X_i,\,Y_i,\,Z_i]\}\cdot\sum_j Y_j\cdot[X_j,\,Y_j,\,Z_j] + \{(Y_i+1)\cdot[X_i,(Y_i+1),(Z_i-1)] - Y_i[X_i,\,Y_i,\,Z_i]\}\cdot\sum_j X_j\cdot[X_j,\,Y_j,\,Z_j]] \quad (22)$$

Results for TEOS – Water system Detailed Approach

The system of differential equation obtained by writing eq. (22) for all 15 species from the TEOS – Water system was solved in Matlab. The results are presented in the following plots (Figure 3). The initial reactants ratio is TEOS : H_2O = 1 : 5.

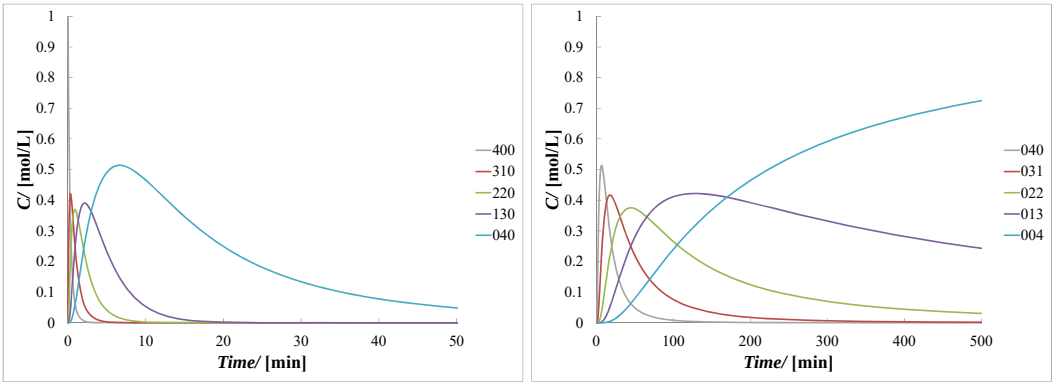

Fig. 3. Time dependence for: left – 400, 310, 220, 130, 040 species; right – 040, 031, 022, 013, 004 species.

As expected, the concentration of TEOS (species 400) decreases due to hydrolysis. The hydrolyzed species (left plot) are gradually formed until a maximum concentration, being consumed afterwards. The same behavior is observed for the

species formed through condensation, although the maximum appears later. The only increasing concentration is the silica polymer product (the 004 compound).

3. Aluminum encapsulation modeling: TEOS – Water – Aluminum system

A more complex system is formed when aluminum is added to the TEOS – Water mixture.

3.1. TEOS – Water – Aluminum Basic Approach

In addition to the hydrolysis - condensation reactions (r_1, r_2 and r_3) occurring in the TEOS – Water system ("*Basic Approach*"), the condensation reactions with hydrolyzed aluminum surface are also considered (r_4, r_5).

$\boldsymbol{r_1}$: $SiOR + H_2O \xrightarrow{k_H} SiOH + ROH$
$\boldsymbol{r_2}$: $2SiOH \xrightarrow{k_{CW}} Si - OSi + H_2O$
$\boldsymbol{r_3}$: $SiOH + SiOR \xrightarrow{k_{CA}} Si - OSi + ROH$
$\boldsymbol{r_4}$: $SiOH + MOH \xrightarrow{k_{MSCW}} Si - OM + H_2O$
$\boldsymbol{r_5}$: $SiOR + MOH \xrightarrow{k_{MSCA}} Si - OM + ROH$

When a hydroxyl group at Al surface (*MOH*) reacts with a species which has an „–OH" group, a *Si-OAl* bond and water will result. When *MOH* reacts with a species which has an „–OR" group, *Si-OAl* bond and alcohol will be the products.

The evolution of species concentration will be the following:

$$\frac{d[SiOR]}{dt} = -r_1 - r_3 - r_5 \quad (23)$$
$$\frac{d[SiOH]}{dt} = r_1 - 2r_2 - r_3 - r_4 \quad (24)$$
$$\frac{d[Si-OSi]}{dt} = r_2 + r_3 \quad (25)$$
$$\frac{d[H_2O]}{dt} = -r_1 + r_2 + r_4 \quad (26)$$
$$\frac{d[ROH]}{dt} = r_1 + r_3 + r_5 \quad (27)$$
$$\frac{d[MOH]}{dt} = -r_4 - r_5 \quad (28)$$
$$\frac{d[SiOM]}{dt} = r_4 + r_5 \quad (29)$$

where:

$$r_1 = k_H \cdot [SiOR][H_2O] \quad (30)$$
$$r_2 = k_{CW} \cdot [SiOH][SiOH] \quad (31)$$
$$r_3 = k_{CA} \cdot [SiOR][SiOH] \quad (32)$$

$$r_4 = k_{MSCW} \cdot [SiOH][MOH] \quad (33)$$
$$r_5 = k_{MSCA} \cdot [SiOR][MOH] \quad (34)$$

3.2. TEOS – Water – Aluminum Detailed Approach

The TEOS – Water – Aluminum Detailed Approach, presented in Figure 4, will follow the same rules as described in section 2.2. The same three types of reactions are valid inside every sub-system (TEOS – Water sub-system and Aluminum sub-system): hydrolysis, water-forming condensation and alcohol-forming condensation with a possibility of various species formation. Every of the species from TEOS – Water sub-system can react with *MOH* through condensation reactions and form the corresponding species.

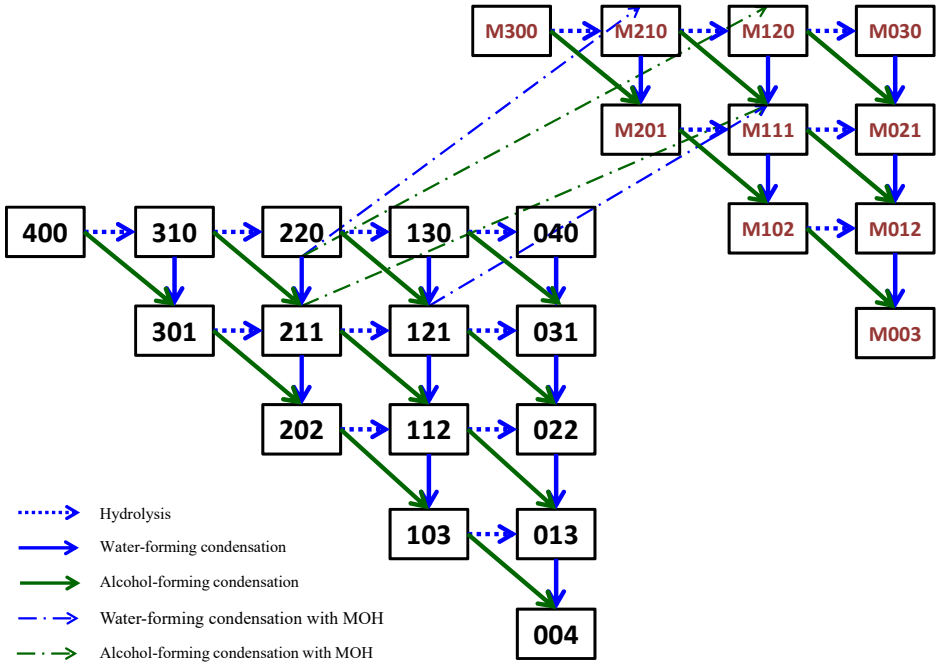

Fig. 4 The species matrix within TEOS – Water – Aluminum system Detailed Approach

For example, the compound *M111* from the diagram, which contains one *Si – OAl* bond, one „–OR" group, one „–OH" group and one „–OSi" group can be formed via hydrolysis from *M201*, water-forming condensation from *M120* or alcohol-forming condensation from *M210*. In the same time, the *M111* compound can result from the basic TEOS – Water sub-system, namely from *121* and *211* species through condensation with *MOH*.

The mathematical expressions are similar to eq. (22), but additionally include two terms describing the reaction between species from the bulk TEOS – Water sub-system with hydrolyzed aluminum surface.

Chemical species from bulk (TEOS – Water):

$$\frac{d[X_i,Y_i,Z_i]^{(b)}}{dt} = k_H \cdot \{(X_i+1)\cdot[(X_i+1),(Y_i-1),Z_i]^{(b)} - X_i\cdot[X_i,\ Y_i,\ Z_i]^{(b)}\}\cdot[H_2O] + k_{CW}\cdot\{(Y_i+1)\cdot[X_i,(Y_i+1),(Z_i-1)]^{(b)} - Y_i\cdot[X_i,\ Y_i,\ Z_i]^{(b)}\}\cdot\sum_j Y_j\cdot\left[X_j,\ Y_j,\ Z_j\right]^{(b)} + k_{CA}\cdot\left[\{(X_i+1)\cdot[(X_i+1),Y_i,(Z_i-1)]^{(b)} - X_i\cdot[X_i,\ Y_i,\ Z_i]^{(b)}\}\cdot\sum_j Y_j\cdot\left[X_j,\ Y_j,\ Z_j\right]^{(b)} + \{(Y_i+1)\cdot[X_i,(Y_i+1),(Z_i-1)]^{(b)} - Y_i\cdot[X_i,\ Y_i,\ Z_i]^{(b)}\}\cdot\sum_j X_j\cdot\left[X_j,\ Y_j,\ Z_j\right]^{(b)}\right] - X_i\cdot k_{MSCA}\cdot[MOH]\cdot[X_i,\ Y_i,\ Z_i]^{(b)} - Y_i\cdot k_{MSCW}\cdot[MOH]\cdot[X_i,\ Y_i,\ Z_i]^{(b)} \quad (35)$$

Chemical species attached to aluminum:

$$\frac{d[X_i,Y_i,Z_i]^{(M)}}{dt} = k_H \cdot \{(X_i+1)\cdot[(X_i+1),(Y_i-1),Z_i]^{(M)} - X_i\cdot[X_i,\ Y_i,\ Z_i]^{(M)}\}\cdot[H_2O] + k_{CW}\cdot\{(Y_i+1)\cdot[X_i,(Y_i+1),(Z_i-1)]^{(M)} - Y_i\cdot[X_i,\ Y_i,\ Z_i]^{(M)}\}\cdot\sum_j Y_j\cdot\left[X_j,\ Y_j,\ Z_j\right]^{(M)} + k_{CA}\cdot\left[\{(X_i+1)\cdot[(X_i+1),Y_i,(Z_i-1)]^{(M)} - X_i\cdot[X_i,\ Y_i,\ Z_i]^{(M)}\}\cdot\sum_j Y_j\cdot\left[X_j,\ Y_j,\ Z_j\right]^{(M)} + \{(Y_i+1)\cdot[X_i,(Y_i+1),(Z_i-1)]^{(M)} - Y_i\cdot[X_i,\ Y_i,\ Z_i]^{(M)}\}\cdot\sum_j X_j\cdot\left[X_j,\ Y_j,\ Z_j\right]^{(M)}\right] + (X_i+1)\cdot k_{MSCA}\cdot[MOH]\cdot[(X_i+1),\ Y_i,\ Z_i]^{(b)} + (Y_i+1)\cdot k_{MSCW}\cdot[MOH]\cdot[X_i,\ (Y_i+1),\ Z_i]^{(b)} \quad (36)$$

Results for TEOS – Water – Aluminum system Detailed Approach

The model of the TEOS – Water – Aluminum system is solved in order to predict the evolution of different species, at different reactants ratios. Also, the ingredients can be mixed from the beginning or added separately. Few species were chosen to present the main results.

Mixing all the ingredients, with initial concentrations TEOS:Water:Aluminum =1:2:1

General species behavior, depicted in Figure 5, is similar to those in Fig. 3: Hydrolyzed species appear, have a maximum peak and are consumed through different reactions. Because the Water:TEOS ratio is high, water is used for hydrolysis first. After the species have been hydrolyzed, water is a product of condensation reaction. The hydrolyzed species attached to aluminum have the same behavior (right plot). *MOH* concentration decreases as aluminum proceeds with encapsulation. Final products are *M003* and *004*. Species attached to aluminum have a greater concentration.

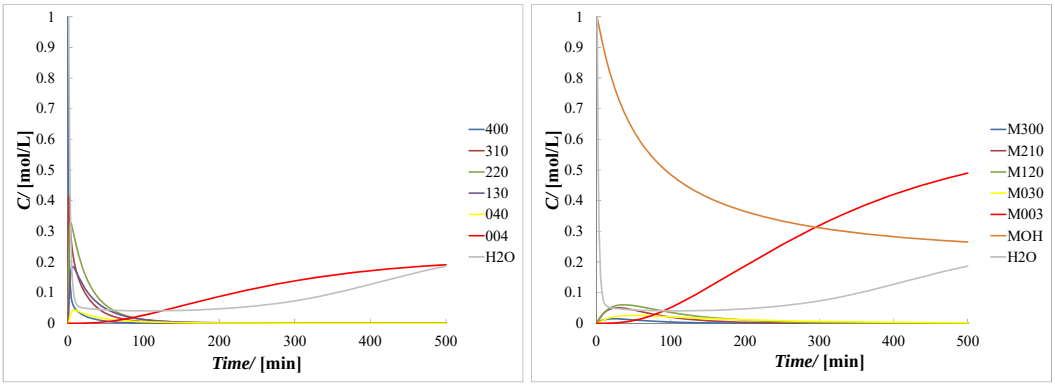

Fig. 5 Time dependence for: left – 400, 310, 220, 130, 040, 004 species; right – M300, M210, M120, M030, M003 species

TEOS – Water pre-hydrolysis, followed by addition of aluminum; $Si(OH)_4$:Water:Aluminum =1:0:1

Another way of performing encapsulation is to start with a pre-hydrolysis. Therefore, Aluminum pigment is added only after all *TEOS* has been hydrolyzed. Pre-hydrolysis is performed in the acid environment. Aluminum pigment is added together with a strong base in order to switch the pH to basic, favorable for condensation reactions.

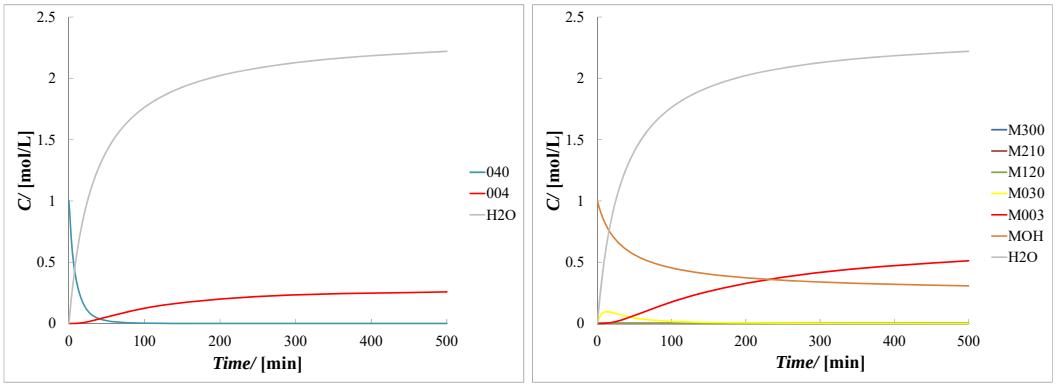

Fig. 6 Time dependence for: left – 040, 004 species; right - M300, M210, M120, M030, M003 species

As it can be seen in the Figure 6, the hydrolyzed reactant $Si(OH)_4$ and *MOH* are consumed in the reactions, while the concentration of the products (*M003* and *004*) is increasing. In the mass of reaction, there is twice more *M003* compared to *004* (SiO_2). Because aluminum was added in the mass of reaction when the *SiOR* groups were already hydrolyzed, water is a product with significant concentration.

4. Mathematical models verification

Because of the large number of species and because the equations describing their temporal evolution are often difficult to follow, moieties conservation relationships were formulated. Thus, for TEOS – Water – Aluminum model, the concentrations of Metal, Hydrogen, Oxygen and "–OR" groups do not change during the reaction.

Aluminum concentration sums all the species attached to aluminum pigment and the rest of unreacted hydrolyzed aluminum.

$$C_M = \sum_{Z=0}^{3}(\sum_{Y=0}^{3}[3-Y,\ Y,\ Z]) + [MOH] \quad (37)$$

The hydrogen concentration is related to the number of *SiOH* groups, water, alcohol and "–OH" groups from the aluminum pigment.

$$C_H = \sum_{Z=0}^{4}(\sum_{Y=0}^{4}[Y\cdot(4-Y,\ Y,\ Z)]\ )^{(b)} + \sum_{Z=0}^{3}(\sum_{Y=0}^{3}[Y\cdot(3-Y,\ Y,\ Z)]\ )^{(M)} + 2\cdot[H_2O] + [ROH] + [MOH] \quad (38)$$

The oxygen atoms that have to be counted correspond to *Si-OSi*, *SiOH* and *SiOR* groups from bulk and at the Al surface, and to the oxygen atoms from water, alcohol and *MOH* species:

$$C_O = \sum_{Z=0}^{4}\left[\frac{8-Z}{2}\cdot\sum_{X=4-Z}^{0}(X,\ 4-X,\ Z)\ \right]^{(b)} + \sum_{Z=0}^{3}\left[\frac{8-Z}{2}\cdot\sum_{X=3-Z}^{0}(X,\ 3-X,\ Z)\ \right]^{(M)} + [H_2O] + [ROH] + [MOH] \quad (39)$$

The "–OR" groups occur in the bulk, at Al surface, and in unreacted *ROH*.

$$C_{OR} = \sum_{Z=0}^{4}(\sum_{X=4-Z}^{0}[X\cdot(X,\ 4-X,\ Z)]\ )^{(b)} + \sum_{Z=0}^{3}(\sum_{X=3-Z}^{0}[X\cdot(X,\ 4-X,\ Z)]\ )^{(M)} + [ROH] \quad (40)$$

6. Conclusions

In this article, mathematical models were formulated in order to describe species interactions within TEOS – Water and TEOS – Water – Aluminum systems. The models were built gradually, from basic understanding of TEOS – Water system (only 5 species involved) to the more complex description of the TEOS – Water – Aluminum system involving 28 species. The correctness of the models is ensured by checking the conservation of number of functional groups and atoms during the reaction.

The results show qualitatively the evolution in time of different species. The models can be used to investigate the effect of reaction recipe (for example, reactants addition order, reactants ratio, reaction time) on the relative concentration of various species.

REFERENCES

[1] Assink, R.A., Kay, B.D., Sol-gel Kinetics I. Functional group kinetics, *Journal of Non-Crystalline Solids*, 99, (1988), 359-370.
[2] Deng, Z.Y., Zhu, L.L., Tang, Y.B., Sakka, Y., Ye, J.H., Xie R.J., Role of Particle Sizes in Hydrogen Generation by the Reaction of Al with Water, *Journal of the American Ceramic Society*, 93**,** (2010), 2998-3001.
[3] Kay, B.D., Assink, R.A., Sol-gel Kinetics II. Chemical speciation modeling, *Journal of Non-Crystalline Solids* 104, (1988), 112-122.
[4] Kiehl, A., Greiwe, K., Encapsulated aluminium pigments, *Progress in Organic Coatings*, 37, (1999), 179-183.
[5] Niemann, J., Waterborne Coatings for the Automotive Industry, *Progress in Organic Coatings,* 21**,** (1992), 189-203.
[6] Wissling, P., State-of-the-art technology in aluminium pigments for aqueous paints, *JOCCA-Surface Coatings International* 82**,** (1999), 335.
[7] Zhu, H.W., Chen, Z.X., Sheng, Y., Thi, T.T.L., Flaky polyacrylic acid/aluminium composite particles prepared using in-situ polymerization, Dyes and Pigments, 86**,** (2010), 155-160.

PREPARATION AND CHARACTERIZATION OF Al(III)-PILLARED INTERLAYERED CLAYS BASED ON INDIGENOUS BENTONITE

Ana-Maria GEORGESCU[1*], Vasilica-Alisa ARUŞ[1], Françoise NARDOU[2], Ileana Denisa NISTOR[1]

[1]''Vasile Alecsandri'' University of Bacău, Faculty of Engineering, Chemical and Food Engineering Depart., 157 Marasesti Street, 600115 Bacau, Romania;
[2]University of Limoges/CEC, SPCTS, UMR 7315 CNRS, 12 Rue Atlantis, 87068 Limoges Cedex, France

Abstract

Al-pillared interlayered clays (Al-PILCs) were prepared from Romanian natural calcium bentonite (Orasu Nou deposit) and the effect of some parameters on the textural properties has been investigated. The synthesis of Al-pillared bentonite consists in the following steps: bentonite purification, ionic exchange of bentonite with Cu(II) ions, preparation of pillaring agent, intercalation of ionic exchanged bentonite with pillaring agent and calcination. The synthesized nanomaterials were characterized by X-ray diffraction (DRX) analysis, nitrogen adsorption-desorption technique for the measurement of specific surface area by using of BET method (Brunauer - Emmet - Teller) and the pore size distribution by using the BJH method (Barrett - Joyner -Halenda). The basal spacing, specific surface area and pore size distribution were strongly affected by the varied parameters. The material with the best textural characteristics will be chosen in the aim of its using in environmental remediation.

Keywords: bentonite, basal spacing, specific surface area, porosity

1. Introduction

Pillared clays have attracted a special attention since 1970 at industrial level, due to their porous nature and their catalytic potential [1]. Several types of pillaring agents were used in the literature [2-5]. The inorganic polyhydroxocations lead to the production of chemically modified clays, with high thermal stability and a large specific surface area.

The researches of our work are focused on the achievement of adsorbents based on efficient nanomaterials used for environmental remediation. These adsorbents are realized starting from natural calcium bentonite (Orașu Nou deposit, Romania) that was modified through chemical and thermochemical

*Corresponding author: Email address: ana.georgescu@ub.ro

treatments in order to increase their retention properties by increasing their specific surface area, interlamellar distance and porosity.

The natural calcium bentonite was modified by pillaring process with aluminum(III) polyhydroxocations. Characterization of pillared nanomaterials by different methods (XRD, BET, BJH) were used to select the most efficient adsorbent in order to test them in the future studies on certain heavy metals adsorption from aqueous solutions.

2. Experimental

Raw material and reagents

The raw material used in this study was a Romanian natural calcium bentonite (*CaBent-nat*) from Orasu Nou deposit, supplied from S.C. Bentonita S.A., whose characteristics were presented in a previous paper [6].

The chemicals used in this paper were supplied from Merck (copper(II) chloride dehydrate, 99%; sodium hydroxide, pellets, 98%; silver nitrate, 99.8%) and from Alfa-Aesar (aluminum chloride hexahydrate, 99.99%) and they were used without further purification.

Synthesis of Al(III)-pillared calcium bentonites (Al-PCBs)

The preparation of Al-PCBs consists in the following steps: purification of *CaBent-nat*, ion exchange of purified calcium bentonite (*CaBent-pur*) with Cu(II) ions in order to obtain Cu-bentonite (*Cu-Bent*), intercalation of *Cu-Bent* with Al(III)-pillaring agent and calcination of intercalated bentonites (*ICBs*). The synthesis of Al-PCBs was realized according to experimental procedure described in detail in our previous papers [7, 8], the only difference being the Al/clay ratio.

The synthesis parameters of Al-PCBs are presented in Table 1.

Table 1

Synthesis parameters for obtained materials

Nr. crt.	Nanomaterial	Al/clay ratio ($mmol \cdot g^{-1}$)	Calcination duration (min)	Calcination temperature (°C)
1	ICB-5Al		-	-
2	PCB-5Al-300/1			300
3	PCB-5Al-400/1		60	400
4	PCB-5Al-500/1			500
5	PCB-5Al-300/2	5		300
6	PCB-5Al-400/2		120	400
7	PCB-5Al-500/2			500
8	PCB-5Al-300/3			300
9	PCB-5Al-400/3		180	400
10	PCB-5Al-500/3			500

Characterization methods

The specific surface area and the pore size distribution were measured with a Micromeritics ASAP 2010 device. The samples were degassed at 473 K, for 16 h. The value 0.1620 nm^2 was taken for all samples as the N_2 molecular cross-sectional area. Pore size distribution for materials was calculated according to Barret–Joyner–Halenda (BJH) method from the nitrogen desorption isotherms.

The basal distance of synthesized materials was performed using Bruker D8 Advance diffractometer, which works on monochromatic $k_{\alpha 1}$ radiation of Cu ($\lambda_{CuK\alpha 1}$ =1.540598 Å). X-ray diffraction spectra are recorded in the angular range of 2θ = 2 - 40°, the step size being 0.0197º. For the range 2θ = 2 - 10°, the number of steps is 580, and duration step of 3 s, and for the range 2θ = 10 - 40°, the number of steps is 1695, for duration step of 1s. The analyses are made at a voltage of 40 kV and amperage of 40 mA.

3. Results and discussions

Figure 1 shows the XRD patterns of intercalated and pillared bentonites with Al(III) polyhydroxocations. The physical characteristics of synthesized nanomaterials are presented in Table 2.

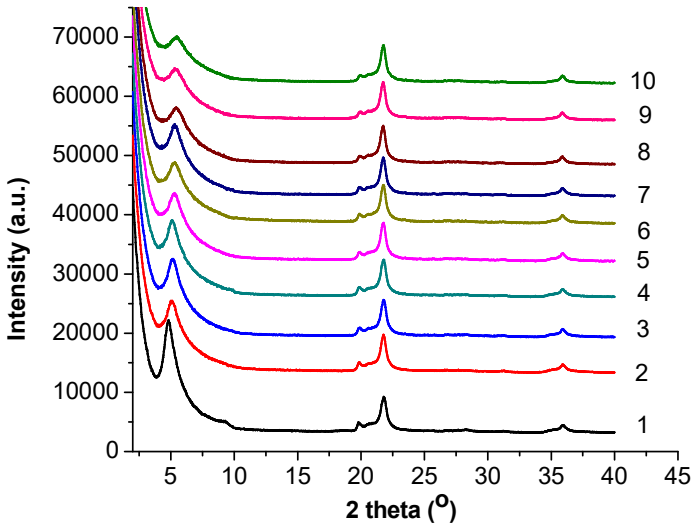

Fig. 1. X-ray diffraction patterns of ICB-5Al (1), PCB-5Al-300/1 (2), PCB-5Al-300/2 (3), PCB-5Al-300/3 (4), PCB-5Al-400/1 (5), PCB-5Al-400/2 (6), PCB-5Al-400/3 (7), PCB-5Al-500/1 (8), PCB-5Al-500/2 (9), PCB-5Al-500/3 (10)

The highest value of basal distance (1.758 nm) was obtained for *PCB-5Al-300/1* material, it being with 0.517 nm higher than the basal distance of *CuBent* [9], which indicates that the pillaring process with Al(III) polyhydroxocations has been successfully achieved. Basal distances of synthesized materials are much smaller as the calcination temperature is higher. If calcination duration is higher

(up to 500ºC), the basal distance tends to diminish. Through X-ray diffraction analysis is can be noticed that clays crystallinity decreases with increasing of duration and temperature calcination. Concerning nonclays minerals (cristobalite and quartz), their crystallinity is not changed.

Table 2

Physical characteristics of synthesized nanomaterials

Nr. crt.	Nanomaterial	Basal distance (nm)	Specific surface area, S_{BET} ($m^2 \cdot g^{-1}$)
1	ICB-5Al	1.835	174.21
2	PCB-5Al-300/1	1.758	166.58
3	PCB-5Al-400/1	1.667	135.78
4	PCB-5Al-500/1	1.629	115.84
5	PCB-5Al-300/2	1.718	152.31
6	PCB-5Al-400/2	1.659	158.24
7	PCB-5Al-500/2	1.624	139.20
8	PCB-5Al-300/3	1.736	149.17
9	PCB-5Al-400/3	1.667	147.10
10	PCB-5Al-500/3	1.618	132.15

It can be noticed that the specific surface area values are increasing from values of about 45 $m^2 \cdot g^{-1}$ in the case of raw clay [10] to about 167 $m^2 \cdot g^{-1}$ in the case of obtained material under the following synthesis parameters: an Al/clay ratio of 5 $mmol \cdot g^{-1}$, calcinated at 300ºC for 1 h. The specific surface areas values are higher, the longer the duration and the temperature calcination are lower.

The determination of pore size distribution in the case of intercalated and pillared bentonites, are shown in Fig. 2.

From the experimental results it is found that ICB-5Al and Al-PCBs contain mainly mesopores, whose dimensions are between 2 ... 50 nm, and a smaller amount of macropores (50 ... 150 nm).

Pore-size distribution curve of synthesized materials is bimodal into mesopore region, showing two peaks at 2.7 nm and 4.3 nm respectively, and in the region of macropores, the most common size is about 58 nm. Materials porosity increases after pillaring process, this fact being confirmed also by the increasing of pore volume at about 0.023 $cm^3 \cdot g^{-1} \cdot nm^{-1}$ as against 0.004 $cm^3 \cdot g^{-1} \cdot nm^{-1}$ in the case of raw material [10].

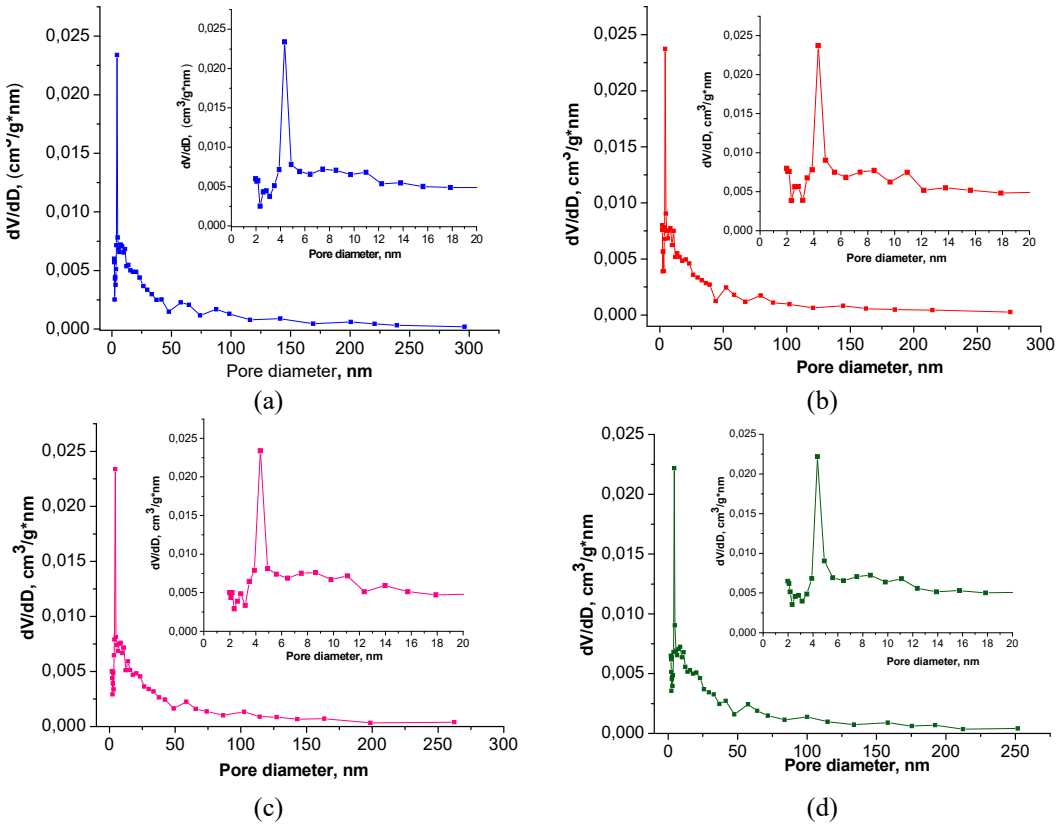

Fig. 2. Pores size distribution curve of ICB-c-5Al (a), PCB-5Al-300/1 (b), PCB-5Al-300/2 (c), PCB-5Al-400/3 (d)

In conclusion it can be said that textural analyses of Al-PCBs confirm that the pillaring process led to the improvement of the most important properties of adsorbents: the porosity. This is due to the formation of new mesopores in the clay structure resulted after pillaring process. The porosity of these pillared bentonites can be controlled by choosing the optimal parameters of various synthesis steps.

6. Conclusions

Physical characteristics of Al(III)-pillared bentonites (basal spacing, specific surface area and pore size distribution) were strongly affected by the synthesis parameters. The highest value of the basal distance (1.758 nm) was in the case of bentonite calcined at 300°C under nitrogen atmosphere for 1h; this value increased with about 0.5 nm in comparison with exchanged bentonite with copper(II) ions, which indicates that the pillaring process has been achieved. The highest value of specific surface area (166.58 $m^2 \cdot g^{-1}$) was obtained for the same

material (*PCB-5Al-300/1*), this being more than 3 times higher than that of natural bentonite. Basal distances and specific surface areas of Al-PCBs decrease with the increasing of calcination temperature and calcination duration. Bentonites porosity increases after Al(III)-pillaring process, as confirmed by the pore size distribution curves. After the intercalation of *Cu-Bent* with pillaring solution, the obtained materials are mesoporous, the mesopore size ranging from 2 to 20 nm.

We recommend the using of Al(III)-pillared calcium bentonites as adsorbents for heavy metals retention from wastewaters due to its superior textural properties in comparison with raw material.

REFERENCES

[1] Vaccari, A., Clays and catalysis: a promising future, *Applied Clay Science*, 14(4), (1999), 161–198.

[2] Gil, A., Korilia,, S.A., Trujillanob R., Vicente, M.A., A review on characterization of pillared clays by specific techniques, *Applied Clay Science*, 53, (2011), 97–105.

[3] Bergaya, F., Theng, B.K.G., Lagaly, G., *Handbook of clay science*, Elsevier Science, 2006.

[4] Platon, N., Siminiceanu, I., Nistor, I.D., Miron, N.D., Muntianu, G, Zavada, R M, Isopencu, G, Nistor, I D, Preparation and characterization of new products obtained by pillaring process, *Revista de chimie*, 62(8), (2011), 799-805.

[5] Muntianu, G., Ursu, A.-V., Djelveh, G., Isopencu, G., Mareş, A.-M., Nistor, I.D., Jinescu, C.V., Dynamic parameters for mixtures of pillared clay-magnetic particles in fluidized bed in coaxial magnetic field, *Revista de Chimie*, 65(9), (2014), 1077-1085.

[6] Georgescu, A.-M., Nardou, F., Penot, C., Brabie, G., Nistor, I. D., Influence of purification process on Romanian calcium bentonite characteristics, *Journal of Engineering Study and Research*, (submitted for publishing).

[7] Georgescu, A.M., Muntianu, G., Nistor, I.D., Nardou, F., Modeling and optimization of pillared process using experimental design procedure, *Ponte Journal*, 72(7), (2016), 226-231.

[8] Georgescu, A.M., Nardou, F., Nistor, I.D., Influence of synthesis parameters on morphological properties of aluminium(III)-pillared bentonites, *Scientific Study & Research, Chemistry & Chemical Engineering, Biotechnology, Food Industry*, (submitted for publishing).

[9] Georgescu A.M., Brabie G., Nistor I.D., Penot C., Nardou F., Textural and morphological characterization of copper(II)-exchanged Romanian calcium bentonite, *Journal of Engineering Studies and Research*, 20(3), (2015), 38-44.

[10] Georgescu, A.M., Brabie, G., Nistor, I.D., Penot, C., Nardou, F., Synthesis and characterization of Cr-pillared clays: modelling using factorial design methodology, *Journal of Porous Materials*, 22(4), (2015), 1009-1019.